New Models and Analytical Frameworks for Power Systems with Wind Generation Penetration

by

Mohamed Hassan Ahmed

A thesis
presented to the University of Waterloo
in fulfillment of the
thesis requirement for the degree of
Doctor of Philosophy
in
Electrical and Computer Engineering

Waterloo, Ontario, Canada, 2012

AUTHOR'S DECLARATION

I hereby declare that I am the sole author of this thesis. This is a true copy of the thesis, including any required final revisions, as accepted by my examiners.

I understand that my thesis may be made electronically available to the public.

Abstract

Wind energy is a proven energy source that does not contribute to emission of greenhouse gases, air and water pollution, or generate large quantities of waste. However, wind generation is dependent on wind speed, which is difficult to predict with high accuracy. The intermittent nature of wind generation makes its operation and planning a complex problem and there is a need for advanced analytical models to embed this uncertainty in its generation profile. This research focuses on the development of innovative mathematical modeling and analysis tools to improve our understanding of the effects of wind generation on power systems.

The overall goal of this research is to introduce novel analytical frameworks to consider the penetration of wind generation sources within the distribution and transmission networks. In particular, two main operational problems are addressed within this thesis; the Distribution Load Flow (DLF) problem and the Unit Commitment (UC) problem in the presence of wind generation.

First for the DLF problem, a novel probabilistic wind generation model is presented. The probabilistic wind generation profile, which is a function of the wind speed, is considered and an appropriate procedure is developed to classify specific levels based on wind speed, in order to reduce the number of probabilistic combinations of wind power generation. Next, a novel Probabilistic Distribution Load Flow (PDLF) approach is used to evaluate the impact of wind penetration into distribution systems. The traditional DLF program is modified to include the wind generation profiles. Three Wind Turbine (WT) models are derived and integrated within the PDLF program to examine and compare their performance. The probabilistic forward-backward sweep algorithm is developed for the first two models of WT. For the third model of WT, a probabilistic compensation-based load flow is presented. The effect of WT penetration is investigated on feeder losses, voltage profile and line flows.

Secondly, a new scenario generation and reduction technique is developed for analyzing the effects of wind generation uncertainties on short-term power system operation. A historical wind speed data set is used to obtain different wind speed clusters which are then processed through Monte Carlo Simulations (MCS), Markov-chains and a forward selection scenario reduction algorithm to obtain a reduced set of scenarios. These reduced scenarios are then incorporated into a Locational Marginal Price (LMP) based electricity market settlement and dispatch model. These UC type models incorporate system constraints and transmission constraints to examine the effects of wind generation

on electricity market prices, UC decisions including generation, reserve requirement, load cleared and social welfare. Markov-chain transition matrices are developed to include the effect of the inter-hour transition correlation of wind speed from one specific hour to the following hour to improve the generation of the wind scenarios. The effect of changing wind farm capacity on system operation is also discussed. Furthermore, the impact of the wake-effect phenomena influencing off-shore wind turbines is explained.

Finally, this research examines the effect of wind generation penetration on the environmental emissions. A novel methodology is developed to evaluate the environmental impact of wind generation penetration into electrical power systems. The solution of the market dispatch UC model is studied for different cost functions with an emission cap. The relationship between changing the emission caps and the penetration level of wind energy is investigated. Furthermore, the effect on market prices is also examined when emission caps are imposed by external agencies, on the System Operator (SO).

Acknowledgements

I would like to express my sincere gratitude to several people who have contributed in various ways to the completion of this thesis. First and foremost, I would like to thank my supervisors, Professor Magdy Salama and Professor Kankar Bhattacharya, for their continuous guidance, support and encouragement throughout the period of my Ph.D. studies at the University of Waterloo. Their invaluable suggestions and precious ideas have helped me walk through various stages of my research, while their passion and extraordinary dedication to work have always inspired and encouraged me to work harder.

My appreciation is also extended to my Ph.D. committee members: Professor Claudio Cañizares, Professor Jatin Nathwani and Dr. Tarek El-Fouly. Special thanks to Professor Mahmoud Saleh, Professor Metwally Awad El-Sharkawy, Professor Mohamed Abdel-Latif Badr, Professor Yasser Hegazy, Professor Ramadan EL-Shatshat, Professor Ehab El-Saadany, Dr. Tarek Abdel-Galil and Dr. Mostafa Marei for their continuous support, interest, assistance and technical discussions during the course of this research.

I would like to express my sincere thanks to Dr. Hassan Sadek, my father, who rests in peace, forged my personality and share credit on every goal I achieve. To my mother, Neemat Habib, for her years of love and devotion, and for supporting my academic career even though it meant being away from her. Last but not least, I would never find the right words to express my gratitude to my caring wife, Nihal Salem, for her endless love, understanding, patience, and support during all these years of my Ph.D. studies.

Dedication

To the soul of my father,

To my mother,

To my wife, Nihal, and my children, Ziad and Hassan

Table of Contents

List of Figures

List of Tables

Nomenclature

Sets and Indices

G	Set of selected scenarios
d	Index for days
h	Index for customer bid blocks
I, i, q	Set of indexes of bus bars
I_W, i_w	Set of indexes of wind farm buses
J, j	Set of indexes of generating units
K, k, t	Set of indexes of the time periods
l	Index for generator bid blocks
m	Index for months
N, n, z	Set of indexes of generated scenarios
S, s	Set of indexes of reduced scenarios
y	Index for years
W	Set of wind speeds
B, β	Set of random events
L	Set of system branches
b, m	Branch index
n	Number of bus bars
N	Number of power intervals
$\mathbb{R}$	Euclidean space

Parameters

ω	Wind speed, m/sec
ω_0	The initial free stream of wind speed, m/sec
ω_I	Wind turbine cut-in speed, m/sec
$\omega_{cut\text{-}out}$	Wind turbine cut-out speed, m/sec
ω_r	Wind turbine rated speed, m/sec
$\varpi_{i_w,k,m}$	Mean wind speed, m/sec
$\sigma_{i_w,k,m}$	Standard deviation of wind speed, m/sec
λ_n	Probability of scenario n
Y	Set of vectors of wind generation profile
$\mu_{l,j,k}$	Bid price of unit j, $/MWh
β	Number of periods of the time span
$\gamma_{h,i,k}$	Bid price of customer i, $/MWh
$D_{n,n'}$	Distance between scenario pair (n, n')
h	Scenario with minimum $D_{n,n'}$
F_z	Probability distance measure of scenario z
z	Scenario with minimum F_z
ε	Tolerance error

B	Susceptance of transmission lines, per unit
c	Scale index for Weibull distribution.
C_j	Shut-down cost of unit j, $
C_{Thrust}	Thrust coefficient
CF	Capacity factor for hydro station.
D	Wind turbine diameter, meter
D_j	Number of periods of unit j that must be initially online due to its minimum down time
D_{j0}	Number of periods of unit j is offline prior to the first period of the time span
D_m	Number of days of month m
D_{Tj}	Minimum down-time for unit j, hour
E_i	The group of generators connected to bus i
$f(\omega)$	Probability density function of wind speed
$F(\omega)$	Cumulative distribution function of wind speed
$F_{l,j,k}$	Generator bid power of block ℓ, MW
G_j	Number of periods unit j initially online due to its minimum up time constraint.
K_{jt}	Cost of the interval t of the stair wise start-up cost function of unit j, $
M_j	Number of bid blocks of generator bid function
N_i	Number of bid blocks of customer bid function
ND_j	Number of intervals of the stair-wise startup cost
NW_i	Number of wind turbines connected to bus i
$P_{hydro,k}$	Hydro generated power, MW
P_{hydro}^{rated}	Hydro station rated power, MW
$\overline{P}j,k$	Maximum power output of unit j, MW
$\overline{P}_{w i_w,n}$	Vector of 24-hour wind generation profile
$P_j max$	Capacity of unit j, MW
$P_j min$	Minimum power output of unit j, MW
P_{rated}	Rated power of wind turbine, MW
$\overline{P}_{TL_{i,m}}$	Transmission line capacity, MW
P_T	Injected wind turbine power, MW
$P_{w i_w}$	Injected wind farm power, MW
$Q_{h,i,k}$	Bid power of block h of customer i, MW
R_k	Spinning reserve requirement, MW
RD_j	Ramp-down limit for unit j, MW/hour
RU_j	Ramp-up limit for unit j, MW/hour
SD_j	Shut-down ramp limit for unit j, MW/hour
SU_j	Start-up ramp limit for unit j, MW/hour
T	Time in years for available historical data.
U_{j0}	Number of periods of unit j is online prior to the first period of the time span
UT_j	Minimum up-time for unit j, hour

w	Wake effect decay constant
V_{j0}	Initial commitment state of unit j (0 or 1)
λ_s	Probability of occurrence of s
a_1, a_2, a_3	Constants of the parabolic part of Pw
c	Scale index
f	Probability Distribution Function (PDF)
F	Cumulative Distribution Function (CDF)
P_w	Active power of Wind Turbine
$P(\beta)$	The probability of event β
R	Shape index
X	Total reactance of induction generator, W
X_m	Reactance of magnetization branch of induction generator, W
X_c	Reactance of induction generator capacitor, W
Variables	
$\delta_{i,k}$	Power angle, radian
$H_{h,i,k}$	Power consumed in block h, MW
$P_{j,k}$	Committed output power for unit j, MW
$PD_{i,k}$	Load cleared in the auction, MW
$step_{l,j,k}$	Power generated in block ℓ, MW
$v_{j,k}$	Binary variable is equal to 1 if unit is online and 0 otherwise
$V_i(\omega)$	Voltage of bus i at speed level ω
$I_i(\omega)$	The nodal current injection
$\Delta I_{q,i}(\omega)$	Change of reactive current injected by WT
$I_{q,i}(\omega)$	The total reactive current injected by WT to maintain the voltage at specific value
$I_L(\omega)$	Current in branch (L)
$I_m(\omega)$	The sum of branch currents in all branches connected to bus i

Chapter 1
Introduction

1.1 Motivation

In recent years, there has been a dramatic increase in wind power capacity installations around the world, with further plans to increase wind capacity in many countries, such as in Denmark, Germany, Spain, U.S. and Canada. The renewable energy resources contribute minimally to greenhouse gases emissions at the production stage, or through lifecycle emissions resulting from equipment manufacturing, installation, material requirements and construction. Wind energy is now a mature renewable energy technology; it is clean, abundant, and most importantly large amounts of electrical power can be generated from a wind-farm (WF). A WF may consist of hundreds of individual wind turbines (WTs) aggregated and spread over hundreds of square kilometers.

In many electric utility systems, wind energy has become a significant electrical supply resource in the past 15 years, from 1996 to 2010, with almost 200,000 MW of capacity installed worldwide at the end of 2010 [1], as presented in Figure 1-1.

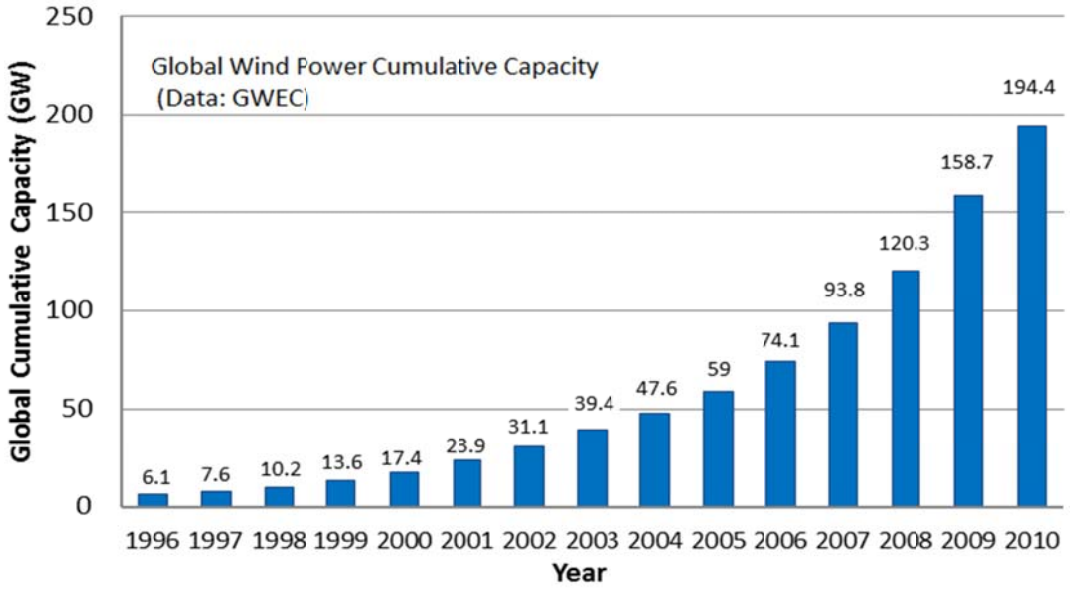

Figure 1-1 Global Cumulative Installed Wind Capacity 1996-2010 [1]

Canada has outstanding and bountiful wind resources, alongside its large landmass and long coastlines. The current total installed wind capacity in Canada is 5.4 GW which contributes to 2% of the country's electricity demand. According to the Canadian Wind Energy Association [2] , 20% of

Canada's electricity demand could be supplied by wind energy by the year 2025. Each province has its own independent programs for renewable energy development and incentives [3]. According to the Integrated Power System Plan (IPSP) of Ontario Power Authority (OPA) [4], Ontario's target for renewable resources is 15,700 MW by 2025, out of which 4,685 MW is expected to be wind generation. Ontario's goal is to develop a cleaner energy economy. The Government of Ontario has set a goal of eliminating all coal-fired generation by the end of the year 2014, which is envisaged to decrease the greenhouse gases emissions from electricity generation to below 5 mega tons/year. Ontario energy infrastructure will require refurbishment in the near future, as existing nuclear facilities will reach the end of their life cycle and all coal-fired generation will retire by 2014. Wind generation is expected to be even more than what is planned for in the IPSP, because of the Feed-in-Tariff (FIT) program. Since the initiation of the FIT program in October 2009, the OPA has received over 1700 applications for the FIT and micro-FIT programs [5].

This expected increase in installed wind capacity introduces various challenges to the operation of the power system, from frequency control issues to planning of the transmission system. However, wind generation is dependent on the wind speed at a given instant, which is difficult to predict in advance. This intermittent nature of wind generation makes its operation and planning a complex problem and there is a need for the current analytical models to consider this uncertainty in wind generation appropriately. Figure 1-2 represents two categories of WTs that have found applications in power systems. The first category is the low rating WTs, which have typically been deployed in distribution systems, and the main issues governing their operation are the voltage impacts and power losses. The second category is the high rating WTs, typically found in transmission systems and their main issue being, inclusion in UC and market dispatch programs.

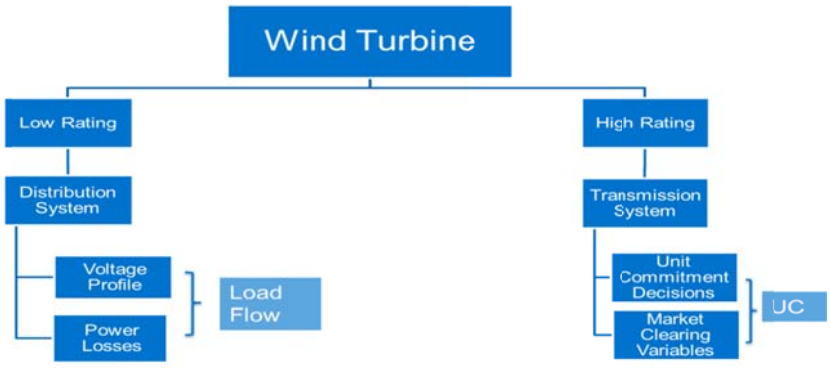

Figure 1-2 Two proposed models of WTs

When connection of WT generators in distribution systems is considered, it is not possible to achieve a realistic evaluation of where and when over-voltages may occur by simply using deterministic distribution load flow analysis. The probability of a given wind speed can be estimated if the probability distribution of the wind speed is known. Once the wind speed is known, the power injected into the grid can be calculated by means of the WT power curve. Thus, to assess the impact of wind generation penetration on system operations aspects, a probabilistic model is needed, using the probability of a given wind speed. Figure 1-3 compares the drawbacks of using a deterministic load flow that have accuracy problems versus using Monte-Carlo Simulations which is very computationally expensive. This calls for a fast and accurate computational platform for distribution load flow.

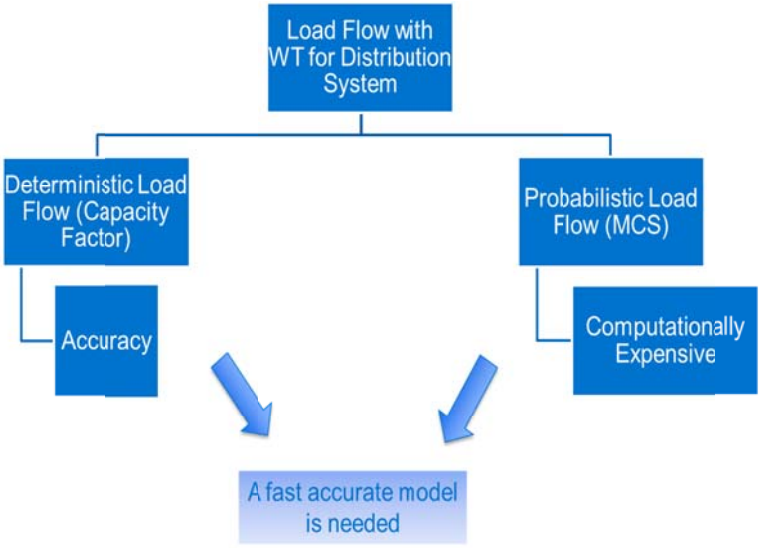

Figure 1-3 A comparison between existing deterministic and probabilistic load flow

Another major challenge associated with wind energy is the way it impacts system Unit Commitment (UC) decisions. With low levels of wind capacity penetration, UC can be treated as a deterministic problem. However, when installed wind capacity is fairly large, vis-à-vis the system capacity, it adds a significant stochastic element to the operation of the system. This is due to the uncertainty associated with wind forecasts. As wind cannot be forecasted to a high degree of accuracy, additional reserve capacity needs to be carried by the system in addition to the reserves already allocated to cater for unit outages and demand forecast error. The issue of system-wide UC and the associated electricity market clearing price formation and real-time dispatch of generators is

also more complicated by the presence of wind generation. Figure 1-4 presents a comparison between the deterministic and stochastic UC formulations, reported in the literature.

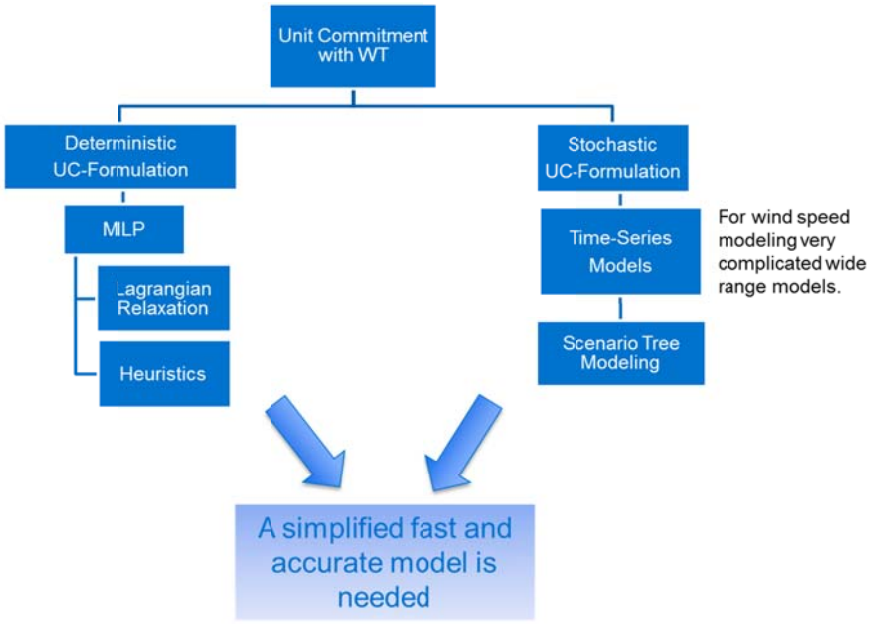

Figure 1-4 A comparison between deterministic and stochastic UC

Moreover, a realistic environmental evaluation model is needed to assess the environmental emissions reduction from a power system which has a supply mix that includes wind power generation. The relationship between the penetration level of wind generation and the resulting reduction in emissions is not linear and policy makers need to determine the optimum level of wind capacity penetration as well as to set the optimum emission cap.

In reality, to address these challenges, it has become clear more than ever that the adoption of advanced, fast and accurate wind models is vital. It is the goal of this research work to improve the accuracy of wind models to improve the efficiency of integrating WTs and WFs into the distribution and transmission systems, respectively.

1.2 Research Objectives

This research focuses on studying the effects of wind generators connected to the low voltage distribution grid and to high voltage transmission system. The specific objectives of this research are outlined as follows:

- Development of probabilistic representation of WT model for inclusion in the traditional Distribution Load Flow (DLF) program. Modify the traditional DLF to include the penetration of WTs, by considering three different WT models.
- Development of a probabilistic approach to evaluate the impact of wind penetration into distribution systems, then study the effect of WT penetration on feeder losses, voltage profile and line flows.
- Proposing of a reliable method for wind power scenarios generation using Monte-Carlo Simulations (MCS) and Markov-chain models, Markov-chain is used to improve the transitions for inter-hour wind speed correlations. These wind power generation scenarios are then reduced using Forward Selection Algorithm.
- Development of an LMP market model that replicates several US electricity market models (for example- the New York, New England, PJM markets), while incorporating the stochastic wind generation at specific locations in the system using the reduced set of wind generation scenarios of previous step. This analysis will not only require the formulation of a stochastic UC-type model but will also include a dc-load flow representation to represent the transmission system and congestion issues. Other electricity market constraints and wind generation effects will be included.
- Development of a UC-model to examine the effects of the stochastic behavior of the wind generation penetration on the total system operation cost and hence, a programming model to evaluate the environmental impact of wind generation penetration into electrical power system is proposed.

1.3 Thesis Outline

The thesis is organized as follows: Chapter 2 presents a literature survey of the available techniques for wind speed modeling and wind farm output power simulation. This chapter also surveys the previously developed models for distribution load flow. The proper fields of application of each model and their usage limitations are discussed. Previously developed unit commitment and algorithms used for solving the stochastic problem with and without wind generation are also reviewed. Finally, the developed studies to investigate possible environmental impact of integrating wind farms to utility grids are surveyed.

The rest of this thesis is divided into two parts: The first part, presented in Chapter 3, investigates the analysis of distribution load flow problem when a connection of WT is considered

(IEEE 34-bus). This problem is an example of snap-shot type problems that can be solved using a probabilistic WT model. It includes developing a new probabilistic model for the WT, and incorporates this model in the distribution load flow algorithms. The second part, Chapters 4, and 5, investigate a different type problem which includes the inter-hour constraints such as ramp-rate constraint. Chapter 4 discusses the operational aspects of wind farms in the transmission system (IEEE RTS). Unit-Commitment model is developed that includes, developing a new scenario wind power generation and reduction algorithm for wind farms power system operation studies. This model facilitates investigating the impact of wind farms integration to utility grids on electricity markets clearing prices. The presented UC-model was formulated as a Mixed Linear Integer Programming Problem (MILP) and solved using the CPLEX solver in the General Algebraic Modeling System (GAMS) environment. This model was used to investigate the impact of wind power variability, wind energy penetration level, wind farm location. Chapter 5 simulates a realistic environmental evaluation that is practically useful for the power sector. The developed models are useful for policy makers to determine the optimum level of wind capacity penetration as well as to set the optimum emission cap. The proposed model is a stochastic UC model that minimizes the total system cost. This model takes into account the existence of an emission constraint that represents the emission cap imposed by ISO. Chapter 6 presents the thesis summary, conclusions and recommendations for future research areas. Figure 1-5 shows the overall layout of the thesis and the gamut of issues addressed in the Chapters.

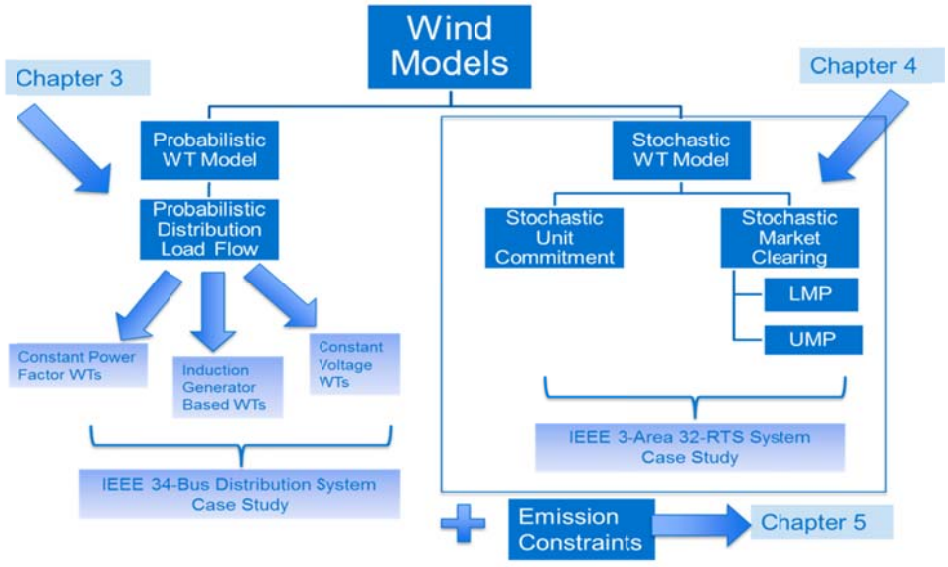

Figure 1-5 Overall layout of the thesis

Chapter 2
Background and Literature Review

2.1 Introduction

In Chapter 1, the motivations of the research work has been discussed and the research objectives are presented. In this chapter, first a literature survey pertaining to wind generation potential and wind turbine modeling is presented. Thereafter, the chapter is divided into two main folds, one for reviewing the power system operational aspects wherein different methods for Distribution Load Flow (DLF) are presented. The second part reviews short-term operational problems in power systems with wind generation penetration, including issues of inter-hour constraints and wind generation models that can handle the correlated transitions of wind speed from one hour to the next. The last part of this chapter presents current practices of including emission constraints to short-term power operations models.

2.2 Wind Potential

From an environmental perspective, wind energy is a proven energy source that does not contribute to climate change, air and water pollution, toxic or nuclear wastes. A single WT of typical capacity of 660 kW is expected to generate annually 2,000 MWh of electrical energy, enough for 250 Canadian homes [2]. It has been estimated in [2] that using wind to produce electricity rather than burning coal will save 900,000 kilograms of coal and reduce 2,000 tons of greenhouse gases annually. Newer and larger WTs can be expected to bring in even greater savings. Figure 2-1 shows the current installed capacity of wind energy generation across all of Canada [2].

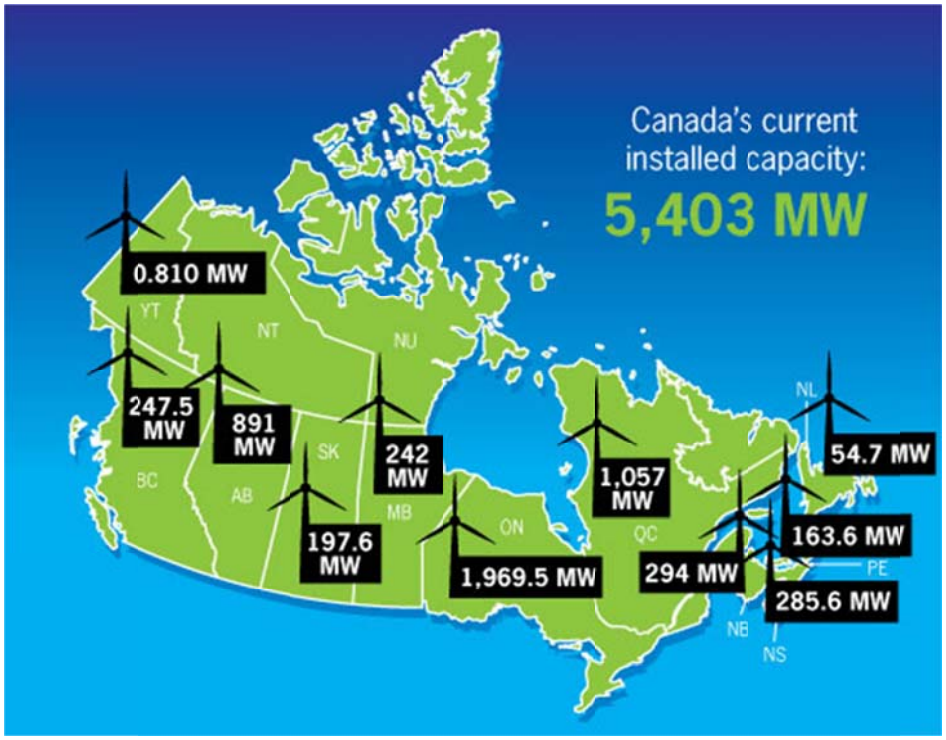

Figure 2-1 Current capacity of wind energy in Canada[2].

In recent years, wind energy has become an important component of the power supply mix in many countries and its importance is growing. Wind energy can substiute for other forms of electricity production to decrease environmental concerns arising. However, wind generation is dependent on the wind speed at a given instant, which is difficult to predict in advance. This very intermittent nature of wind generation makes its operation and planning a complex problem and there is a need for the presently available analytical models to consider this uncertainty in generation appropriately.

2.3 Wind Turbine Model

The analysis of power flows in an electrical network is an essential component of the expansion and operation planning studies. When connection of WT generators is considered, it is not possible to achieve a realistic evaluation of electrical system by simply using deterministic analysis. The probability of a given wind speed can be estimated if the probability distribution is known. Once the wind speed is known, the power injected into the grid can be calculated by means of the WT power curve.

2.3.1 Wind Speed Model using Weibull Distribution

Wind speed is considered as a random variable and is modeled using the Weibull Probability Distribution Function (PDF), the mathematical representation is given by (2.1) [6]:

$$f(\omega) = \frac{r}{c}\left(\frac{\omega}{c}\right)^{r-1} \exp\left[-\left(\frac{\omega}{c}\right)^{r}\right] \tag{2.1}$$

In (2.1), $f(\omega)$ is the wind speed PDF and,

$$r = \left(\frac{\sigma}{\omega_{mean}}\right)^{-1.086} \tag{2.2}$$

$$c = \frac{\omega_{mean}}{\Gamma(1+\frac{1}{r})} \tag{2.3}$$

Where, ω_{mean} is the mean wind speed and σ is the standard deviation for a particular site. The Cumulative Distribution Function (CDF) can be represented mathematically by (2.4),

$$F(\omega) = 1 - \exp\left[\left(-\frac{\omega}{c}\right)^{r}\right] \tag{2.4}$$

2.3.2 Wind Power Output

The generation of active power from WTs can be represented as a function of the wind speed, as given by (2.5) and (2.6), [7]:

$$P_w(\omega) = \begin{cases} 0 & 0 \le \omega \le \omega_1 \\ h(\omega) & \omega_1 \le \omega \le \omega_r \\ P_{rated} & \omega_r \le \omega \le \omega_{cut-out} \\ 0 & \omega \ge \omega_{cut-out} \end{cases} \tag{2.5}$$

Where,

$$h(\omega) = (a_1 + a_2\omega + a_3\omega^2)P_{rated} \tag{2.6}$$

The constant terms a_1, a_2, and a_3 can be expressed in terms of the cut-in speed (ω_1) and the rated wind speed (ω_r), as given by (2.7)-(2.9), [8]:

$$a_1 = \frac{1}{(\omega_1 - \omega_r)^2}\left[\omega_1(\omega_1 + \omega_r) - 4\omega_1\omega_r\left(\frac{\omega_1 + \omega_r}{2\omega_r}\right)^3\right] \tag{2.7}$$

$$a_2 = \frac{1}{(\omega_1 - \omega_r)^2}\left[4(\omega_1 + \omega_r)\left(\frac{\omega_1 + \omega_r}{2\omega_r}\right)^3 - (3\omega_1 + \omega_r)\right] \tag{2.8}$$

$$a_3 = \frac{1}{(\omega_1 - \omega_r)^2}\left[2 - 4\left(\frac{\omega_1 + \omega_r}{2\omega_r}\right)^3\right] \tag{2.9}$$

Using (2.5), the output power characteristic is developed for a WT of type VESTAS 600 kW, as shown in Figure 2-2. The following wind speed data are used: $\omega_{cut\text{-}in}$ = 4 m/s, ω_{rated} = 16 m/s and $\omega_{cut\text{-}out}$ = 25 m/s, for all wind speed models in this thesis.

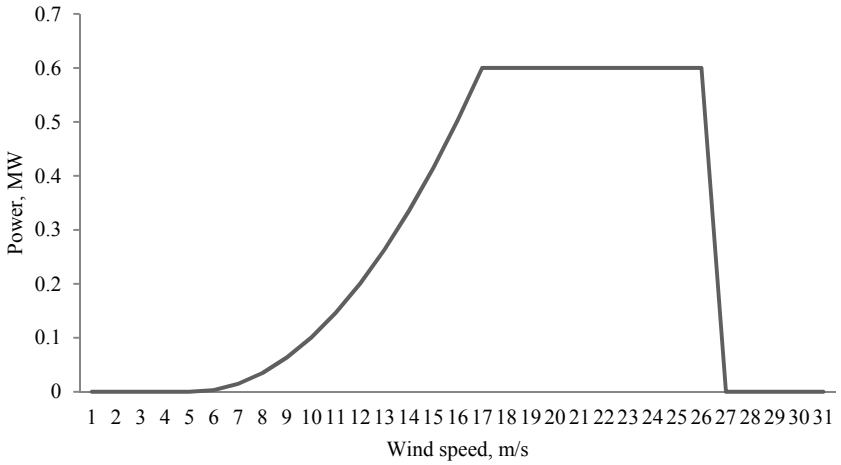

Figure 2-2 Power curve for VESTAS 600 kW wind turbine

2.4 Modeling of Distribution Systems

Generally, distribution networks are radial and the *R/X* ratio is high. For this reason, conventional Newton-Raphson and fast decoupled load-flow methods do not converge [9] but since distribution systems typically have a radial or weakly meshed structure, they need different load flow algorithms [10, 11] for their fast convergence. Many researchers have suggested modified versions of the conventional load-flow methods for solving power networks with high *R/X* ratio [12-14]. Reference [15] develops a load-flow technique for solving radial distribution networks using ladder-network theory. A ladder technique is developed, from the basic ladder-network theory, into a working algorithm, applicable to the solution of radial load-flow problems.

In [16] a method is proposed for solving radial distribution networks based on the direct application of Kirchhoff's voltage and current laws. A branch numbering scheme is proposed that enhances the numerical performance of the solution method. The load-flow solution is obtained by

the iterative solution of three fundamental equations representing real power, reactive power and voltage magnitude.

Reference [17] proposes a new load-flow method for obtaining the solution of radial distribution networks. In [18, 19] a load-flow technique is proposed for solving radial distribution networks by calculating the total real and reactive power fed through any node. A unique node, branch and lateral numbering scheme is used which helps to evaluate exact by the real- and reactive power loads, fed through any node and the corresponding receiving-end voltages. A summary of the DLF methods used in literature is presented in the following subsections.

2.4.1 Distribution Load Flow Methods

2.4.1.1 Forward–Backward Methods

A majority of radial distribution system power flow algorithms use the forward-backward sweep method. These techniques model the distribution network as a tree with the slack bus being the root, and the branch sections being ordered by layers away from the root node. The backward sweep primarily sums either the line currents or power flows from the extremities to the root. The forward sweep is a voltage drop calculation, providing updates to the voltage profile based on the current estimates of the flows [20].

2.4.1.2 Bus-Impedance Methods

These are a family of methods that uses the bus-impedance matrix and equivalent current injections to solve the network equations. The principle of superposition is applied to the bus voltages throughout the network. Two different contributions make up the voltage at a bus- the specified slack bus voltage and the incremental potential due to current injections into the network. Loads and generators are modeled as equivalent current injections. Starting with the assumption of a no-load system, the load bus voltages throughout the network are set equal to the known slack bus voltage, and are then modified using the current flows, which are a function of the connected loads. Since the bus load is a function of the bus voltage, the equivalent current injection is determined iteratively [10, 11, 21].

2.4.1.3 Compensation-Based Power Flow

The compensation-based power flow method is used for solution of weakly meshed distribution systems [16]. In this method, the interconnected grid is split at a number of points (breakpoints) in order to convert it to a radial network. Each breakpoint creates a simple loop. The radial network is

solved efficiently by direct application of KVL and KCL. The flows at the breakpoints are then calculated by injecting currents at their two end-nodes. In the presence of constant P and Q loads, the network is nonlinear and hence requires an iterative compensation process. The solution of the radial network with additional breakpoint current injections completes the solution of the weakly meshed network. This method is extended to a dispersed generation system with PV-node compensation in [22].

2.4.2 Distribution Systems with Presence of DGs

For the last 15 years, distribution generation (DG) has been one of the most attractive subjects for research in power systems. In [23], DG has been defined as, "*as an electric power generation source connected directly to the distribution network or on the customer side of the meter*". Many factors led to the increasing interest in connecting more DGs; there has been a steady growth in electricity demand while the growth in building new assets, such as bulk generation and transmission lines, faces many difficulties, mainly economical. In addition, DG units are always located closer to load center, hence transmission and distribution losses can be reduced. Moreover, the investment risk in DG is not high because the project time is usually small compared to bulk generation projects, the total cost is relatively low and the expected efficiency is typically high.

Because of the growing concern on climate change, the emerging need is for integration of more renewable energy sources into the power system that introduces specific technical challenges. Renewable energy sources, such as wind and solar, are usually characterized by small or medium sizes which are more suitable to be connected to the distribution system.

When WTs are installed in distribution feeders and participate in system operations, the power flow, voltage control, loss reduction and such other issues need to be carefully analyzed. With increased penetration of WTs, reverse power flows may arise and result in unexpected voltage profiles in feeders. Therefore, existent power flow methods need to be modified.

2.4.3 Probabilistic Load Flow

Probabilistic Load Flow (PLF), first proposed in 1974, has been further developed and applied to power system operation, short- and long-term planning, as well as in other areas [24]. PLF requires inputs specified by their PDF or CDF to obtain system states and power flows in terms of PDF or CDF, so that the system uncertainties can be included and reflected in the outcome. PLF can be solved numerically, *i.e.*, using a Monte Carlo method, or analytically, using a convolution method, or

a combination of both [6, 24, 25]. The main concern in the Monte Carlo approach is the need for large number of simulations, while in the analytical approach the complexity of mathematical computations and the accuracy of approximations are important issues. The introduction of DGs has complicated the voltage control of distribution systems. Among others, the steady state voltage rise problem has been identified as one of the most crucial technical difficulties that face the integration of DG into the distribution system.

In Section 2.4, DLF algorithms have been reviewed. The following section reviews the short-term operational problems including inter-hour constrained problems that need a modified wind generation model taking into account wind speed transitions from one hour to the next.

2.5 The Short-Term Power System Operations Problem

The thermal UC problem has been traditionally solved in centralized power systems to determine the start-up and shutdown decisions of thermal generating units and their dispatch to meet the system demand and spinning reserve requirements while satisfying generation constraints (production limits, ramping limits, and minimum up and down times) over a specific time span, so as to minimize the total operation cost. The generation scheduling problems solved by the ISO in current electricity markets [26] are essentially similar but the main difference being that, rather than minimizing operation costs, the ISO maximizes a measure of social welfare, which is a function of market participant bids and offers. The traditional UC problem is described briefly below [27]:

2.5.1 Objective Function

The operator's objective while solving the UC problem is to minimize the total system operation cost. However, because of the extended time-scale of the problem, in addition to the generator's fuel cost, some other cost components are included. The different cost components relevant to an UC program are discussed below.

Fuel Cost: The most common approach has been to use a cost characteristic derived from the heat-rate characteristic and represented by a polynomial function, usually quadratic, and can be written as follows (2.10),

$$C_i = a_i P_i^2 + b_i P_i + c_i \tag{2.10}$$

The quadratic function is usually approximated by a linear function in order to reduce the computation burden of solving a non-linear optimization problem.

Start-up Cost: This component appears in the UC objective function in order to take into account the costs incurred during a start-up operation of the generator. This is most often modeled as a function of the time for which the unit was off-line (2.11).

$$C_{UP,i} = \alpha_i + \beta_i \left(1 - e^{-T_i^{OFF}/\tau_i}\right) \tag{2.11}$$

where α_i is a fixed cost associated with the unit start-up, β_i is the cost involved in a cold start-up of the generator, T_i^{OFF} is the time for which the generator has been off and τ is a time-constant representing the cooling speed of the unit. However, it has been a very common practice to use a constant cost representation for start-up cost in the objective function.

Shut-down Cost: This is not a very significant component compared to other costs. A constant cost representation is generally used and is included when the unit undergoes a shut down.

2.5.2 Constraints in UC Problem:

Demand-Supply Balance- ensures that the operator has scheduled enough generation capacity at a given hour so that the demand at the hour is met.

Minimum-Up and Minimum-Down Time Constraints on Thermal Units- the minimum-uptime constraint ensures that the unit has been committed for a certain minimum number of hours, before it can be shut down; while the minimum down-time constraint ensures the minimum number of hours a unit must be off-line before it can be brought on-line again. These are particularly important constraints for large thermal (including nuclear) generating units.

Generation Limit- describes the allowable range of generation available for scheduling, as defined by the maximum and minimum limits of the unit.

Ramp Rate Constraints on Thermal Units- limits the inter-hour generation changes in a unit and are particularly applicable to coal-based thermal units. While several models of the ramp constraint have been used, these constraints link the generation variables of the previous hour to that of the present hour, and hence introduce a dynamic characteristic in the UC models.

Logic of Status Change- ensures that transitions of the UC states from 0 to 1 (*i.e.* from offline to online, and vice versa) are properly coordinated with the unit start-up and shut-down decisions.

Adequacy Constraint- ensures that enough system capacity is committed so as to meet the system peak demand while also ensuring spinning reserve availability. The *spinning reserve* in the system is a reserve available to the system operator from among its spinning (synchronized & on-line) generators. Therefore, this reserve should typically be available within 10 minutes, from the occurrence of an event, to the operator. The operator has a very important responsibility of

maintaining adequate spinning reserves in the system, not only on a total-MW basis, but also taking care of the location aspect of this reserve, and transmission capacity constraints in the system.

2.5.3 Solving the UC Problem

The UC problem is a nonlinear large-scale mixed-integer programming that has been an active research topic for several years because of the potential savings in operation costs. As a consequence, several solution techniques have been proposed, such as those based on heuristics [28, 29], dynamic programming, mixed-integer linear programming (MILP) [30], Lagrangian relaxation [31], simulated annealing [32], and evolution-inspired approaches [33]. A recent extensive literature survey on UC can be found in [34]. Among the aforementioned methodologies, Lagrangian relaxation is the most widely used approach because of its capability of solving large-scale problems. The main disadvantage of this method is that, due to the non-convexities of the UC problem, heuristic procedures are needed to find feasible solutions, which may be suboptimal. In contrast, the MILP based approaches guarantee convergence to the optimal solution in a finite number of steps [35] while providing a flexible and accurate modeling framework. In addition, during the search of the problem tree, information on the proximity to the optimal solution is available. An efficient MILP solution method, such as the branch-and-cut algorithm has been developed, and commercial solvers with large-scale computational capabilities are currently available. As a consequence, a great deal of attention has been paid to MILP-based approaches.

In [30], MILP was first applied to solve the UC problem. The formulation in [30] is based on the definition of three sets of binary variables to, respectively, model the start-up, shutdown, and on/off states for every unit and every time period. This MILP is extended in [36] to model the self-scheduling problem faced by a single generating unit in an electricity market. Non-convex production costs, time-dependent start-up costs, and inter-temporal constraints such as ramping limits and minimum up and down times are accounted for at the expense of increasing the number of binary variables. For realistic power systems comprising several generators, the models of [30] and [36] require a large number of binary variables. Thus, the resulting MILP problems might be computationally intensive for state-of-the-art implementations of branch-and-cut algorithms. In [37] an alternative mixed-integer linear formulation of the thermal UC problem is presented, requiring a single set of binary variables (one per unit and per period).

In this section, the traditional short-term operation problems is been revisited and the next section reviews the short-term operations problems with wind generation penetration.

2.6 Stochastic UC and Wind Energy Penetration

It can be expected that many problems will arise in renewable energy based hybrid power systems, particularly in system operation and ancillary services management. Daily generation scheduling is a critical task in a modern energy management system. Due to the uncertain nature of wind power, it is widely believed that large wind penetrations would put an increased burden on system operations. One of these issues is the provision of emergency reserve for the system security. In general, the largest proportion of the emergency reserve is carried to cover the loss of the largest generation unit in the system. However, with wind power penetrations increasing in isolated power systems, scheduling of additional emergency reserves will be needed to maintain an adequate level of supply reliability. In addition, maintaining sufficient emergency reserve across several units in the system is much more capable of responding to frequency deviations and system load pickup following a contingency for an isolated system.

The major issue in developing the UC problem formulation is the modeling of the uncertainties, *i.e.*, wind generation and load. In [38] an adaptive particle swarm optimization method is proposed for solving a stochastic UC model using scenario analysis technique proposed in [39], to model the uncertainties. This approach reduces the overall forecast error and also eliminates the dependency on the individual WT. The wind generation and load are considered as two independent random processes.

Solving the stochastic UC problem with a large set of scenarios is computationally too expensive. So an appropriate scenario reduction technique must be used to limit the number of scenarios. A new technique for scenario generation and reduction is proposed in [40]. The scenario reduction process is modeled as a special optimization problem. This method improves the quality of the scenario tree, reduces the modeling error and thus improves the stochastic solution. The stochastic UC problem is solved using a stochastic programming approach in [41] by determining a robust UC schedule common to all scenarios and minimizing the expectation of the daily operating costs over all possible set of scenarios. The volatile nature of wind power generation may impact power system characteristics such as voltages, frequency and generation adequacy which can potentially increase the vulnerability of power systems. Adequacy studies examine the impact of unavailability of wind for an extended period and volatility refers to the smaller and hourly fluctuations of wind [42]. While, the cumulative wind power (representing several wind farms) in a power system might not be intermittent, the power output of a single wind generator is likely to be so, over a 24-h period. There are several techniques for predicting the quantity of intermittent nature of wind power [43] . Although

wind power is predictable to a limited extent, it cannot be forecasted with 100% accuracy for dispatch purposes. Hence, it is possible that the actual wind power would be different from its forecasted value. Wind power forecasting and associated forecasting accuracy issues are important in analyzing its impact on power system operation. Likewise, the volatility of wind power could have a tremendous impact on power system operations, which poses new challenges for the electricity market management [37].

In [44] a simulation method based on wind speed time-series for dealing with volatile wind generation is applied to the security-constrained economic dispatch algorithm to investigate its impact on thermal generation UC and dispatch. A statistical interpolation method applies the aggregated wind power generation to UC and economic dispatch [45]. It has been shown in [46] that by explicitly taking into account the stochastic nature of wind in the UC algorithm, more robust schedules are produced.

2.7 Overview of Electricity Markets

2.7.1 UMP versus LMP Electricity Markets

As per Federal Energy Regulatory Commissions [FERC] standard market design protocols, most electricity markets in US have adopted the Locational Marginal Pricing (LMP) auction mechanism whereas the two functioning markets in Canada (Ontario and Alberta) have adopted the Unified Market Pricing (UMP) auction. In both LMP and UMP, the market operator receives energy bids from producers and customers and determines the market clearing price and actual dispatch of every participant. The target is to maximize the social welfare.

The market operator uses a clearing procedure to determine the accepted and unaccepted energy bids, which is effectively the same as the UC tool in centralized power systems. The market clearing procedure provides, for every interval of the market horizon: market clearing price, defined as the price of the most expensive accepted generating energy bid; set of committed and de-committed units and associated power outputs from committed generators. The system price is obtained by stacking the supply bids in increasing order of prices and the demand bids in decreasing order of their prices. The system price and the amount of energy cleared for trading is obtained from the crossing point of these curves as shown in Figure 2-3.

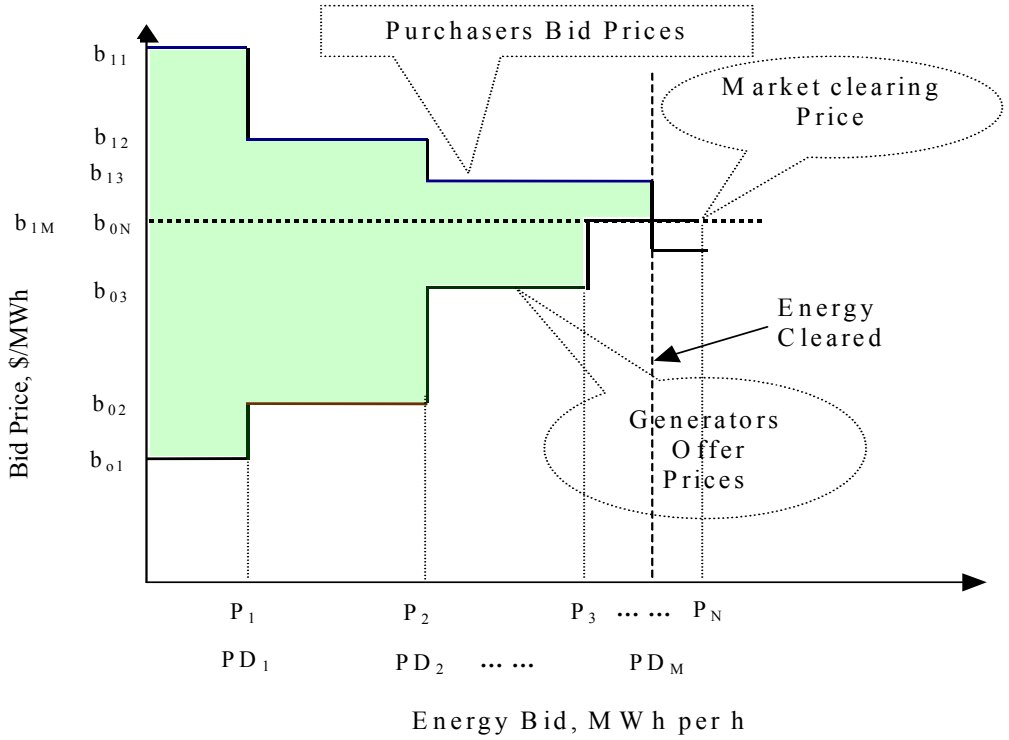

Figure 2-3 Market settlement in double auction power pools [27]

Figure 2-3 shows the typical market clearing process wherein the shaded area denotes the social welfare from market based operation that the market operator seeks to maximize.

In order to properly take into account the inter-temporal constraints, a multi-period market clearing procedure is needed. The data required by the market clearing procedure is the bid information provided by market participants. The economic bidding information provided by any generating unit for every hour consists of a set of energy blocks and their corresponding prices. A generator may also complement this simple bid information by declaring a start-up price. The constraint bidding information that any generating unit may provide for every hour consists of minimum up time, minimum down time, ramp-up and ramp-down limits, start-up and shunt-down ramp rates.

Reference [47] proposes the use of Lagrangian relaxation technique to solve the market dispatch problem. However, this method presents relevant shortcomings associated with the fact that the problem which is solved is the dual of the original problem [48]. The dual problem usually has many similar solutions in terms of objective function value which are different in terms of scheduling variables. Another model of a stochastic UC problem in a pool market with uncertain market prices is

solved using Lagrange relaxation, stochastic dynamic programming, and Benders decomposition in [49].

2.7.2 Market Clearing Dispatch with Wind Power Generation

The effect of intermittency and volatility of wind power generation on LMP markets is discussed in [42], wherein a method is proposed for solving the UC problem with the forecasted intermittent wind power generation. Possible scenarios of wind power generation are simulated for representing wind power variability.

The performance of multi-stage optimization models depends heavily on the quality of the underlying scenario model, describing the uncertain processes influencing the objective function. Moreover, solving the UC problem with a large set of scenarios is computationally expensive. Some recent works are reported on implementing different methods for scenario generation and reduction. In [50], Monte Carlo Simulations (MCS) for scenario generation are discussed. These methods are based on sparse grids and optimal quantization and they provide some convergence based on multivariate integration.

In [51], an optimal scenario reduction method is proposed to determine the scenario subset of prescribed cardinality. A probability measure is used to determine the set that is closest to the initial distribution, in terms of a natural probability metric.

In [52], the scenario reduction problem is modeled as an optimization problem that approximates a given distribution with a distance function. The resulting optimization problem is viewed as a multi-dimensional facility location problem, and is solved using heuristic algorithms.

Moreover, the participation of wind generation in electricity pools compulsorily yields a certain volume of imbalances that would not occur if only conventional units are on the market. Combining wind generation with conventional means or storage allows one to lower the amount of imbalances on the market. For instance, combined wind-storage systems are studied in [53], and the possibility of combining wind and hydro power generation is considered in [54-56].

2.8 Short-term Power System Operations with Environmental Constraints

As widely acknowledged, energy consumption is one of the most reliable indicators of the development and quality of life and the need to satisfy a forecasted energy demand, over a certain time period, is the basis of energy planning. With increased awareness of global climate change,

policy makers are promoting renewable energy sources, such as wind generation, as a means of meeting emissions reduction targets.

At present, thermal power plants, which account for the great majority of generating installations over the world are being operated under a number of constraints with regard to fuel quality and operating conditions, and so forth as a measure against air pollution [50]. These constraints are in accordance with the Air Pollution Control Act and agreements with each local government [51]. Consequently, conventional methods of load dispatching to minimize the total fuel cost have become more and more difficult to implement.

The Air Pollution Control Act limits the air pollutants SO_2, NO_x by regulating the pollutant concentration in fuel ducts. In addition to this act, agreements [52] with local governments often impose additional regulations on such factors as fuel quality, amounts of pollutants emitted per hour, and power output cut down when a severe photochemical smog occurs. These agreement controls have become severer year by year due to an ever-increasing desire of local inhabitants for clean air.

In the literature many researchers have attempted to find the optimum generation schedules that minimize the total operation and generation costs while satisfying emission and others system constraints. In [57] a method is developed for obtaining the optimal mix of high and low sulphur fuels for uses such as electric utilities and large industrial complexes. The mix is determined so that the environmental limits are met and plant operating schedules are fully maintained. The problem is formulated in a minimum energy with penalty function format and well known optimal control methods are applied to obtain the solution. In [58] an optimization method is used to determine economic load dispatching and also the optimum mix ratio of high- and low-sulphur fuels (fuel mix), when a constraint is imposed on total sulphur dioxide emission per hour.

In [59] the economical operation of cogeneration system is studied under emission constraints. It attempts to control the production of atmospheric emissions such as NO_x and SO_x caused by the operation of fossil-fuelled thermal generation. For a more effective operation, many operational strategies have been developed in [60, 61]. Co-generation systems have to operate efficiently according to the system schedule. Various fuels, such as Fuel Oil, Liquid Nature Gas, and coal are available for dispatch. The optimal operating strategy determines the optimal distribution among the in-plant generations, fuels dispatch, and energy purchase to minimize the overall energy cost for a given electric and steam demand while satisfying the system constraints.

In [61] a bottom-up energy system optimization model is proposed in order to support planning policies for promoting the use of renewable energy sources. A linear programming

optimization methodology based on the energy flow optimization model is adopted, detailing the primary energy sources exploitation (including biomass, solid waste, and process by-products), power and heat generation, emissions and end-use sectors. The modeling framework is enhanced in order to adapt the model to the characteristics and requirements of the region under investigation.

The effect of wind energy penetration on electrical system emissions is discussed in [21], the Irish electricity system is studied, wind generation operated in a system that incorporates wind generation forecasts in its dispatch decisions provides superior emission reduction benefits over a system that simply accommodates wind generation when it is available. With increasing levels of installed wind capacity, CO_2 is reduced; however, to significantly reduce emissions of SO_2 and NO_x, wind generation must be combined with alternative emission reduction measures such as alteration in the treatment of peat fired plant, or load reduction schemes. The optimization model discussed in [21] neglects inter-hour generation constraints (such as minimum down time and minimum up time constraints). These constraints will greatly affect the solution of the problem due to the hour-to-hour correlations of wind speed.

It becomes increasingly important to develop realistic environmental evaluation techniques that are practically useful for electric power energy sector that are expected to include a rapidly growing proportion of wind generation in the coming years. The benefits from wind sources are largely dictated by the wind regime at the wind farm site. It is, therefore, very important to obtain suitable wind speed simulation models and appropriate techniques to develop power generation model for WFs to get their environmental impact.

2.9 Summary

The brief review of literature presented in this chapter shows that some research work has been undertaken to incorporate wind generation sources within distribution and transmission systems. The distribution load flow models and short-term operational models of power systems which include UC programs have been discussed extensively. Modeling the uncertain behavior of wind, and the consequent uncertain production profile is a challenging problem when considering a connection of WT or WF to distribution system or transmission system respectively.

Chapter 3
Wind Modeling in Distribution Systems

3.1 Introduction

In the previous chapter, different DLF methods are reviewed and it is concluded that there is an essential need to modify these methods to include the stochastic behavior of wind power generation. This chapter presents a set of new Probabilistic Distribution Load Flow (PDLF) formulations that include a probabilistic WT model. This model can be used to analyze the effects of wind generation on the distribution system. The PDLF is solved using the forward-backward sweep algorithm [62] and the analysis provides insight into the effects on system losses, voltage regulation and sub-station power import/export in the presence of WT units at different locations. WTs may use different types of rotating generators or control topologies which consequently determine the characteristic of their output power. In this work, three different classes of WT models are considered within the PDLF:

Model-1: Constant power factor WTs

Model-2: Induction generator WTs

Model-3: Constant voltage WTs

All the above models are derived and integrated within the PDLF to examine and compare their performance. The main objectives of this chapter are summarized as follows:

a. Develop a probabilistic representation of WT model, considering the WT output power as a random variable function of wind speed.
b. Propose a novel formulation of the PDLF by modifying the traditional formulations of DLF to include the developed probabilistic model of WT.
c. Develop different PDLF formulations, considering different WT models, as listed above.
d. Solve the three different probabilistic models, individually and simultaneously, then study the effect of WT generation penetration on feeder losses, voltage profile and sub-station powers.

3.2 Probabilistic Wind Model

In this work, the novel feature of probabilistic wind modelling is that the wind output power P_w is considered to be a random variable, as a function of another random variable, the wind speed ω. The fundamental theorem of calculating the PDF of a random variable [63] is applied to determine the probability $p(P_w)$ of the active power produced by WTs when the probability distribution of the wind

speed is known. From Figure 2-2 and (2.5), it follows that for a given hour in the 24-hour cycle, the WT production falls into one of the following categories:

a. *For* $P_w=0$, when $0 \le \omega \le \omega_{cut-in}$ *and* $\omega \ge \omega_{cut-out}$

$p(P_w=0)=p(\omega \le \omega_{cut\text{-}in})+p(\omega \ge \omega_{cut\text{-}out}) = F(\omega_{cut\text{-}in})+(1-F(\omega_{cut\text{-}out}))$

b. *For* $P_w=P_{rated}$, when $\omega_{rated} \le \omega \le \omega_{cut-out}$

$p(P_w=P_{rated})=p(\omega_{rated} \le \omega \le \omega_{cut\text{-}out}) = F(\omega_{cut\text{-}out})-F(\omega_{rated})$

c. *For* $P_w=k(\omega)$, when $\omega_{cut-in} \le \omega \le \omega_{rated}$

For wind speed variations in the interval $\omega_{n-1} \le \omega \le \omega_n$, the corresponding active power produced by WT ranges between P_{n-1} *and* P_n, respectively. The probability of generating P_w, which is the average of P_{n-1} and P_n is $p(P_w)$ and can be approximated as (3.1):

$$p(P_w = \frac{P_{n-1}+P_n}{2}) = p(\omega_{n-1} \le \omega \le \omega_n) = F(\omega_n) - F(\omega_{n-1}) \tag{3.1}$$

Thus by dividing the closed interval $[0, P_{rated}]$ in which the active power produced by the WT can be considered in N-2 segments, the PDF of P_w can modeled as a discrete distribution with N discrete values each having a probability $p(P_w)$, as defined in (a), (b), and (c) above. These N values of P_w and their corresponding probabilities can be considered independent levels of wind generation. In this work, N=30 is considered.

Since the random variable P_w is a function, where $P_w: \omega \in \mathbb{R}$, this random variable can be composed with a function $h:\mathbb{R} \to \mathbb{R}$. The resulting new function $h \circ P_w : \omega \to \mathbb{R}$ is a new random variable denoted by $h(P_w)$, *i.e.,* $h(P_w(\omega))$. For example, in the following description of the WT Models, the reactive power Q_w for Model-1 is a function of P_w, so $Q_w=h(P_w(\omega))$is a random variable, the PDF of Q_w can be computed from the PDF of P_w as in (3.2):

$$\begin{aligned} P(Q_w \in B) &= P(\{\omega \in \Omega : Q_w(\omega) \in B\}) \\ &= P(\{\omega \in \Omega : h(P_w(\omega)) \in B\}) \\ &= P(\{\omega \in \Omega : P_w(\omega) \in h^{-1}(B)\}) \\ &= P(P_w \in h^{-1}(B)) \end{aligned} \tag{3.2}$$

In (3.2), $h^{-1}(B) = \{r \in \mathbb{R}: h(r) \in B\}$ and r is a real number. If P_w is a discrete random variable, so using (3.2), the relation between the PDF of P_w and the PDF of Q_w can be computed as in (3.3):

$$f_{Q_w}(q_w) = P(Q_w = q_w) = P(h(P_w) = q_w)$$
$$= P(P_w \in h^{-1}(\{q_w\})) = \sum_{p_w : h(p_w) = q_w} f_{P_w}(p_w) \tag{3.3}$$

3.3 Proposed PDLFs with Different WT Models

The novel feature of the proposed PDLF algorithm is that it includes P_w as a random variable, and consequently the state-of-the art distribution load flow model needs to be modified to include P_w.

3.3.1 Model-1: Constant Power Factor WTs

The constant power factor WT model, which is the most commonly used and can be used for power electronics based WTs, the reactive power can be adjusted by controlling the WT trigger angles. Knowing the required power factor (pf_{WT}), which is almost unity for most utilities, the random variable representing the reactive power Q_w can be calculated as follows (3.4):

$$Q_w(\omega) = P_w(\omega) \times \tan(\cos^{-1}(pf_{WT})) \tag{3.4}$$

In (3.4), P_w is a random variable representing the WT real power and pf_{WT} is the power factor for WT installed at bus *i.* Using the PDF of P_w from Section 3.2, the PDF of Q_w can be obtained using (3.2, 3.3).

This active and reactive power of the WT will be subtracted from the load at the connected bus of the WT. The injected apparent power at the WT connected bus is thus given by (3.5), as:

$$S_w(\omega) = (P_w(\omega) - P_{load}) + j(Q_w(\omega) - Q_{load}) \tag{3.5}$$

Backward Sweep: the nodal current injected in iteration k, at node i, $I_i^{(k)}$, is calculated as in (3.6),

$$I_i^{(k)}(\omega) = \left(\frac{S_i}{V_i^{(k-1)}(\omega)} \right)^* - Y_i V_i^{(k-1)}(\omega) \quad \forall\, i = 1,2,\ldots,n \tag{3.6}$$

In (3.6), $V_i^{(k-1)}(\omega)$ is the bus voltage random variable during the *(k-1)* iteration and S_i is the specified power injected at node i and Y_i is the sum of all the shunt elements connected to node *i.* In iteration k, starting from the branches that are connected to end nodes and moving towards the branches connected to the substation node, the current in branch L, given by I_L, is calculated as in (3.7):

$$I_L^{(k)}(\omega) = -I_i^{(k)}(\omega) + \sum_{m \in L} I_m(\omega) \quad \forall\, L = b, b-1, \ldots, 1 \tag{3.7}$$

In (3.7), I_m is the sum of the currents in all branches, b, connected to bus i.

Forward Sweep: Nodal voltages are updated in a forward sweep from branches connected to substation node toward the end nodes. For each branch L, the voltage at node *i* is calculated using the updated voltage at the previous node and branch currents are calculated in the preceding backward sweep as follows:

$$V_i^{(k)}(\omega) = V_h^{(k)}(\omega) - Z_L I_L^{(k)}(\omega) \qquad \forall \;\; L = 1,2,...,b \tag{3.8}$$

In (3.8), Z_L is the series impedance of branch L. The previous steps are repeated until convergence is achieved.

3.3.2 Model-2: Induction Generator WTs

By using a squirrel cage induction generator based WT, and knowing the active power P_w, the reactive power output can be formulated as a function of the real output power, bus voltage, and generator impedances as given in (3.9) [64].

$$Q_w(\omega) = \frac{X_c - X_m}{X_c X_m}(V_i(\omega))^2 + \frac{X}{(V_i(\omega))^2} P_w^2(\omega) \tag{3.9}$$

In (3.9), $V_i(\omega)$ is the bus voltage random variable, X is the sum of the stator and rotor leakage reactances, X_c is the reactance of the capacitors bank while X_m is reactance of the induction generator. The same procedure, as in Model-1 WT, is applied to solve for the voltages iteratively using (16)-(19). The only exception here is to update the value of Q_w using (3.9), after iteration is completed. It should be noted that Q_w for Model-2 is a function of two random variables V_i and P_w *i.e.* $Q_w = d(V_i, P_w)$. When, an iteration of backward-forward sweep is completed, the PDF of V_i is obtained, which is used in (3.9) to obtain the PDF of Q_w, as follows:

- Find $f_1(Q_w|V)$ by transformations, V is fixed, using (3.10).

$$f_1(Q_w|V) = f_{P_w}(P_w).\left|\frac{dP_w}{dQ_w}\right| \tag{3.10}$$

where $P_w = d^{-1}(Q_w)$

- Obtain the joint density of Q_w and V, which is $f_1(Q_w, V) = f_1(Q_w|V) f_V(V)$
- Then obtain the PDF of Q_w by integrating joint density over V as in (3.11):

$$f_{Q_w}(Q_w) = \int_{-\infty}^{\infty} f_1(Q_w \mid V)\, f_V(V)\, dV \tag{3.11}$$

3.3.3 Model-3: Constant Voltage WTs

In this WT model, the bus at which the WT is connected is modeled as a *P-V* node, where *V* is fixed at a specific value. The compensation-based method for power flow analysis uses a *P-V* node sensitivity matrix to eliminate the voltage magnitude mismatch for all *PV* nodes. The following steps describe the novel probabilistic compensation-based method for Model-3 WT:

1) Construct *PV* node sensitivity matrix Z_V. The wind generator of the *PV* node is disconnected. In Z_V, the diagonal elements are sum of the impedances of lines which can be formed from the *PV* node to the feeder node and the off-diagonal elements are the sum of impedances in the lines connecting two *PV* nodes (if any).
2) Perform backward current and forward voltage sweep iterations, as discussed earlier. If the maximum power mismatch at all buses is less than the power convergence criterion, then proceed to the next step.
3) Calculate *PV* node voltage mismatch ΔV_i. For *PV* node *i*

$$\Delta V_i(\omega) = V_i(\omega) - V_{i,specified} \tag{3.12}$$

In (3.12), $V_{i,specified}$ is the magnitude of specified voltage at node *i* and $V_i(\omega)$ is the voltage at the *PV* node of the final iteration of Step-2. If the maximum *PV* node voltage mismatch is greater than the *PV* node voltage convergence criterion ε, update *PV* node current injection $I_{q,i}(\omega)$ using the following equations (3.13 and 3.14) and then go to Step- 2, otherwise, the final power flow solution is obtained.

$$\Delta I_{q,i}(\omega) = [Z_V]^{-1} \Delta V_i(\omega) \tag{3.13}$$

$$I_{q,i}(\omega) = \left|\Delta I_{q,i}(\omega)\right| \times e^{j(\frac{\pi}{2} + \delta_{v_i}(\omega))} \tag{3.14}$$

This random variable $I_{q,i}(\omega)$, is representing the current added to or subtracted from the load current at bus *i* based on the sign of $\Delta V_i(\omega)$. If $\Delta V_i(\omega)$ is negative, less reactive power generation is injected into the *PV* node while if $\Delta V_i(\omega)$ is positive, more reactive power generation is injected into *PV* node.

In any iteration *k*, the change of the reactive power injection required by the WT at bus *i*, ΔQ_w, to maintain its voltage at a specific value can be calculated using (3.15),

$$\Delta Q_w(\omega) = \frac{Q_i^{k-1}(\omega) - Q_i^{k-2}(\omega)}{\left|V_i^{k-1}(\omega)\right| - \left|V_i^{k-2}(\omega)\right|} \left[\left|V_{i,specified}\right| - \left|V_i^{k-1}(\omega)\right|\right] \tag{3.15}$$

This model is used for large scale controllable WTs, the specified values for this model are P_w and bus voltage magnitude. A capacity cap is imposed on the WT rated apparent power.

$$\sqrt{P_w^2(\omega) + Q_w^2(\omega)} \leq S_w(\omega) \tag{3.16}$$

This type of WT requires special treatment in power flow analysis to maintain its voltage magnitude as well as to monitor its reactive power capability.

This formulation of Model-3 WT is a nonlinear programming (NLP) problem with an objective function of minimizing the error mismatch between the specified voltage at the WT-bus and the bus voltage calculated from the iterations, as in (3.12). The model constraints ensure that other bus voltages are within a specified range and the complex power injected meets the capacity cap of the WT.

The three WT models discussed earlier are now integrated with the PDLF with all the proposed changes, considering the wind output active and reactive power as random variables.

3.4 Distribution System Case Study Description

In this section, the three models of WTs are connected to the IEEE 33-bus distribution system at different locations. These locations are the remote buses (18, 25 and 33). Different wind speed profiles extracted from [65] are used to mimic the wind speed variations at the selected buses. A clustering technique will be applied in Section 3.4.2 to get the hourly PDF of wind speed for a specific month.

3.4.1 System under Study

A case-study is presented considering the 33-bus distribution system shown in Figure 3-1. The complete data of this system can be found in [52, 66] (Appendix A). Although the selection of location of WT generators is entirely arbitrary in this work, there is no loss of generality. In a real-life, the WT generators would be located at a bus after carrying out detailed planning studies and techno-economic validation, which is beyond the scope of this thesis. The WTs are considered to be located at one of the remote buses (bus-18, 25 or 33). It is to be noted that the proposed PDLF can be applied to a 3-phase unbalanced distribution system also, by carrying out a detailed modeling of the system.

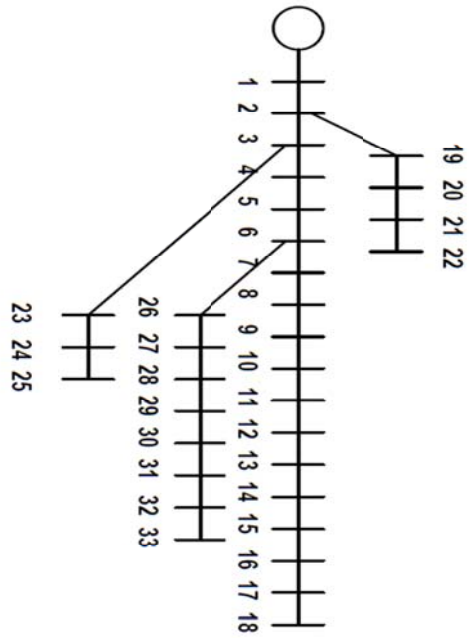

Figure 3-1 IEEE 33-bus distribution system with WT.

Model-1 and Model-2 are solved using MATLAB with error tolerance not to exceed 0.001 for all voltages at all buses, while Model-3 is a non-linear programming problem, and is solved using the MINOS NLP solver in GAMS [51]. When a single WT is considered, all three WT models are examined individually, and it is assumed that the WT is connected at bus-18, 25, or 33, at a time. When three WTs are considered connected simultaneously, it is assumed that WT at bus-18 is of Model-1 type, at bus-25 and bus-33 are of Model-2 and Model-3 types, respectively.

3.4.2 Wind Speed Data Clustering

Wind speed data clustering is carried out using three different data sets, extracted from [65]. These wind speed profiles mimic those at buses 18, 25 and 33. Different data mining techniques are applied to study the wind speed correlation between the three buses. The spatial, temporal and auto correlations between the three buses are calculated to determine the conditional probabilities and joint probabilities, these probabilities are used later in Section 3.5.2, when three WTs are connected at the remote buses simultaneously. The wind speed data is clustered into 12 monthly sets, one for each month, based on the clustering technique proposed by the authors in [67], wherein it is shown that monthly clustering results in a better correlation than daily or yearly clustering. Figure 3-2 shows the

average wind speed at the different buses for July. Using the mean, standard deviation of the clustered wind speed and (2.1), the scale and shape indices are calculated (Table 3-1), for a particular hour (*i.e.*, 6 PM) in each month. It should be noted that for the rest of this study, the wind speed profile for July is considered.

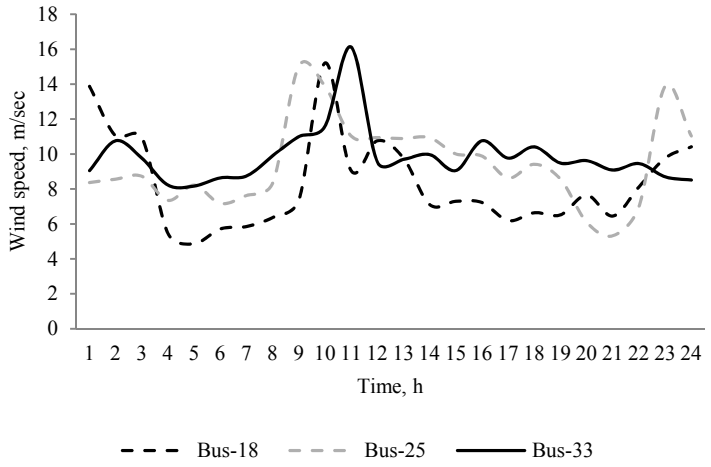

Figure 3-2 Hourly mean wind speed profile at different buses for July

Table 3-1 Wind speed Parameters at 6 PM

	shape index (r)			scale index (c)		
	Bus-18	Bus-25	Bus-33	Bus-18	Bus-25	Bus-33
Jan	1.93	2.26	2.21	5.52	7.50	7.35
Feb	1.95	2.24	2.20	5.87	7.43	7.58
Mar	2.38	2.69	2.63	6.09	7.53	7.57
Apr	2.18	2.52	2.53	6.73	8.17	7.70
May	2.16	2.74	2.70	5.89	7.74	7.09
Jun	1.90	2.25	2.29	5.66	7.13	7.11
Jul	1.72	1.90	2.10	5.14	6.67	6.88
Aug	1.85	2.07	2.15	5.00	7.17	6.86
Sep	1.98	2.37	2.20	6.89	9.21	8.98
Oct	2.16	2.47	2.71	6.54	9.31	9.55
Nov	1.69	2.18	2.06	5.85	8.43	8.28
Dec	1.52	1.87	1.77	6.06	8.47	7.97

Using (2.1), and the values from Table 3-1, the PDFs at 6 PM for wind speed profiles at the three buses are shown in Figure 3-3

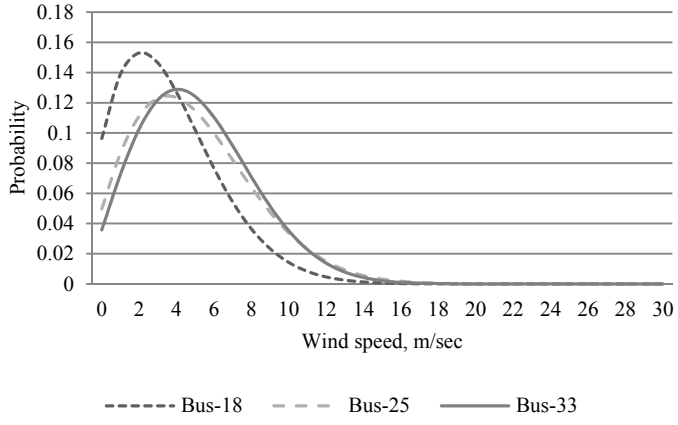

Figure 3-3 PDFs for wind speed profiles for different WTs at 6 PM

3.5 Analysis and Results

The solution of the PDLF is carried out considering Model-1 WT and then compared with the DLF solution obtained using the WT as a deterministic source with a capacity factor (i.e. 0.3), which is the common practice by many utilities, calculated from historical data. It is assumed that the WT is connected at bus-18. Figure 3-4 shows a comparison of the voltage profiles for the above two cases. The voltages at buses 1-5 and 19-22 are very close to each other in both cases, whereas for other buses there is a considerable difference between the two approaches.

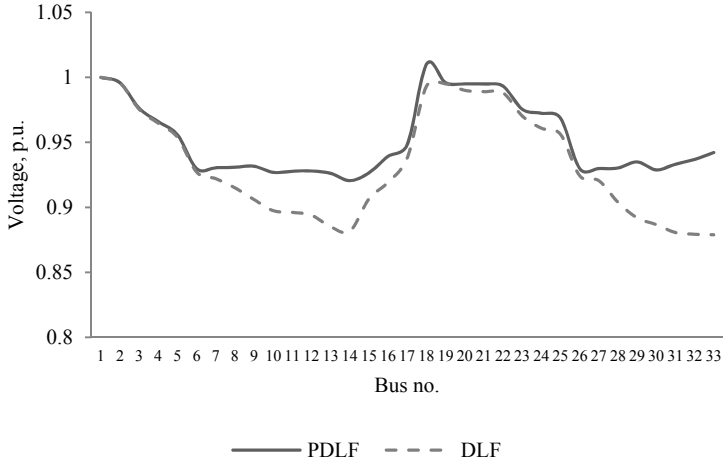

Figure 3-4 Expected bus voltage profile with PDLF compared to that with DLF

The PDFs of the bus voltage random variables (Figure 3-5) are obtained by solving the PDLF, with the WT injecting power at bus-18. This is one of the characteristics of the PDLF solution where all the PDFs of the system random variables can be computed. Afterwards, these PDFs are used to obtain the expected value of all system variables (the expected voltages of buses 18, 25 and 33 are given in Table 3-2). In the rest of the results presented in the following sub-sections, comparisons are made between expected values for different WT models, with their different locations.

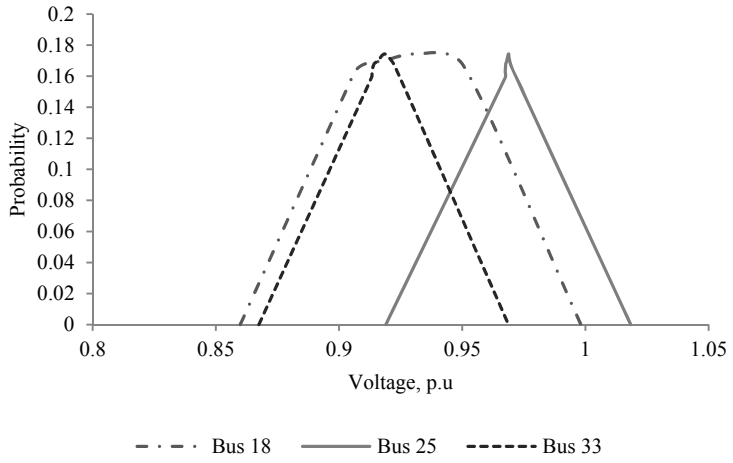

Figure 3-5 PDF of remote bus voltages when Model-1 WT is connected at bus-18

Figure 3-6 shows the PDF for the total system loss, which can be used to calculate total expected loss of (0.016 p.u.), as per Table 3-2, in the distribution system when Model-1 WT is connected at bus-18. Another comparison is made between the results obtained from PDLF, DLF with WT as a deterministic source, and DLF with actual wind speed data (Table 3-2). It is observed that the bus voltages resulting from the PDLF are very close to those obtained using DLF with one snap shot of the historical data. Table 3-2 shows a sample set of bus voltages at remote buses, V_{18}, V_{25} and V_{33}. The power loss calculated using DLF is almost two times that of the actual value.

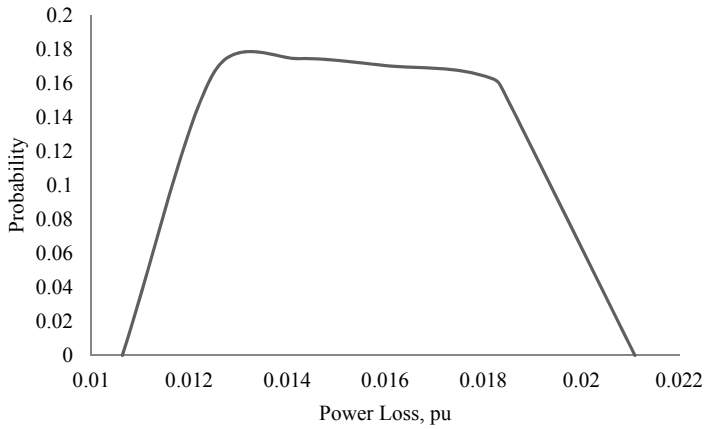

Figure 3-6 PDF for total distribution loss when WT is connected at bus-18

Table 3-2 DLF Solution by Different Methods (pu)

	Model–1 (WT at 18)		
	DLF	PDLF	Historical
V_{18}, pu	0.993	1.010*	0.998
$V_{25,}$ pu	0.956	0.968*	0.966
V_{33}, pu	0.878	0.942*	0.931
Power loss, pu	0.042	0.016*	0.019
Sub. Power, P, pu	0.462	0.368*	0.372
Sub. Reactive power, Q, pu	0.312	0.240*	0.251

(*) Denotes expected values

Furthermore, a comparison between solving the PDLF using the proposed algorithm, solving the PDLF using MCS, and solving the DLF with a capacity factor deterministically is presented. Table 3-3 shows the summary of results and it can be observed how the proposed algorithm is fast and efficient with less number of iterations. The maximum error is the maximum difference between voltages attained from different algorithms compared with the voltages from the solution of DLF using the historical data. It is to be noted that the proposed algorithm results is the minimum error.

Table 3-3 Comparison of Solutions by Different Methods (pu)

	Proposed PDLF		PDLF (MCS)		DLF	
	Model-1	All	Model-1	All	Model-1	All
Iterations[1]	134	352	276*	1363*	20	234
CPU time, s	32.23	51.31	78.13	122	1.26	22.12
Max error in bus voltage	4.1%	5.2%	5.76%	7.31%	16.23%	25.34%

[1] Total Iterations in Sweep Algorithm
* This denotes total iterations on N samples of MCS

3.5.1 Study of Single WT: Different Models and Locations

The PDLF calculations are carried out using the three different models of WT, discussed in Section 3.3. The WTs are tested at different remote buses. In the following discussions, the results obtaining using Model-1 (most common type of WT) are illustrated separately, followed by a comparison of the three models.

The distribution system has traditionally been designed as a one-directional passive system, *i.e.* the power flows from the substation towards the loads. The inclusion of WTs as a distributed generation source has changed the design philosophy of the distribution system because of the reverse power in the system, so all protection system, relays, and switching devices should accept and adapt this reverse power. When a WT injects power at a node, the voltage at this node rises. The voltage difference between the node where the WT is connected and the adjacent node, V_i - V_w, can be written in per unit as $\Delta V = PR + QX$. If the Model-1 WT injects active power, P_w, into the system, the voltage difference can be re-written as, $V_i - V_w = (P - P_w)R + QX$. It is clear that the voltage at the injection node rises, depending on the WT injected power. Accordingly, Figure 3-7 shows the expected bus voltages at the three remote buses when Model-1 WT injects power at buses-18, 25 and 33 individually. It is observed that the expected voltage at a bus attains the best profile, when a WT is connected to it.

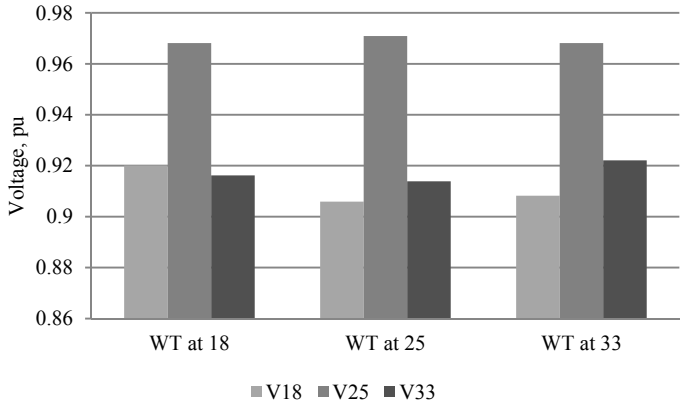

Figure 3-7 Expected voltages for different locations of Model-1 WT

Using PDLF runs, a comparison is made between the three different WT models located at different buses. It is observed from Figure 3-8 that Model-2 WT has a better expected voltage profile than Model-1 and Model-3 because of its ability to inject reactive power (Q_w) without a pre-defined voltage set-point. From the earlier definition of voltage drop between adjacent buses, for Model-1 and Model-2, (3.17) and (3.18):

$$\Delta V_{Model-1} = (P - P_w)R + QX, \tag{3.17}$$

$$\Delta V_{Model-2} = (P - P'_w)R + (Q - Q_w)X \tag{3.18}$$

where $P'_w = \sqrt{(P_w^2 - Q_w^2)}$.

From the above two voltage drop equations and given that R>X, it can be concluded that $\Delta V_{Model-1} > \Delta V_{Model-2}$. Therefore, the voltage profile resulting with Model-2 WT is better than that with the Model-1 WT. For Model-3 WT, the voltage is pre-specified to be at a fixed value of the sub-station voltage of 1 p.u. This requirement of fixed voltage, limits the voltage regulating capability of the WT bus when compared to Model-2 WT, in which the voltage has no pre-defined set point.

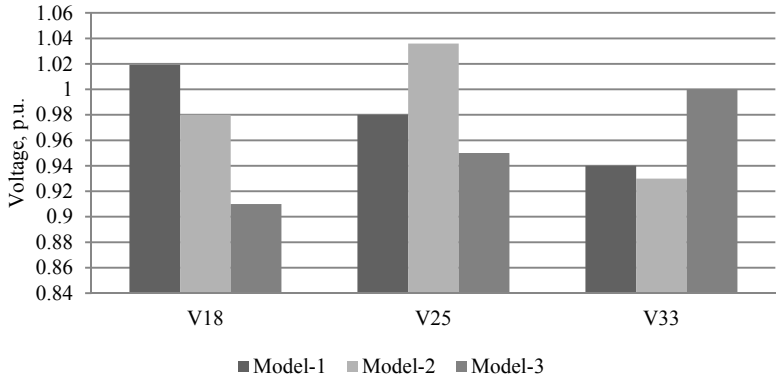

Figure 3-8 Expected bus voltages for different WT models at bus-18

Figure 3-9 shows the substation power export/import at different wind speeds for the three WT models. It is observed that the Local Distribution Company (LDC) imports power from the external grid when the wind speed is less than 9 m/s or greater than 23 m/s. On the other hand it exports power when the wind speed lies in the above range. It is also noted that with WT Model-3, the LDC requires more power to import and has less power to export, because, part of the WT apparent power is used to maintain the voltage at the connected bus at the fixed value.

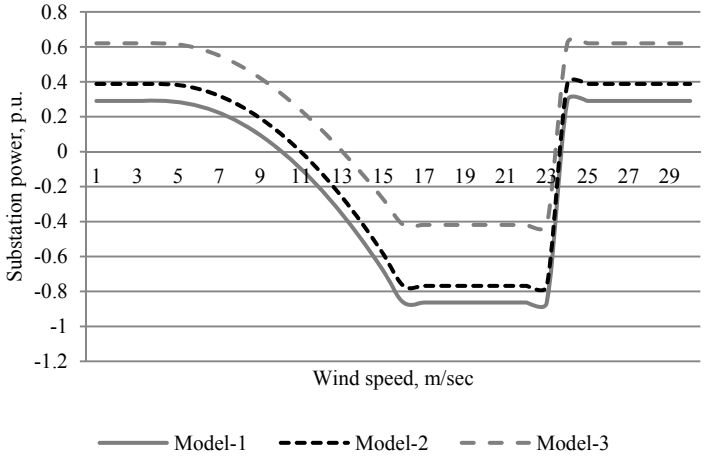

Figure 3-9 Power transferred over substation transformer (Positive: import, Negative: export)

The PDF for substation power import/export of Model-1 WTs at two different hours (1:00 AM and 6:00 PM) are shown in Figure 3-10. Since the wind speed PDFs change from hour to hour, the resultant expected values for the sub-station power also changes on an hourly basis. Table IV shows the expected power imported/exported by the sub-station considering different WT models. It is

observed from Table 3-4 that the power exported by the LDC is maximum at 1 AM considering the Model-1 WT, when there is excessive wind speed and light load conditions.

Meanwhile, the power imported by LDCs attains a maximum at 6 PM with Model-2 WT. On the other hand, the sub-station is always importing reactive power and the lowest imported value at 6 PM is when Model-2 WT is connected. This is due to the fact that Model-2 WT injects reactive power as function of the active power, and thus, the reactive power is higher than the reactive power injected by Model-3 WT because it has a fixed voltage that limits the injection of its reactive power.

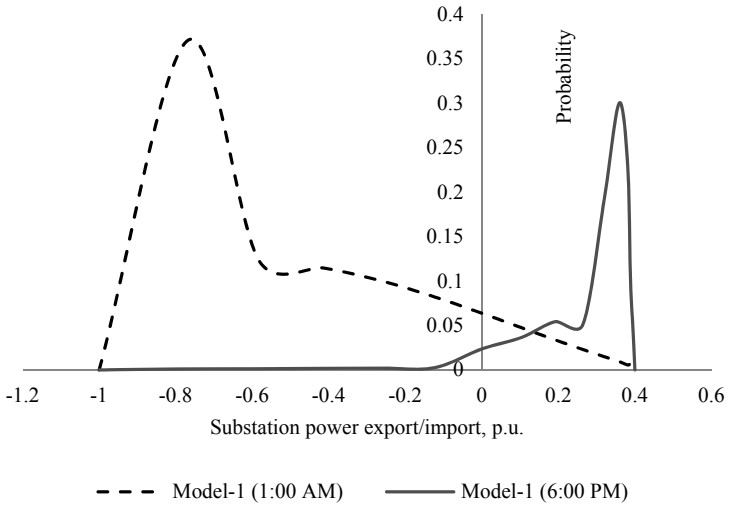

Figure 3-10 PDF of substation power considering Model-1 WT

Table 3-4 Substation Expected Power

	Model-1		Model-2		Model-3	
	1:00 AM	6:00 PM	1:00 AM	6:00 PM	1:00 AM	6:00 PM
Expected Active Power	-0.41	0.34	-0.25	0.43	-0.13	0.38
Expected Reactive Power	0.18	0.41	0.12	0.32	0.16	0.35

3.5.2 Connection of Multiple WTs

In the previous subsection, the case of connection of a single WT of Model-1, Model-2 or Model-3 one at a time to a distribution system is studied. This section presents the case of multiple WTs of different models that are connected simultaneously to the distribution system.

Wind speeds vary in the range 0-30 m/sec, which is classified into 30 levels, denoted by ω_{Level}, as in Section 3.2. With three different WTs connected simultaneously as shown in Figure 3-11, and each having 30 wind speed divisions, the possible number of combinations, *scenarios* (denoted by index *s*), of gross wind penetration will be too large (30 x 30 x 30), *i.e.*, *s = 27,000*.

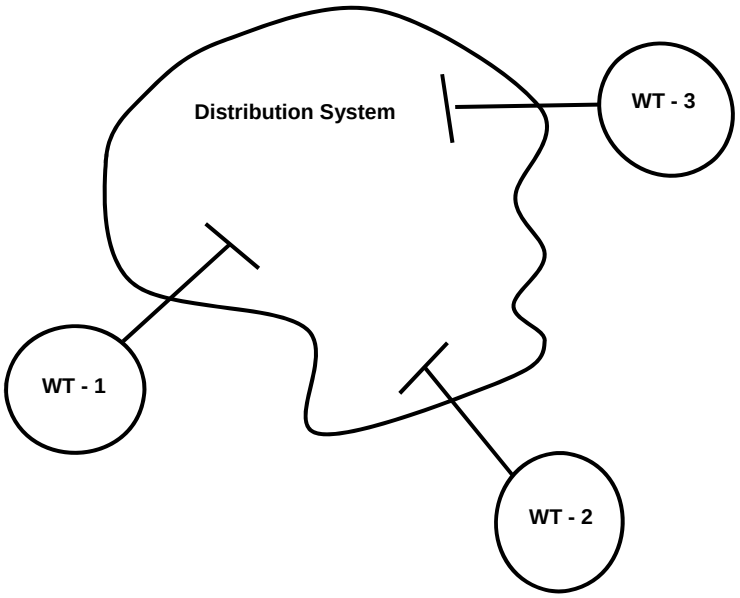

Figure 3-11 Three WTs connected simultaneously to the distribution system

In order to reduce the computational burden, the 30 wind speed levels are re-classified into four levels by re-defining the ranges of wind speed appropriately (Table 3-5), as [67]:

Level-1: 0 m/s $\leq \omega \leq$ 4 m/s and 25 m/s $< \omega \leq$ 30 m/s

Level-2: 4 m/s $< \omega \leq$ 11 m/s

Level-3: 11 m/s $< \omega \leq$ 14 m/s

Level-4: 14 m/s $< \omega \leq$ 25 m/s

Level-1 denotes WT operation below the cut-in speed or above the cut-out speed, when the output power is zero. Level-4 denotes the WT operation at the 90% of the rated output power. Levels 2 and 3 are the intermediate ranges of operation of the WT that give 15% and 50% average active

power respectively of the rated capacity of WT. This classification helps to reduce the number of scenarios to (4 x 4 x 4), *i.e.*, *S = 64*, since each WT may operate in any of the four wind speed levels.

Table 3-5 Proposed wind speed levels

ω (m/sec)	P_{out} (MW)	P_{out} (%)	Levels
0-4	0	0	Level 1
4-5	0.003	0.51	Level 2
5-6	0.014	2.45	
6-7	0.034	5.81	
7-8	0.063	10.59	
8-9	0.100	16.79	
9-10	0.146	24.41	
10-11	0.200	33.45	
11-12	0.263	43.92	Level 3
12-13	0.334	55.81	
13-14	0.414	69.11	
14-15	0.503	83.84	Level 4
14-25	0.6	100	
25-30	0	0	Level 1

The probability of a given ω_{Level}, denoted by $p(\omega_{Level})$, is calculated as (3.19):

$$p(\omega_{Level}) = \int_{\omega_{lower}}^{\omega_{upper}} f(\omega).d\omega \qquad (3.19)$$

In (3.19), ω_{upper} and ω_{lower} are the upper and lower ranges respectively, of each wind speed level.

The expected power generation associated with the new wind speed levels is calculated using (3.20) as:

$$E\{P_w(\omega_{Level})\} = \int_{-\infty}^{\infty} P_w(\omega_{Level}).f(\omega_{Level})\,dP_w \qquad (3.20)$$

To validate the accuracy of the above approximation, a comparison is made between the bus voltages obtained using a PDLF (with 30 levels of wind speed), a PDLF (with 4 levels of wind speed) and a DLF (with deterministic wind capacity factor), considering that one WT of Model-1 is connected at bus-18 (Figure 3-12). It is observed that the bus voltages resulting from the PDLF

solutions are superior to those obtained from the DLF; and that the PDLF (4 level) voltage profile is close to that obtained using the PDLF (30 level).

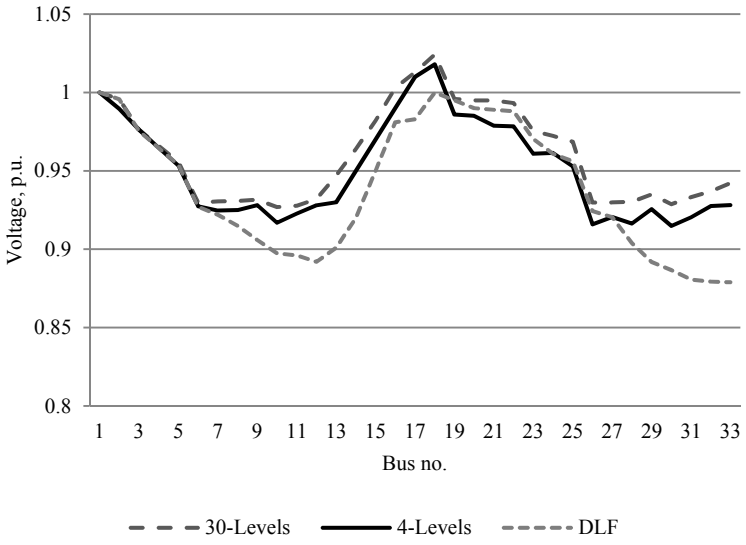

Figure 3-12 Expected bus voltage profile with PDLF (30 & 4) Levels compared to that with DLF

Different power generation scenarios can be represented as (3.21):

$$s = \left\{P_{WT_1}(\omega_{Levelx}),\, P_{WT_2}(\omega_{Levely}),\, P_{WT_3}(\omega_{Levelz})\right\} \tag{3.21}$$

As mentioned before, there will be $s = 64$ expected power generation scenarios, which can be represented as:

$$s_1 = \left\{P_{WT_1}(\omega_{Level\ -1}),\, P_{WT_2}(\omega_{Level\ -1}),\, P_{WT_3}(\omega_{Level\ -1})\right\},\ s_2 = \left\{P_{WT_1}(\omega_{Level\ -1}),\, P_{WT_2}(\omega_{Level\ -1}),\, P_{WT_3}(\omega_{Level\ -2})\right\}$$

$$s_3 = \left\{P_{WT_1}(\omega_{Level\ -1}),\, P_{WT_2}(\omega_{Level\ -1}),\, P_{WT_3}(\omega_{Level\ -3})\right\},\ldots,\ s_{64} = \left\{P_{WT_1}(\omega_{Level\ -4}),\, P_{WT_2}(\omega_{Level\ -4}),\, P_{WT_3}(\omega_{Level\ -4})\right\}$$

Corresponding to each scenario s, a probability of occurrence of s, given by λ_s is determined using the conditional and joint probabilities (Section 3.4.2) as given by (3.22)-(3.23):

$$\begin{aligned}\lambda_s &= P(\omega_{Level_x,WT\,1}\ and\ \omega_{Level_y,WT\,2}\ and\ \omega_{Level_z,WT\,3}) \\ &= P(\omega_{Level_x,WT\,1}\,|\,\omega_{Level_y,WT\,2}\ and\ \omega_{Level_z,WT\,3})\,\lambda_\alpha\end{aligned} \tag{3.22}$$

where,

$$\begin{aligned}\lambda_\alpha &= P(\omega_{Level_y,WT\,2}\ and\ \omega_{Level_z,WT\,3}) \\ &= P(\omega_{Level_y,WT\,2}\,|\,\omega_{Level_z,WT\,3})\,P(\omega_{Level_z,WT\,3})\end{aligned} \tag{3.23}$$

The above model comprises three WTs connected simultaneously to the distribution system. The total model is solved using GAMS MINOS solver. The capacity of each WT is reduced to 200 kW to

result in the same connected rated capacity of 600 kW, as was considered in Section 3.5.1. The simultaneous modeling of the three WTs is complicated, and the proposed algorithm can solve the system with a maximum error of 5.2% when compared to the DLF with actual data. The optimization solver requires 51.31 seconds to solve the system (Table 3-3). Figure 3-13 shows the voltage profile when all the three WTs are connected simultaneously. It can be observed that the width of the window of voltage variation is the best when all WTs are connected together.

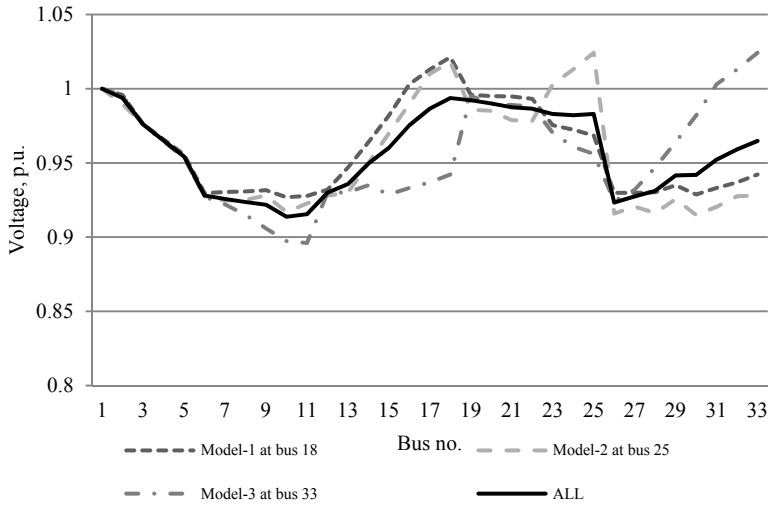

Figure 3-13 Expected voltage profile for different cases.

3.6 Summary

This chapter presents a probabilistic distribution load flow model to examine the effects of wind generation at various remote buses in a radial distribution system. Details of the probabilistic distribution load flow mathematical model including wind turbine models are presented. The proposed models are applied to steady-state analysis of a realistic distribution feeder with dispersed wind generation in order to assess the effects of wind turbine operation on distribution power loss and voltage profiles. Test results show that the proposed method can be effectively and efficiently used to analyze the penetration of wind turbines to distribution feeders.

Chapter 4
Short-Term Operation of Power System with Wind Generation Penetration

4.1 Introduction

In the previous chapter, a probabilistic WT model is developed. This probabilistic model can be used for solving distribution load flow problems at specific hour when the distribution system has one or more WTs. When it comes to short-term operation problems that include inter-hour constraints, a more sophisticated wind generation model is needed to track not only the changes of wind speed at a specific hour but also the transition correlations of wind speed from one hour to the next. This chapter presents a mathematical modeling framework to examine the effect of wind generation on short-term power systems operations. The work considers penetration of wind generation sources using a stochastic wind speed profile to obtain different scenarios of wind power generation. A new scenario generation and reduction technique is proposed to be applied for analysing the effects of wind generation variability on short-term power system operation with particular emphasis on electricity market prices using MCS and Markov-chain model. A UC-type model that includes dc-load flow equations to represent the transmission system and congestion issues is developed for this study. Subsequently, an LMP energy market model is also developed by incorporating the different reduced scenarios of wind power generation. The model include unit commitment constraints, transmission constraints and wind generation effects to examine the impact of wind generation on price settlement, load dispatch, and reserve requirements. The work further examines how the LMP markets are affected by wind farm capacity and when wake effect is considered.

The main objectives of this chapter are summarized as follows:

- Propose a clustering and classification technique for developing a wind speed model for WF.
- Apply MCS using the clustered wind speed model for a WF, to generate a large set of wind generation scenarios.
- Use Markov-Chain model to improve the correlation between the inter-hour changes of the wind speed variations.
- Develop a scenario reduction technique using *Forward Selection Algorithm* to obtain a reduced set of wind generation scenarios.

- Incorporate the reduced set of scenarios into an LMP based electricity market settlement and dispatch model to examine the effects of wind generation on various market variables and on system operation.
- Extend the analysis to include the *wake-effect*, *i.e.*, to take into account the differing impact of wind speed incidence on each wind turbine arising from their layout, and hence study the impact on electricity market variables and on system operation.

4.2 Problem Formulation

A central challenge of large-scale wind integration is the ability to absorb the wind generation with a thermal fleet of reduced flexibility. One measure of the system's ability to absorb wind is the wind uncertainty cost, which is the extra cost of operating the system due to the short-term wind uncertainty. Simple statistical analysis cannot determine this cost, because the dispatchable elements, which balance the wind intermittency, are subject to inter-temporal constraints that limit their responsiveness. Examples of these constraints are start-up times for thermal generators, and limitations to the amount of storable energy. In order to understand the effect that these limitations have on the system's ability to absorb wind, the scheduling of the entire system must be simulated in the time domain, accounting for the inter-temporal constraints at some level. The costs of integrating wind are assessed using time-domain simulation in a number of studies, as summarized in [68].

Time-domain scheduling simulation is the most effective tool for simulating the operational costs in wind-integrated power systems, because it can represent the inter-temporal constraints that limit the balancing actions of the thermal plant, storage, and demand-side measures. High wind penetrations demand just-in-time commitment decisions that reflect the uncertainties in the wind penetration, so that it is desirable to generate the scheduling decisions using unit commitment (UC) with rolling planning. However, the computational burden can make such methods impractical in long simulations. In this work, an efficient formulation of the UC problem is presented that is designed for use in scheduling simulations of power systems. Unlike traditional UC techniques, the proposed formulation uses a simple and efficient scenario generation and reduction structure that simulates the inter-hour transition correlations using Markov-chains. The proposed method compare favorably with scenario tree tool.

The contributions of this work are twofold. First, a new formulation of the UC problem that allows an efficient representation of simplified, large-scale power systems in scheduling simulations

is presented. Second, scenario reduction can be constructed so as to avoid the need for explicit reserve constraints against the wind output uncertainty.

In this work, it has been assumed that all commitment and dispatch decisions are made by an SO who seeks to maximize the system operating social welfare using mixed integer linear programming to optimize the schedules. For simplicity, only wind power uncertainty is assumed. The wind realization is generated using an aggregated wind model developed later, in Section 4.4. The sudden nature of generator failures requires extra fast-acting primary reserves that are not modeled here. It is possible in this work to build up scenarios of arbitrary complexity that span the full range of the forecast error distribution. Including scenarios that cover the worst-case tail of the distribution allows the UC to be solved without explicit reserve constraints. In this work, the number of decision variables and constraints is reduced by assuming a linear fuel usage. Ramp rate constraints are presented as they tend to be active with an hourly time-step in conventional generators. The proposed model accounts for all inter-temporal generator constraints.

4.3 Mathematical Model

4.3.1 Objective Function

The stochastic LMP market model is formulated with the objective of maximizing the social welfare (J_s), as in (4.1):

$$J_{s\in S} = \sum_{k\in K}\sum_{i\in I}\sum_{h=1}^{N_i} \gamma_{h,i,k} \times H_{h,i,k} - \sum_{k\in K}\sum_{j\in J}\left(c^u_{j,k} + c^d_{j,k} + \sum_{\ell=1}^{M_j} \mu_{\ell,j,k} \times step_{\ell,j,k} \right) \tag{4.1}$$

The first term in (4.1) represents the gross surplus of customers, where a customer at bus i has a biddable power to buy $PD_{i,k}$ at interval k. A step load model is assumed with N_i steps, where each load block h has a bid price $\gamma_{h,i,k}$ and quantity $Q_{h,i,k}$, as given by (4.2)-(4.3).

$$PD_{i,k} = \sum_{h=1}^{N_i} H_{h,i,k} \quad , \forall i \in I, \forall k \in K, \ \forall h = 1 \cdots N_i \tag{4.2}$$

$$H_{h,i,k} \le Q_{h,i,k} \tag{4.3}$$

The last term in (4.1) denotes the total cost of gencos, where each generator j has a biddable power to sell $P_{j,k}$ at interval k. For every generator, a step generation model with M_j steps is used, each generated power block ℓ has an offer price $\mu_{\ell,j,k}$ and quantity $F_{\ell,j,k}$, as given by (4.4)-(4.5).

$$P_{j,k} = \sum_{\ell=1}^{M_j} step_{\ell,j,k} + P_j^{\min} v_{j,k}, \ \forall j \in J, \forall k \in K, \quad \forall \ell = 1 \cdots M_j \tag{4.4}$$

$$step_{\ell,j,k} \leq F_{\ell,j,k} \tag{4.5}$$

In (4.1), $c_{j,k}^{u}$ is the start-up cost of a generator represented by an exponential start-up cost function [37]. Since the time span is discretized into intervals, the start-up cost also needs to be a discrete function. The discrete start-up cost is asymptotically approximated by a staircase function. A mixed-integer linear formulation for the staircase start-up cost, proposed in [37, 69] is used in this work, as given in (4.6).

$$c_{j,k}^{u} \geq K_j^{t}[v_{j,k} - \sum_{t} v_{j,k-t}] \ , \ \forall j \in J, \forall k \in K, \ \ \forall t = 1 \cdots ND_j \tag{4.6}$$

In (4.1), $c_{j,k}^{d}$ is the shut-down cost of a generator, a constant shut-down cost C_j is assigned if unit *j* is brought to offline at interval *k*. Constraint (4.7) depicts the equivalent formulation for the shut-down cost.

$$c_{j,k}^{d} \geq C_j[v_{j,k-1} - v_{j,k}], \forall j \in J, \forall k \in K \tag{4.7}$$

4.3.2 Model Constraints

Demand Supply Balance: Constraint (4.8) ensures that the total generation from generating units including WF generation contribution, is able to meet the forecasted demand of interval *k*. It is to be noted that the WF generation contributions, $P_{w_{i_w},k}$, in (4.8) are obtained from the reduced set of scenarios that will be discussed in Section 4.4.4.

$$\left(\sum_{j \in E_i} P_{j,k} \right) - PD_{i,k} + P_{w_{i_w},k} = \sum_{q \in I} B_{i,q} \times [\delta_{i,k} - \delta_{q,k}] \tag{4.8}$$

Transmission Constraint: Constraint (4.9) ensures that the power transfer on a transmission line is within the specified limit

$$B_{i,q}[\delta_{i,k} - \delta_{q,k}] \leq \overline{P}_{TL_{i,m}} \tag{4.9}$$

Spinning Reserve Constraint: Constraint (4.10) ensures that the total maximum available output power from all committed generators meets the system demand and spinning reserve allocations at interval *k*.

$$\sum_{j \in J} \overline{P}_{j,k} \geq \sum_{i \in I} PD_{i,k} + R_k \tag{4.10}$$

Generation Limits: Constraint (4.11) ensures that the output power of a generator at an interval k is bounded by its upper and lower limits.

$$P_j^{\min} v_{j,k} \leq P_{j,k} \leq P_j^{\max} v_{j,k} \ , \quad \forall j \in J, \quad \forall k \in K \tag{4.11}$$

Hydro-Generation Constraint: Constraint (4.12) ensures that the total energy generated from each hydro station over a period of 24-hours is less than the total stored energy.

$$\sum_{k \in K} P_{hydro,k} \leq P_{hydro}^{rated} \times 24 \times CF \tag{4.12}$$

Ramp-up and Start-up Ramp Rate Constraint: Constraint (4.13) ensures that the inter-hour generation changes are within the limits specified by generator ramping-up capabilities. It also ensures that when a unit status changes from OFF-state to ON-state, the ON-state generation should be within the specified start-up ramp-rate.

$$P_{j,k} \leq P_{j,k-1} + RU_j v_{j,k-1} + SU_j [v_{j,k} - v_{j,k-1}], \ \ \forall j \in J, \ \forall k \in K \tag{4.13}$$

Shut-down Ramp Rate Constraint: Constraint (4.14) ensures that when a unit status changes from ON-state to OFF-state, the last ON-state generation should be within the specified shut-down ramp-rate.

$$\overline{P}_{j,k} \leq P_j^{\max} v_{j,k+1} + SD_j [v_{j,k} - v_{j,k+1}], \quad \forall j \in J, \quad \forall k = 1 \cdots \beta - 1 \tag{4.14}$$

Ramp-down and Shut-down Ramp Rate Constraint: Constraint (4.15) ensures that the inter-hour generation changes are within the limits specified by generator ramping-down capabilities.

$$P_{j,k-1} - P_{j,k} \leq RD_j v_{j,k} + SD_j [v_{j,k-1} - v_{j,k}], \ \forall j \in J, \ \ \forall k \in K \tag{4.15}$$

Minimum Up-time Constraints: Constraints (4.16)-(4.19) ensure that when a generator is brought online, it remains in the ON-state for a certain minimum number of hours before it can be shut-down.

$$\sum_{k=1}^{U_j} [1 - v_{j,k}] = 0, \quad \forall j \in J \tag{4.16}$$

$$\sum_{n=k}^{k+UT_j-1} v_{j,n} \geq UT_j [v_{j,k} - v_{j,k-1}], \ \ \forall j \in J, \ \ \forall k = U_j + 1 \cdots \beta - UT_j + 1 \tag{4.17}$$

$$\sum_{n=k}^{\beta} \left\{ v_{j,n} - [v_{j,k} - v_{j,k-1}] \right\} \geq 0, \quad \forall j \in J, \quad \forall k = \beta - UT_j + 2 \cdots \beta \tag{4.18}$$

$$U_j = Min\left\{\beta, [UT_j - U_j^0]V_j^0\right\} \tag{4.19}$$

Minimum Down-time Constraints: Constraints (4.20)-(4.23) ensure that when a generator is brought offline, it remains in the OFF-state for a certain minimum number of hours before it can be start-up.

$$\sum_{k=1}^{D_j} v_{j,k} = 0, \quad \forall j \in J \tag{4.20}$$

$$\sum_{n=k}^{k+DT_j-1}[1-v_{j,n}] \geq DT_j[v_{j,k-1} - v_{j,k}], \quad \forall j \in J, \qquad \forall k = D_j + 1 \cdots \beta - DT_j + 1 \tag{4.21}$$

$$\sum_{n=k}^{\beta}\left\{1 - v_{j,n} - [v_{j,k-1} - v_{j,k}]\right\} \geq 0, \quad \forall j \in J, \qquad \forall k = \beta - DT_j + 2 \cdots \beta \tag{4.22}$$

$$D_j = Min\left\{\beta, [DT_j - D_j^0][1 - V_j^0]\right\} \tag{4.23}$$

The LMP market model is a mixed integer linear programming model and is solved using the CPLEX solver in GAMS [64].

4.4 Stochastic Wind Generation Model

This section presents the clustering of wind speed data for three WF sites. The wind speed data used in this work has been extracted from [65]. These data, which is available over a year on an hourly basis, is clustered into 12 groups, one for each month. For the rest of the study the wind speed data for month of July is used to model the WFs. Figure 4-1. shows the hourly mean wind speed profile for July for the three WFs.

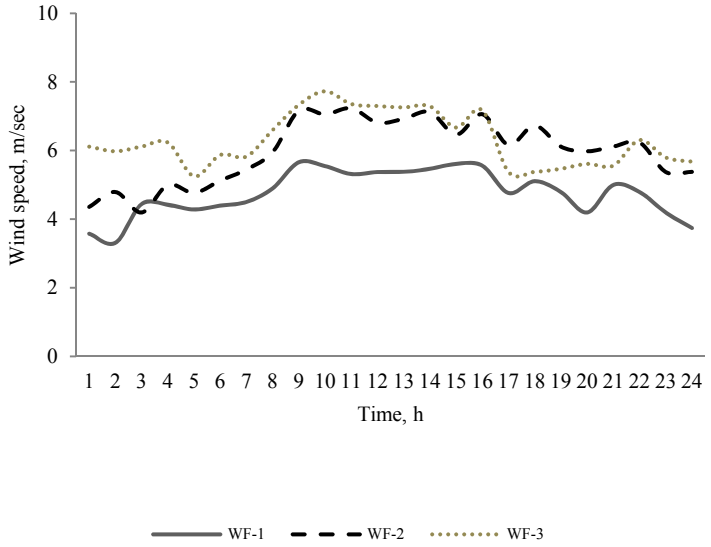

Figure 4-1 Hourly mean wind speed profile for different sites in July

Historical, hourly, wind speed data ($\omega_{iw,k,d,m,y}$) is clustered to develop a typical daily wind speed profile for each month for a WF connected at bus i_w. A monthly wind speed profile is obtained by averaging the wind speed for each hour of the month ($\varpi_{iw,k,m}$), over the entire data set of T years (4.24). Subsequently, the hourly standard deviation of the monthly wind speed profile ($\sigma_{iw,k,m}$) is obtained using (4.25).

$$\varpi_{i_w,k,m} = \frac{\sum_{y=1}^{T}\sum_{d=1}^{Dm} \omega_{i_w,k,d,m}}{D_m \times T} \tag{4.24}$$

$$\sigma_{i_w,k,m} = \sqrt{\frac{1}{D_m \times T}\sum_{y=1}^{T}\sum_{d=1}^{Dm} (\omega_{i_w,k,d,m,y} - \varpi_{i_w,k,m})^2} \tag{4.25}$$

From (4.24), (4.25), and using (2.2)-(2.3) the shape index $r_{k,m}$ and the scale index $c_{k,m}$ of the clustered wind speed PDF for each hour, of a given month, is obtained. The corresponding CDF for the clustered wind speed PDF is obtained from (2.4). Using (2.1) and hourly mean wind speed values (Figure 4-1), 24-hourly PDFs can be developed for each WF. Figure 4-2 shows the PDFs at 5 PM, for three sites (WF-1, WF-2 and WF-3), while Figure 4-3 shows the PDFs for 5 PM, 6 PM and 7 PM at WF-3 site.

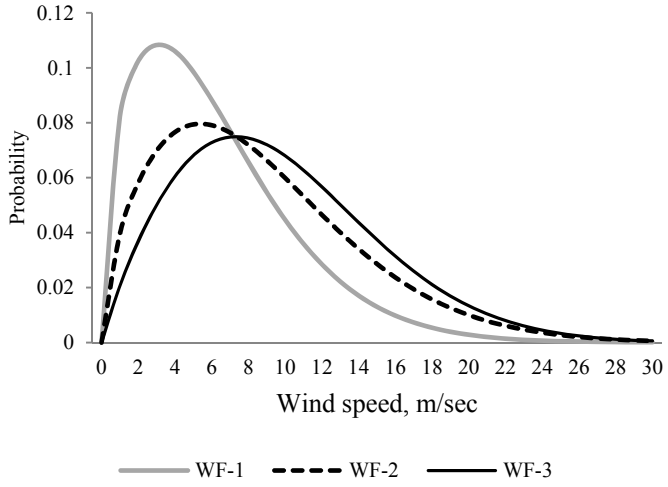

Figure 4-2 Clustered wind speed PDFs for three WFs at 7 PM.

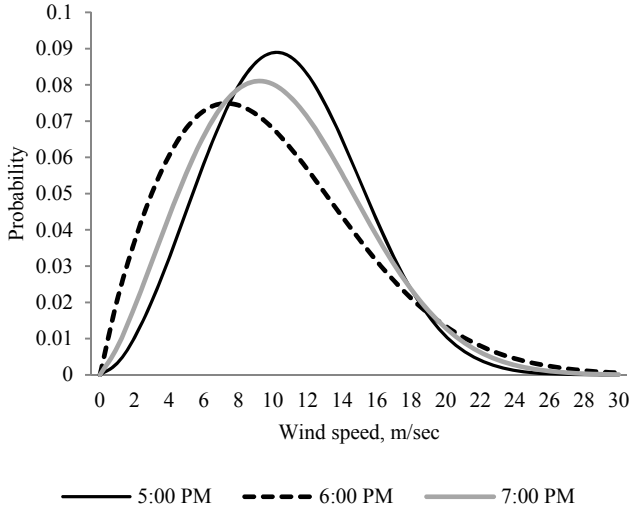

Figure 4-3 Clustered wind speed PDFs at WF-3 site at 5, 6 and 7 PM.

4.4.1 Monte-Carlo Simulation

The Monte-Carlo Simulation method requires a sequential string of wind speed data which can be generated either from historical data or synthetically. In this work, the wind speed data are generated synthetically using CDF. The CDF of the clustered wind speed profile, F(ϖ), and hence the function [1-F(ϖ)] will lie in the range [0,1]. By considering F(ϖ) to be a uniformly distributed random variable

in [0,1], MCS can be carried out to arrive at a large set of wind speed values for each hour, $\omega_{iw,k,n}$, $\forall$ n $\in$ N, using (2.4).

This procedure is repeated for each hour to generate N, 24-hour wind speed profiles for each WF. In order to reach the desired accuracy, the MCS stops after N simulated scenarios, when the ratio of standard deviation of the sample mean of wind speed at given hour of interest to the sample mean of the same hourly wind speed becomes less than certain predetermined tolerance (ε).

Thereafter, the WF output power for each wind speed profile is calculated using (2.5). Let $\bar{P}_{w_{i_w,n}}$ is a vector that represent the 24-hour wind generation profile for a scenario *n* which can be defined as (4.26):

$$\overline{P}_{w_{i_w,n}} = [P_{w_{i_w,k=1,n}}, P_{w_{i_w,k=2,n}}, ..., P_{w_{i_w,k=24,n}}] \quad (4.26)$$

This is a combination of the 24-hour WF power generation samples together for the interval under study to form N, 24-hour generation profiles (*i.e.* scenarios). Figure 4-4 describes the steps for wind scenario generation algorithm.

4.4.2 Markov Chain Improvement of Inter-Hour Changes of Wind Speed

For improving the generating of sequences of wind speed states for a specific wind speed vector at a given hour, wind speed vectors are those produced using MCS in previous section to generate large number of samples, $\omega_{iw,k,n}$, for each hour. The Markov-chain transition matrices are used in this section order to include the inter-hour transition correlation to form a better correlated 24-hour daily profiles.

4.4.2.1 Markov-Chain Model

For the Markov-Chain process, the probability of the given condition in the given moment may be deduced from information about the preceding conditions. A Markov chain represents a system of elements moving from one state to another over time. The order of the chain gives the number of time steps in the past influencing the probability distribution of the present state, which can be greater than one. Many natural processes are considered as Markov processes.

In fact, the probability transition matrix is a tool for describing the Markov chains' behavior. Each element of the matrix represents probability of passage from a specific condition to a next state. The Markov chain modeling approach has frequently been used for the synthetic generation of rainfall data. In [70] and [71] used and recommended a first order Markov chain model to generate annual rainfall data. In [72] compared performance of stochastic approaches for forecasting river

water quality. However, very little work has been done on the synthetic generation of wind speed data using Markov chain models as reported in [73].

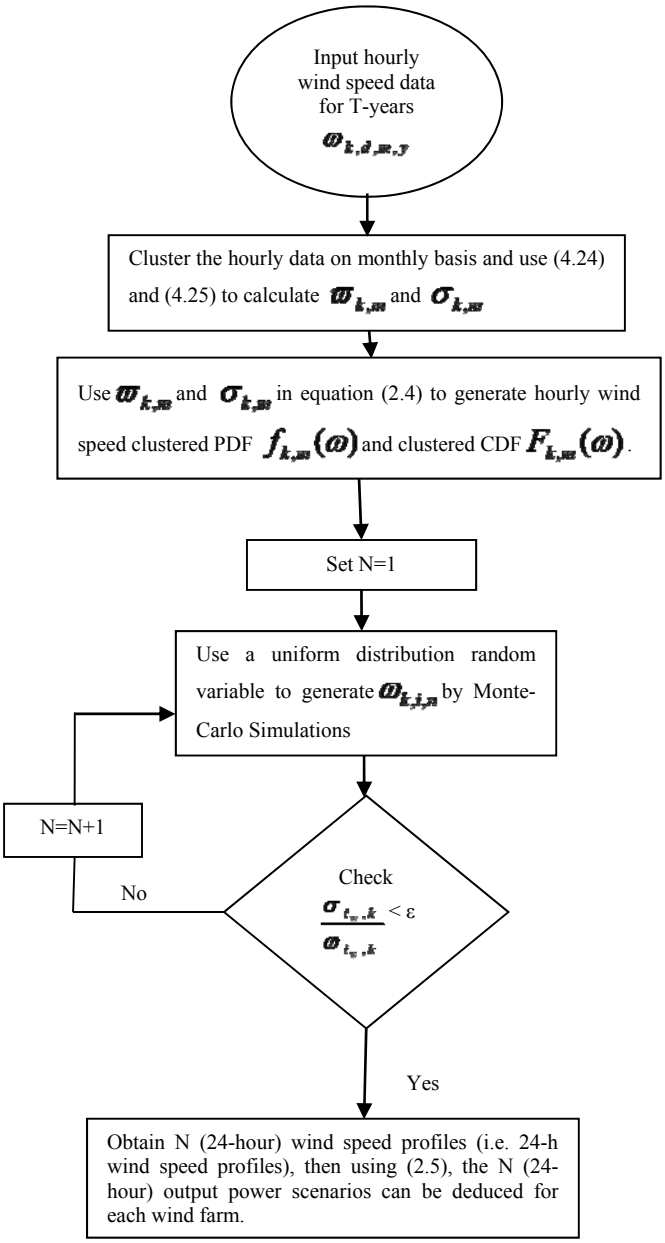

Figure 4-4 Flowchart for the proposed MCS scenario generation

In [74] compared alternative approaches including first and second Markov chain models, and embedded Markov chain model for the synthetic generation of wind speed time series using the

wind speed data for a short period. References [73] and [75] used first order Markov chain models for synthetic generation of hourly wind speed time series. A first order Markov chain model is generally used for modeling and simulation of wind speed data. In this section, Markov-chain is used to improve the inter-hour changes of wind speed to improve the generation of the wind scenarios discussed in Section 4.4.2.

Markov chains are stochastic processes that can be parameterized by empirically estimating transition probabilities between discrete states in the observed systems [71]. The Markov chain of the first order is one for which each subsequent state depends only on the immediately preceding one. Let *X(t)* be a stochastic process, possessing discrete state space *S={1,2,..., K}*. In general, for a given sequence of time points $t_1<t_2<t_3<\ldots<t_{n-1}<t_n$, the conditional probabilities should be [76] (4.27):

$$\Pr\{X(t_n)=i_n \,|\, X(t_1)=i_1,\ldots, X(t_{n-1})=i_{n-1}\} = \Pr\{X(t_n)=i_n \,|\, X(t_{n-1})=i_{n-1}\} \qquad (4.27)$$

The conditional probabilities $\Pr\{X(t)=j \,|\, X(s)=i\} = P_{ij}(s,t)$ are called transition probabilities of order $r=t-s$ from state i to state j for all indices $0 \le s \le t$, *with* $1 \le i$ *and* $j \le k$. Number of states in this parts are 50 states (*i.e.* k=50). They are denoted as the transition matrix *P*. For k states, the first order transition matrix *P* has a size of $k \times k$ and takes the form (4.28):

$$P = \begin{bmatrix} p_{1,1} & p_{1,2} & \cdots\cdots & p_{1,k} \\ p_{2,1} & p_{2,2} & \cdots\cdots & p_{2,k} \\ \cdot & & & \\ \cdot & & & \\ \cdot & & & \\ p_{k,1} & p_{k,2} & \cdots\cdots & p_{k,k} \end{bmatrix} \qquad (4.28)$$

The state probabilities at time t can be estimated from the relative frequencies of the k states. Different transition matrices (*i.e.* 24 transition matrices) are developed from the historical available data. If n_{ij} is the number of the transitions from state i to state j in the sequence of speed data, the maximum likelihood estimates of the transition probabilities is (4.29):

$$p_{ij} = \frac{n_{ij}}{\sum_j n_{ij}} \qquad (4.29)$$

The transition probabilities of any state vary between 0 and 1. The summation of transition probabilities in a row equals one. Mathematically, it can be expressed as (4.30):

$$\sum_j p_{ij} = 1 \qquad (4.30)$$

For evaluating the validity of the Markov chain for wind speed hourly data, the following properties of the Markov chains are tested [77].

4.4.2.1.1 Dependency Test

The Markov chain properties can be tested statistically by checking whether the successive events are independent or dependent on each other. They form Markov chains if they are dependent [77]. For successive events to be independent, the statistic α, mathematically defined by (4.31):

$$\alpha = 2\sum_{i,j}^{k} n_{ij} \ln \frac{p_{ij}}{p_j} \tag{4.31}$$

is distributed asymptotically as χ^2 having $(k\text{-}1)^2$ degrees of freedom. In probability theory and statistics, the chi-squared distribution (χ^2-distribution) with k degrees of freedom is the distribution of a sum of the squares of k independent standard normal random variables. It is one of the most widely used probability distributions in inferential statistics, e.g., in hypothesis testing or in construction of confidence intervals. The chi-squared distribution is used in the common chi-squared tests for goodness of fit of an observed distribution to a theoretical one, the independence of two criteria of classification of qualitative data, and in confidence interval estimation for a population standard deviation of a normal distribution from a sample standard deviation. The chi-squared distribution is a special case of the gamma distribution.

The marginal probabilities p_j for the *jth* column of the transition probability matrix are given as (4.32):

$$p_j = \frac{\sum_i^m n_{ij}}{\sum_{i,j}^m n_{ij}} \tag{4.32}$$

where n_{ij} is the frequency in state i followed by state j. The tests have been carried out by taking the whole available time series at the three different locations. The values of α is higher in all cases than the χ^2 values. These values of α for the three locations for the first order Markov chain shows that the transition of hourly wind speed has the first order Markov chain property.

4.4.2.1.2 Spatial Correlation Test

Markov chain properties for spatial correlation are checked if analysis of data at more than one location is carried out. If the Markov chain propertied for successive events n different location are homogenous, the γ statistic defined by (4.33):

$$\gamma = 2\sum_{s}^{S}\sum_{i,j}^{k} n_{i,j}(s)\ln\frac{p_{ij}(s)}{p_j} \tag{4.33}$$

is distributed asymptotically as χ^2 having *(S-1)*×*k*×(*k*-1) degrees of freedom, where S is the number of stations. If $\gamma > \chi^2$, then the process is homogenous in the defined confidence interval otherwise heterogeneous. For the available data, the value of γ is greater than the limiting value of χ^2 for the three locations. So it is included that the Markov chain properties are spatially correlated and the wind speeds are dependent on different sites.

4.4.2.2 Proposed Model for Inclusion of Wind Speed Inter-Hour Changes

For improving the generating of the sequences of wind speed states, the initial state, say *i*, is selected from a specific wind speed vector, these wind speed vectors are produced using MCS in Section 4.4.2 to generate large number of samples, $\omega_{iw,k,n}$, for each hour. The transition matrices are used to order these wind speed vectors to form a better correlated 24-hour daily profile. Random values between 0 and 1 are produced by using a uniform random number generator. For next wind speed state in Markov process, the value of the random number is compared with the elements of the ith row of the cumulative probability transition matrix. If the random number value is greater than the cumulative probability of the previous state but less than or equal to the cumulative probability of the following state, the following state is chosen from the next wind speed vector. The row is decided based on the current and preceding states in which current state will be the previously selected state. The modified WF output power, $\overline{P}_{w_{i_w,n}}$ for each wind speed profile is calculated using (2.5). Figure 4-5 shows how MCS and Markov-Chain transition matrices are used to produce 24-hour profiles of wind power generation.

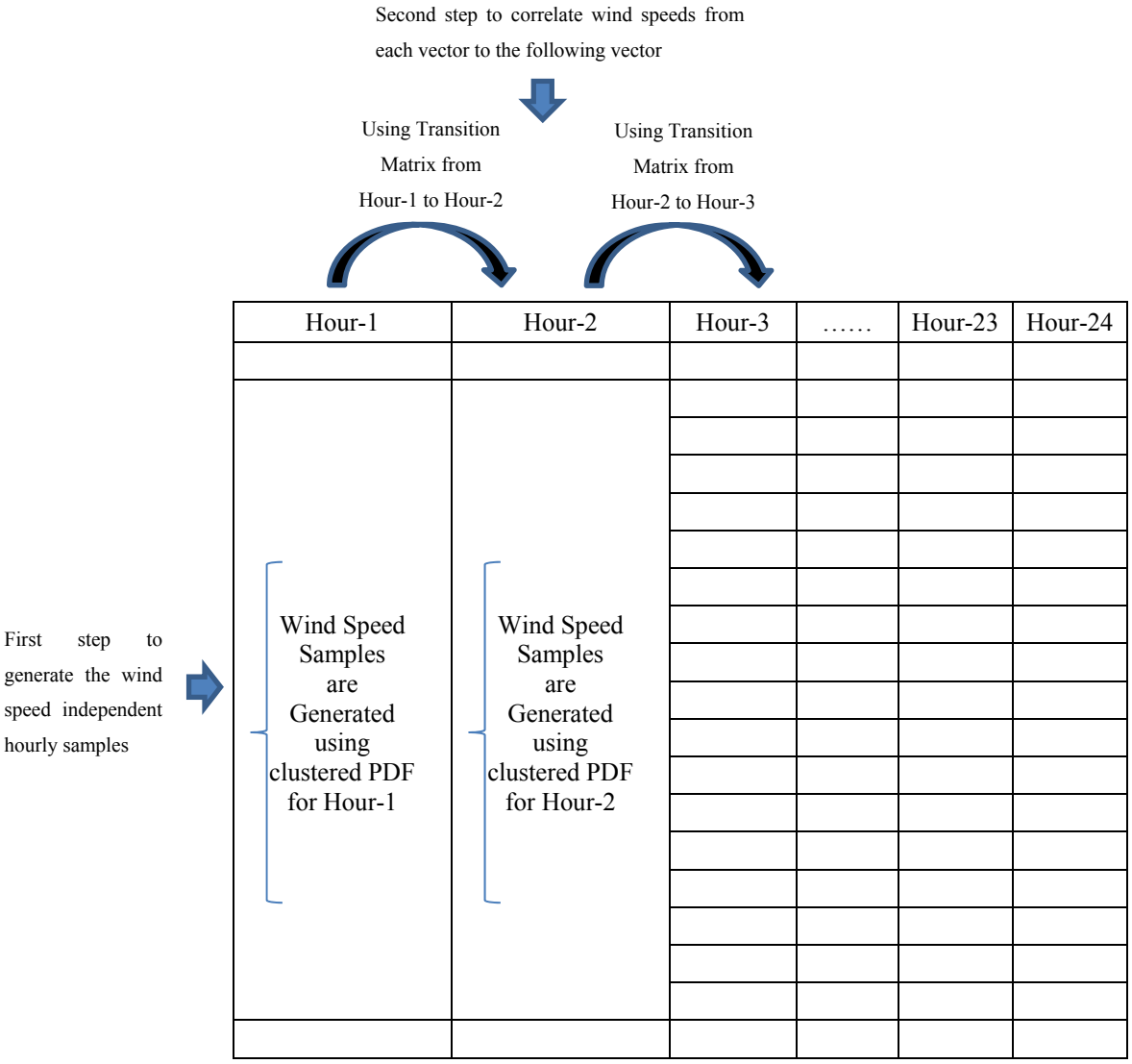

Figure 4-5 Combined MCS and Markov-Chains for scenario generation

4.4.3 Proposed Scenario Reduction

For practical-sized systems the optimization problem that considers all possible scenarios can often be too large. Because of computational complexities and time limitations, the analysis is often carried out considering a much smaller number of scenarios. The scenario selection algorithms determine a subset of the initial set of scenarios and assign new probabilities to the preserved scenarios. The selection algorithms exploit a certain probability distance of the original and the reduced probability measure. The probability distance trades off scenario probabilities and distances of scenario values.

Therefore, deletion will occur if scenarios are close or have small probabilities. In this chapter the Forward Selection Algorithm [7] is used to obtain the reduced set of scenarios, since the objective is to preserve only a few selected scenarios from a large initial set (*N=1,000*).

The Forward Selection Algorithm, discussed below, works recursively, until the preserved number of scenarios *S* is selected. Let Ψ_n (n = 1, 2… N) denote the N data sets, such that,

$$\begin{aligned}
&\Psi_1 = (\overline{P}_{w1,1}, \overline{P}_{w2,1}, \overline{P}_{w3,1}),\\
&\Psi_2 = (\overline{P}_{w1,2}, \overline{P}_{w2,2}, \overline{P}_{w3,2}),\\
&\Psi_3 = (\overline{P}_{w1,3}, \overline{P}_{w2,3}, \overline{P}_{w3,3}),\\
&.\\
&\Psi_n = (\overline{P}_{w1,n}, \overline{P}_{w2,n}, \overline{P}_{w3,n}),\\
&.\\
&\Psi_N = (\overline{P}_{w1,N}, \overline{P}_{w1,N}, \overline{P}_{w1,N})
\end{aligned} \tag{4.34}$$

Each data-set scenario Ψ_n in (4.34) has an equal probability λ_n of $1/N$, and $\Delta_{n,n'}$ is the distance of a scenario pair (n, n'), defined as (4.35):

$$\Delta_{n,n'} = \Psi_n - \Psi_{n'} \tag{4.35}$$

The Forward Selection Algorithm is described as follows:

- Define set Γ, such that $\Gamma = \{\Psi_1, \Psi_2, \ldots, \Psi_N\}$
- Let Ω be the set of scenarios to be deleted. Set Ω is a null set at the outset.
- Compute distances of all scenario pairs $\Delta_{n,n'}$ where $n, n' \in 1,\ldots,N$.
- Compute $\Phi_z = \Sigma_{u\neq z} \lambda_u \Delta_{u,z}$ where $u, z = 1,\ldots,N$
- Identify $u = \eta$, such that, $\Delta_{u,z}$ is minimum.
- Identify $z = \xi$, such that Φ_z is minimum.
- Update set Γ to exclude the scenario corresponding to $n = \xi$ and hence, $\Gamma = \{\Gamma - \Psi_\xi\}$.
- Update set Ω to include the scenario corresponding to $n = \xi$ and hence, $\Omega = \{\Omega + \Psi_\xi\}$.
- Update λ_η to be $\lambda_\eta + \lambda_\xi$.

In the next section, the reduced set of wind generation scenarios is used to mimic the wind speed variations of three WF located at three different buses of the RTS-IEEE system (*i.e.* 101, 201 and 301). The detailed LMP-based electricity market model is then solved for each scenario of the reduced set of scenarios.

4.5 System under Study

The overall system under study is shown in Figure 4-6. The high-voltage transmission system is represented as a three-area system, where each area is modeled using the IEEE RTS-32 system [78]. There are three WFs one in each area, denoted by WF-1, WF-2 and WF-3, and injecting power directly to the transmission system, at buses 101, 201 and 301 respectively. Each WF is considered to comprise 10 wind turbines, of type VESTAS V82-1.65 MW, with a total capacity of 16.5 MW. The overall system comprises 73 buses and 96 generators. The complete data of this system can be found in [78] (Appendix B).

Each of the three areas of the high-voltage transmission system is represented by an individual IEEE-RTS test system model. The IEEE-RTS comprises 24 buses and the configuration is shown in Figure 4-7. The figure shows all the generators, transformers and transmission line for one area (the three areas have the exact same configuration). Figure 4-8 provides the detailed representation for the three areas interconnected.

Although the selection of location of WF generators is entirely arbitrary in this work, there is no loss of generality. In a real-life system, WF generators would be located at a bus after carrying out detailed planning studies and techno-economical validation, which is beyond the scope of this work.

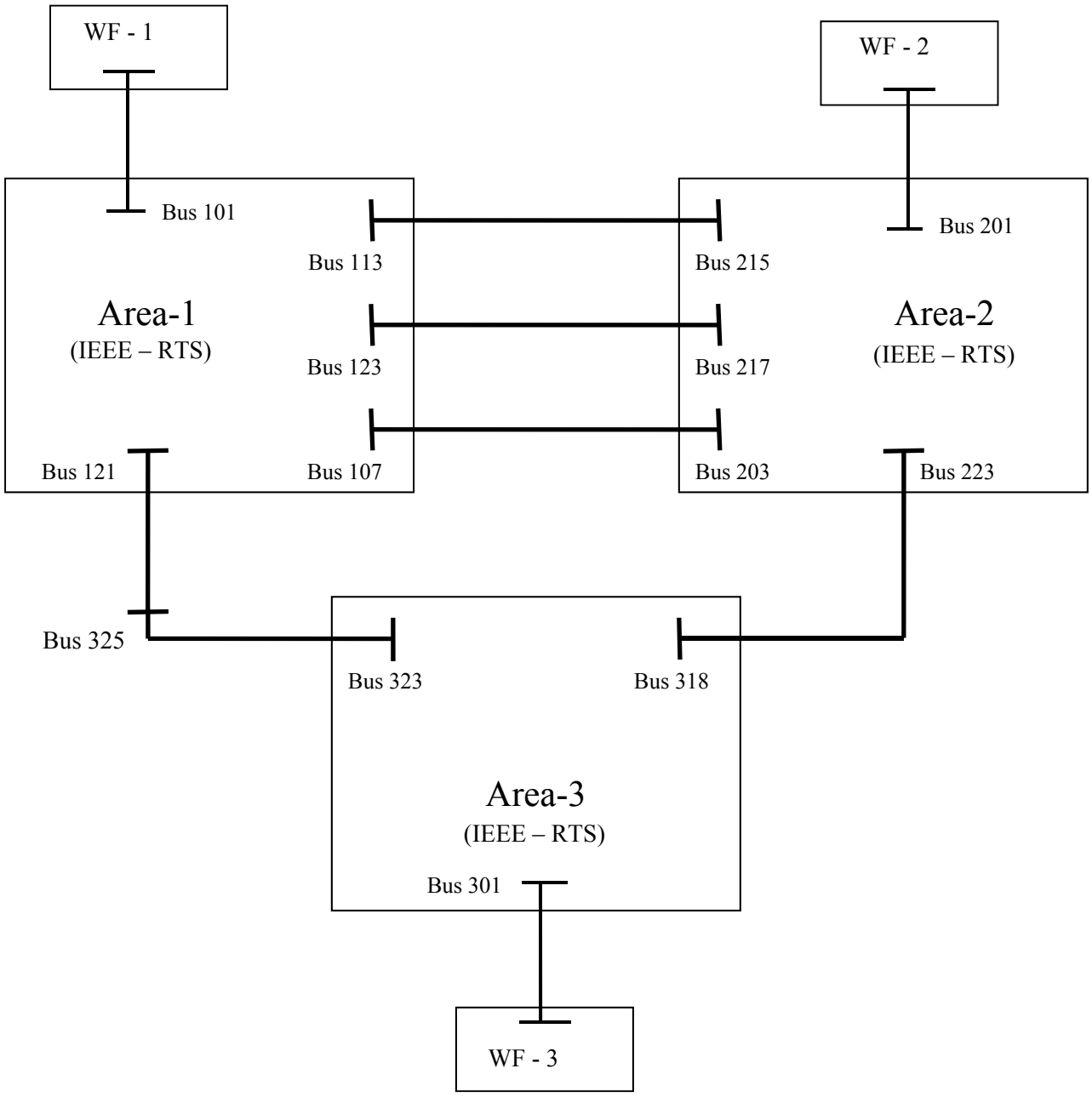

Figure 4-6 Overall transmission system configuration

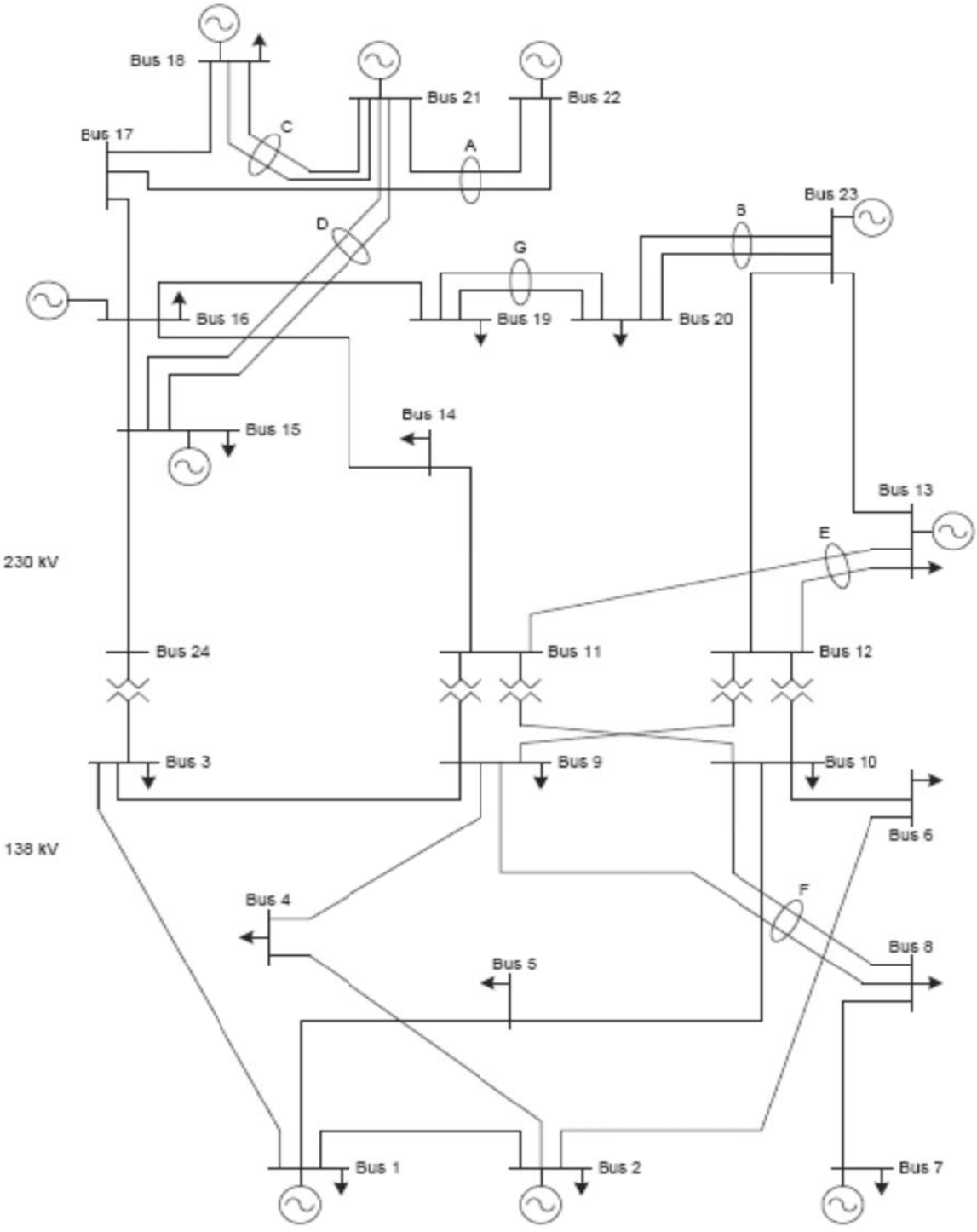

Figure 4-7 IEEE-RTS - One area system

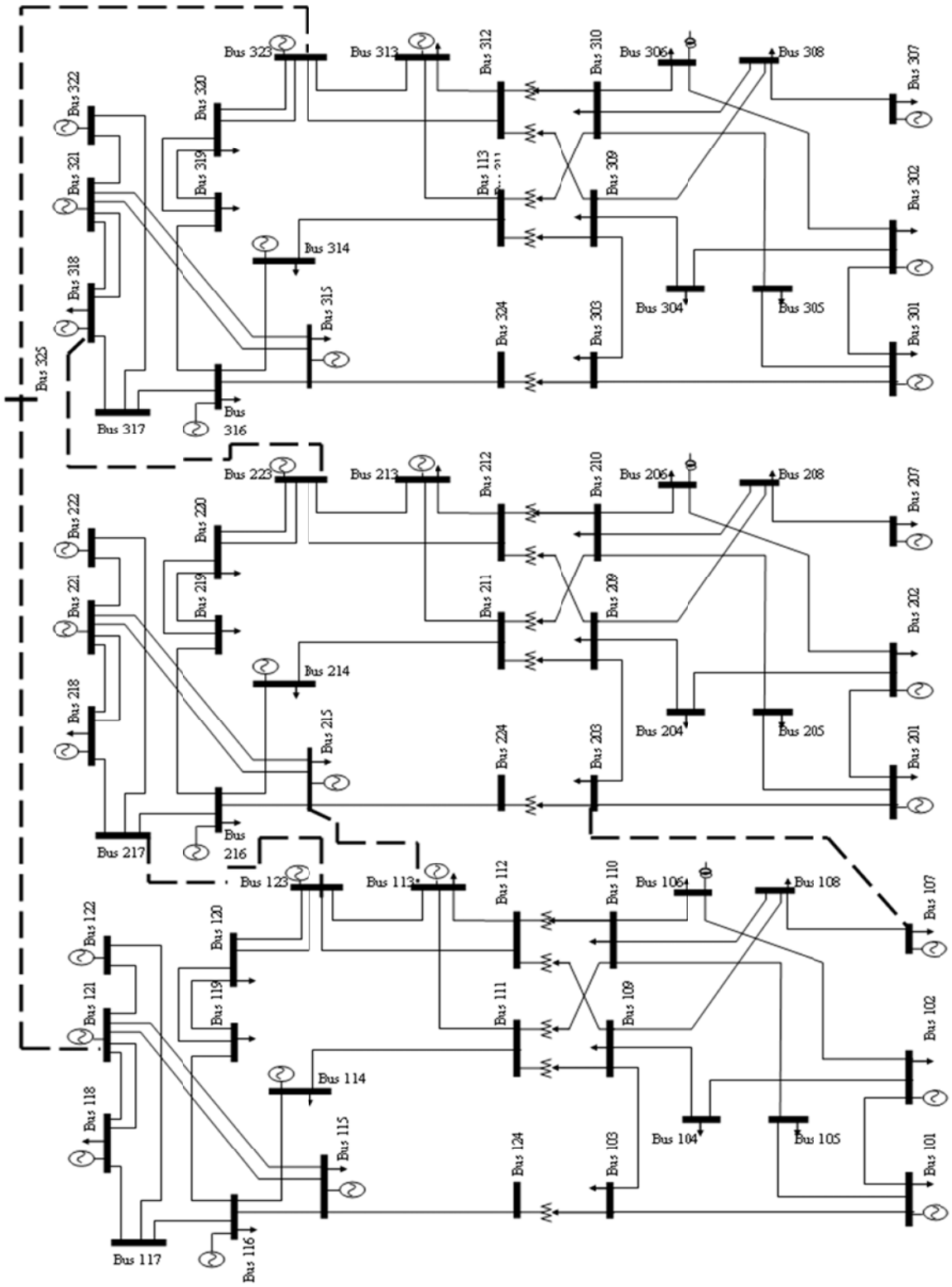

Figure 4-8 IEEE RTS-1996 system with 73 buses: representing overall transmission system

4.6 Analysis and Results

Using MCS and Markov-chain transitions matrices, a large set (*N*) of random wind speed samples is generated for different hours. The *N* wind speed samples are used to generate the *N, 24*-hour wind speed profiles (*i.e.,* vector $\overline{P}_{w_{i_w,n}}$) for the three WFs. These wind speed profiles are used to generate *N* data-set (i.e., Ψ_n). It should be noted that each data set contains three vectors of $\overline{P}_{w_{i_w,n}}$, one for each WF. The *Forward Selection Algorithm* is then used to reduce the number of scenario from (*N*) to (*S*). Figure 4-9 shows a selected reduced data set Ψ_1 ($\overline{P}_{w_{1,1}}, \overline{P}_{w_{2,1}}, \overline{P}_{w_{3,1}}$).

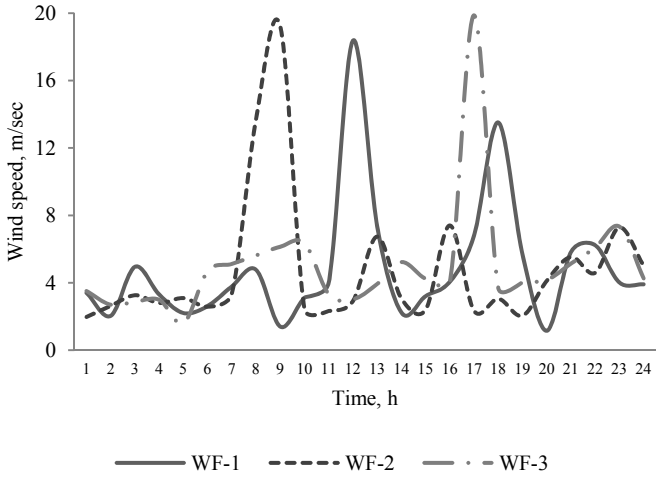

Figure 4-9 A typical reduced scenario for three WFs

4.6.1 Model Validation

A comparison between solving the LMP model uses the proposed scenario generation and reduction algorithm, using Wind Power Generation in Liberalized Electricity Markets project (WILMAR) scenario tree tool (STT) discussed in [79], and using the historical wind speed data is presented in Table 4-1. It shows the summary of results and it can be observed how the proposed algorithm is fast and efficient with less number of iterations. An index error parameter is defined to measure the total deviation in the scenarios from the two algorithms and using the historical data. It seems that the proposed scenario generation algorithm gives closest results to the using the actual data scenarios.

Table 4-1 Comparison of Solutions by Different Methods

	Proposed Algorithm	WILMAR - STT	Historical Data
Iterations	3134	5363	8341
CPU time, s	122.55	156.78	222.12
Error Index	10.73%	15.31%	N/A

4.6.2 Analysis of Stochastic Wind Generation Model

4.6.2.1 Case Study Considering Typical WFs

The detailed market settlement model for the LMP market, presented in Section 4.3 is solved for the reduced set of scenarios (*S=64*). The PDF and the CDF for LMP_{201} at any specific hour is constructed considering all 64-scenarios of wind generation. The PDF can be used to calculate the probability of achieving a specific value of LMP. Figure 4-10 presents the CDF for LMP_{201} at 6 PM. The CDF can be used to calculate the probability of obtaining an LMP equal to or less than a specified value, for example, it can be inferred that the probability that LMP_{201} is less than 90 $/MWh is 0.63.

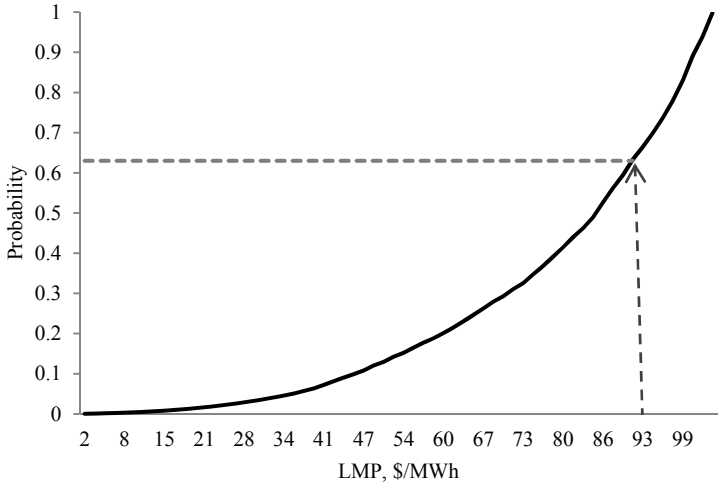

Figure 4-10 CDF for LMP_{201} at 6:00 PM

Figure 4-11 shows a 24-hour comparison of the expected LMPs at buses 101, 201 and 301 (*buses where WFs are connected to the grid*). It is observed that the LMPs have almost the same trend

for all three buses, but LMP_{201} is higher than the other two. This is because of the congested lines between buses 201-202, 201-203 and 201-205.

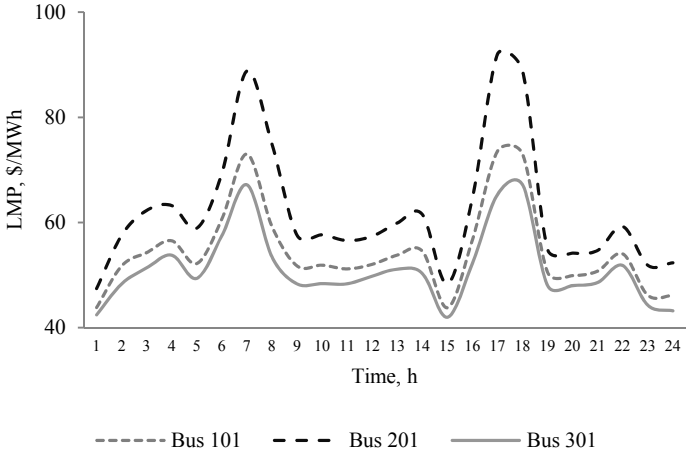

Figure 4-11 Expected LMP for 24 hours at buses 101, 201 and 301

Figure 4-12 presents the PDF of social welfare, constructed considering all *64-scenarios* of wind generation. The expected social welfare is 1.041 million dollars whereas; it is 0.936 million dollars when no WF is connected to the system. It is observed that the social welfare increases when WF generation penetrates the market.

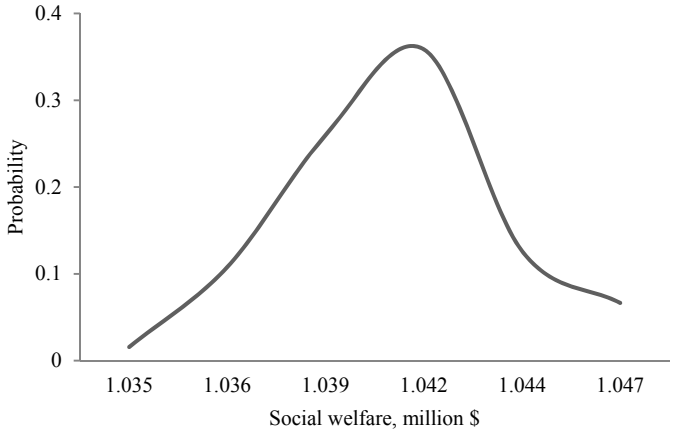

Figure 4-12 PDF of the social welfare with WF penetration

It is observed from Figure 4-13 that the total expected load cleared in the market during the peak hours (9 AM – 10 PM) is increased when wind generation penetrated the system as compared to the case with no WF. This is because wind generation is cheap compared to conventional generation. On the other hand, during off-peak hours (1 AM- 8 AM) some of the conventional units are de-committed when WFs are present in the system and thus the total load cleared in the market during these hours is less than without WFs.

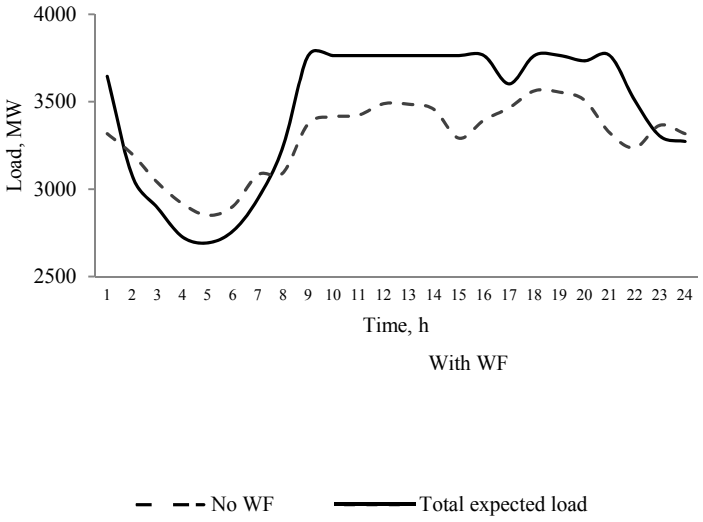

Figure 4-13 Total expected load cleared in market with and without WF

4.6.2.2 Effect of Large Capacity WFs on LMP Market

In this case study, the level of total capacity of wind generation is considered almost to be 5% of the total generation capacity of the system. Each WF is considered to comprise 100 wind turbines, for a total capacity of 165 MW. As seen from Figure 4-14, the social welfare is significantly increased when WF capacity increases. However, the expected LMPs are significantly lower with increased WF capacity (Figure 4-15), especially during peak load hours because of the presence of a large quantity of cheap wind generation.

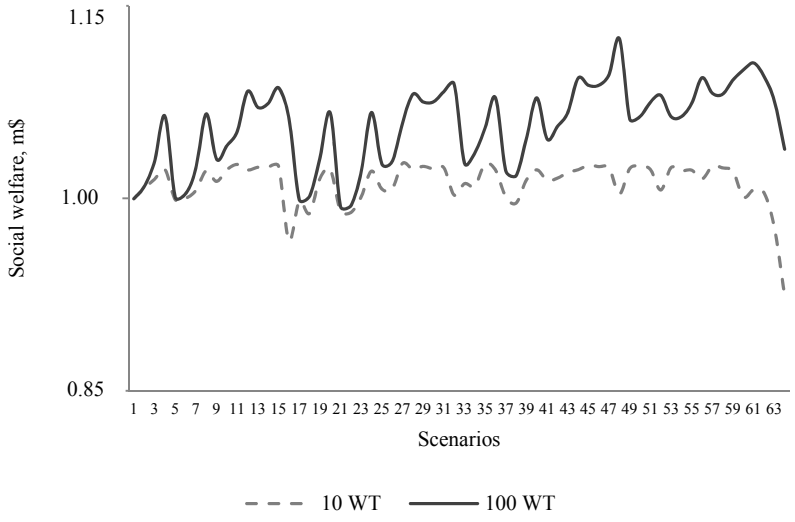

Figure 4-14 Social welfare for different levels of WF capacity

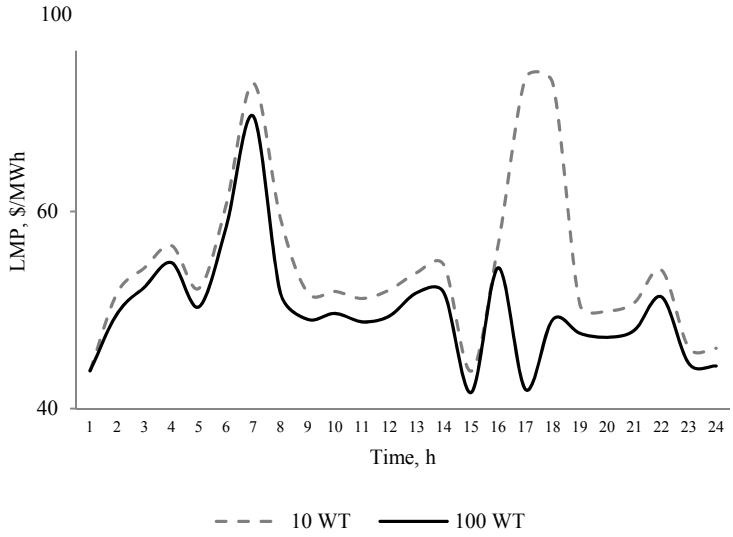

Figure 4-15 Expected LMP_{201} for different levels of WF capacity.

4.6.2.3 Wake Effect

In this case study, the level of total wind generation capacity is increased to 5% of total generation capacity of the system. Each WF is now considered to comprise 100 WTs, of type VESTAS V82-1.65 MW, with a total capacity of 165 MW. The WTs are assumed to be placed in a rectangular configuration, arranged in 5 rows with each row having 20 WTs. The wake effect is taken into consideration by assuming that the wind speed profile is identical for WTs sharing the same row,

while the wind profile differs across rows. This results in a different operating condition for each row. Therefore, a given WF can be considered to be an aggregate of five equivalent WTs, each of 33 MW (20 x 1.65 MW) capacity. Accordingly, the wake effect is modeled by reducing the incident wind speed values from one row to the next row, in the direction of the incident wind [80], given by (4.36):

$$\omega_x = \omega_0 \times \left(1 - \frac{\left(1 - \sqrt{1 - C_{Thrust}}\right)}{\left(1 + 2w\frac{x}{D}\right)^2} \right) \tag{4.36}$$

In (4.36), the following parameters are selected: w= 0.075 for on-shore sites [81], C_{Thrust} = 0.547, D = 82 m [50]. Since each row has the same wind profile, the 24-hour PDF is the same for each row, but the PDF is not the same for different rows. For each wind speed level there are five output powers, one for each equivalent WT. Consequently, the expected power for each wind speed level can be calculated and hence used to solve the LMP model.

From a comparison of the cases with and without the wake effect, it is observed that the social welfare (Figure 4-16) is reduced when wake effect is included in the LMP market model. This is because of the reduced level of wind intercepted by the second and later rows of the WF.

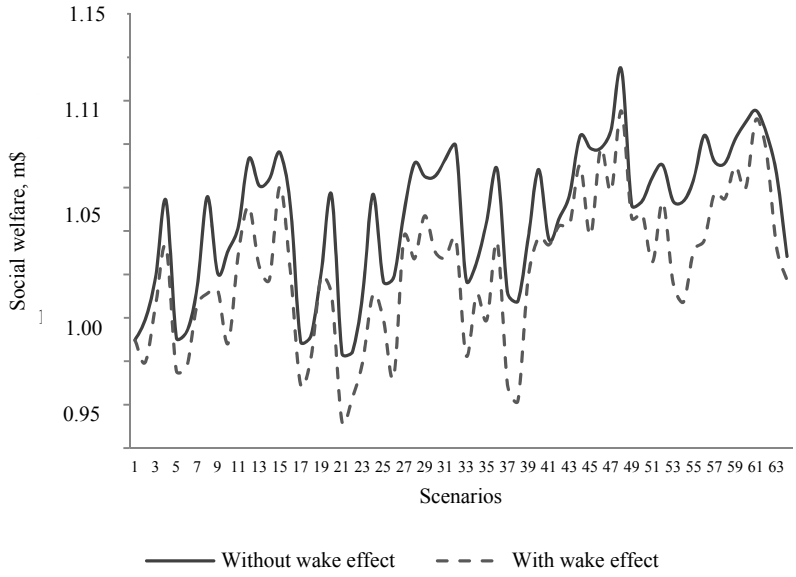

Figure 4-16 Social welfare with and without wake effect

4.7 Summary

In this chapter, a novel scenario generation and reduction technique is proposed using clustered technique through Monte-Carlo Simulations, Markov-chain and the forward selection algorithm, to obtain a reduced set of wind generation scenarios. The reduced set of scenarios is used to examine the effects of wind generation variability on power system operation and market prices. This approach significantly reduces the computational burden arising from large scale simulations for uncertainty analysis of intermittent generation sources such as wind.

An LMP market model is considered in detail and the impact of wind generators located at various buses on market price settlement, and load clearance is studied. The analysis can be used by operators and planners to understand the expected range of variation of LMPs when there is significant penetration of wind in the system. Studies reveals that wind generation has a significant effect on market prices, and overall expected social welfare which is increased with wind penetration. The effect of wind generation capacity is also examined and results depict that LMPs are expected to reduce with large capacity WFs. Analysis of wake-effect on the market is reported for the first time and it is observed that the social welfare reduces with inclusion of wake-effect in wind generation models. The inclusion of several scenarios to capture the worst-case tail of the distribution enables the optimizer to schedule dynamic levels of reserves that weigh the cost of providing them against the potential cost of load shedding or running high-cost generators.

Chapter 5
Evaluation of the Environmental Impact of Wind Generation Penetration

5.1 Introduction

In the previous chapter, a novel scenario generation and reduction algorithm is presented, that is useful for short-term operations that include inter-hour constraints. The analysis of the short-term power system operations with WF generation penetration is investigated. In this chapter the work is extended to study the effect of the wind generation penetration on short-term power system operations when emission constraints are imposed by policy makers.

A comprehensive mathematical modeling framework is proposed in this chapter that can be used to evaluate the impact of wind generation penetration on environmental emissions in short-term power system operations. This model can be useful for policy makers to determine the optimum level of wind capacity penetration as well as to set the optimum emissions cap. The relationship between the penetration level of wind generation and the resulting reduction in emissions is not linear. Increasing the level of penetration of wind generation must be kept within a specific limit, which is investigated in this chapter. Furthermore, A UMP-based market electricity dispatch model is considered and the impact of wind generation on market price settlement and emissions reduction is presented.

5.2 Short-term Operations with WF Generation and Environmental Constraints

5.2.1 Objective Function

A short-term operation model is presented in this chapter with the following objective function to minimize the operation cost (C_s), as given in (5.1):

$$C_{s\in S} = \sum_{k\in K}\sum_{j\in J}\left(c^{u}_{j,k} + c^{d}_{j,k} + c^{p}_{j,k}\right) \tag{5.1}$$

In (5.1), $c^{u}_{j,k}$ is the start-up cost of a generator, the dashed line in Figure 5-1 shows a typical exponential start-up cost function of a thermal generator [37]. Since the time span is discretized into hourly periods, the start-up cost also needs to be a discrete function. The discrete start-up cost can be asymptotically approximated by a staircase function.

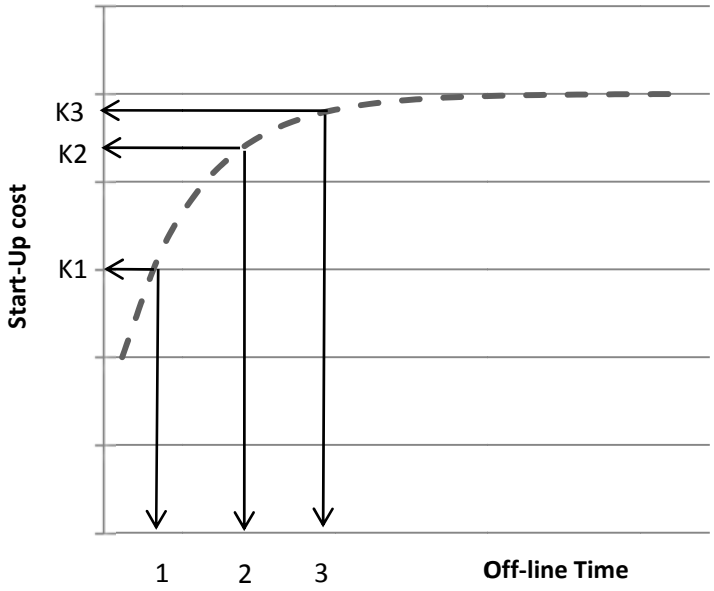

Figure 5-1 Exponential and staircase start-up cost function

A mixed-integer linear formulation for the staircase start-up cost is proposed in [69], as given in (5.2) – (5.4), The same model has been considered in this work.

$$c^{u}_{j,k} \geq K^{t}_{j}[v_{j,k} - \sum_{n=1}^{t} v_{j,k-n}], \forall j \in J, \forall k \in K, \forall t = 1 \cdots ND_{j} \tag{5.2}$$

Where,

$$K^{t}_{j} = \begin{cases} hc_{j}, & if \quad t = 1 \cdots t^{cold}_{j} + DT_{j,} \forall j \in J, \\ cc_{j}, & if \quad t = t^{cold}_{j} + DT_{j} + 1 \cdots ND_{j.} \end{cases} \tag{5.3}$$

$$c^{u}_{j,k} \geq 0, \forall j \in J, \forall k \in K \tag{5.4}$$

In (5.1), $c^{d}_{j,k}$ is the shut-down cost of a generator, a constant shut-down cost C_j is assigned if unit *j* is off-line at hour *k*. The constraints (5.5) and (5.6) depict the equivalent formulation for the shut-down cost:

$$c^{d}_{j,k} \geq C_{j}[v_{j,k-1} - v_{j,k}], \forall j \in J, \forall k \in K \tag{5.5}$$

$$c^{d}_{j,k} \geq 0, \forall j \in J, \forall k \in K \tag{5.6}$$

The last term in (5.1) denotes the total cost of energy generation, wherein, for every generator, a linearized generation cost model is considered, as follows:

A piece-wise linearization of the cost function is carried out to develop linear equivalents. The following brief summary of the linearization approach is applied to the quadratic cost function. As shown in Figure 5-2, a general quadratic cost function can be approximated by a set of piecewise blocks,

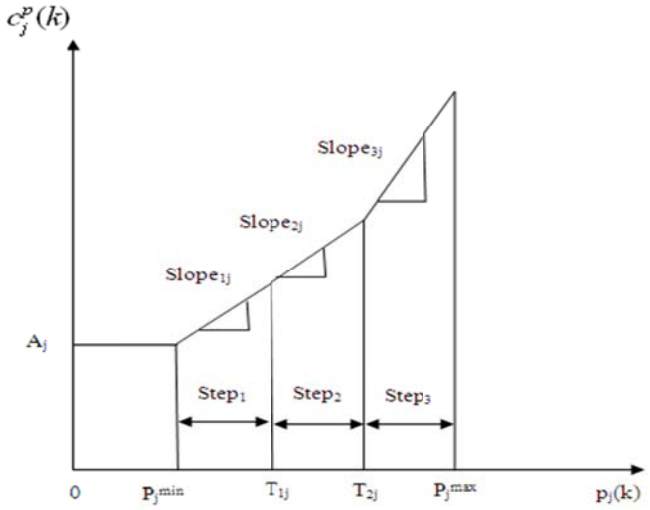

Figure 5-2 Piecewise linear production cost

The analytical form of this linear approximation is given as follows, in equations (5.7) to (5.13) [37]:

$$c_{j,k}^{p} = A_j v_{j,k} + \sum_{\ell=1}^{NL_j} Slope_{\ell,j} \times Step_{\ell,j,k} \forall j \in J, \forall k \in K \tag{5.7}$$

$$P_{j,k} = \sum_{\ell=1}^{NL_j} step_{\ell,j,k} + P_j^{\min} v_{j,k}, \forall j \in J, \forall k \in K \tag{5.8}$$

$$Step_{1,j,k} \le T_{1j} - P_j^{\min}, \forall j \in J, \forall k, K \tag{5.9}$$

$$Step_{\ell,j,k} \le T_{\ell j} - T_{(\ell-1)j} \forall j \in J, k \in K, \forall \ell = 2 \cdots (NL_j - 1) \tag{5.10}$$

$$Step_{NL_{j,j,k}} \le P_j^{\max} - T_{(NL_j-1)j}, \forall j \in J, \forall k \in K \tag{5.11}$$

$$Step_{\ell,j,k} \ge 0, \forall j \in J, \forall k \in K, \forall \ell = 1 \cdots NL_j \tag{5.12}$$

$$A_j = a_j + b_j P_j^{\min} + c_j (P_j^{\min})^2 \tag{5.13}$$

5.2.2 Model Constraints

Demand Supply Balance: Constraint (5.14) ensures that the total generation from generating units is able to meet the forecasted demand of interval *k*.

$$\left(\sum_{j\in E_i} P_{j,k}\right) + P_{w_{i_w},k} = PD_{i,k} \tag{5.14}$$

Spinning Reserve Constraint: Constraint (5.15) ensures that the total maximum available output power from all committed generators meets the system demand and spinning reserve allocations.

$$\sum_{j\in J} \overline{P}_{j,k} \geq \sum_{i\in I} PD_{i,k} + R_k \tag{5.15}$$

Generation Limits: Constraints (5.16) and (5.17) ensure that the output power of a generator at an interval *k* is bounded by its upper and lower limits.

$$P_j^{\min} v_{j,k} \leq P_{j,k} \leq \overline{P}_{j,k}\ , \quad \forall j \in J, \quad \forall k \in K \tag{5.16}$$

$$0 \leq \overline{P}_{j,k} \leq P_j^{\max} v_{j,k}\ , \quad \forall j \in J\ , \quad \forall k \in K \tag{5.17}$$

Ramp-up and Start-up Ramp Rate Constraint: Constraint (5.18) ensures that the inter-hour generation changes are within the limits specified by generator ramping-up capabilities.

$$P_{j,k} \leq P_{j,k-1} + RU_j v_{j,k-1} + SU_j[v_{j,k} - v_{j,k-1}],\ \ \forall j \in J,\ \forall k \in K \tag{5.18}$$

Shut-down Ramp Rate Constraint: Constraint (5.19) ensures that when a unit status changes from ON-state to OFF-state.

$$\overline{P}_{j,k} \leq P_j^{\max} v_{j,k+1} + SD_j[v_{j,k} - v_{j,k+1}], \quad \forall j \in J, \quad \forall k = 1 \cdots \beta - 1 \tag{5.19}$$

Ramp-down and Shut-down Ramp Rate Constraint: Constraint (5.20) ensures that the inter-hour generation changes are within the limits.

$$P_{j,k-1} - P_{j,k} \leq RD_j\, v_{j,k} + SD_j[v_{j,k-1} - v_{j,k}],\ \forall j \in J,\ \ \forall k \in K \tag{5.20}$$

Minimum Up-time Constraints: Constraints (5.21)-(5.24) ensure that when a generator is brought online, it remains in the ON-state for a certain minimum number of hours before it can be shut-down.

$$\sum_{k=1}^{U_j} [1 - v_{j,k}] = 0, \quad \forall j \in J \tag{5.21}$$

$$\sum_{n=k}^{k+UT_j-1} v_{j,n} \geq UT_j[v_{j,k} - v_{j,k-1}],\ \ \forall j \in J, \quad \forall k = U_j + 1 \cdots \beta - UT_j + 1 \tag{5.22}$$

$$\sum_{n=k}^{\beta}\left\{v_{j,n}-[v_{j,k}-v_{j,k-1}]\right\}\geq 0,\quad \forall j\in J,\qquad \forall k=\beta-UT_j+2\cdots\beta \tag{5.23}$$

$$U_j = Min\left\{\beta,[UT_j-U_j^0]V_j^0\right\} \tag{5.24}$$

Minimum Down-time Constraints: Constraints (5.25)-(5.28) ensure that when a generator is brought offline, it remains in the OFF-state for a certain minimum number of hours before it can be start-up.

$$\sum_{k=1}^{D_j} v_{j,k} = 0,\quad \forall j\in J \tag{5.25}$$

$$\sum_{n=k}^{k+DT_j-1}[1-v_{j,n}]\geq DT_j[v_{j,k-1}-v_{j,k}],\quad \forall j\in J,\qquad \forall k=D_j+1\cdots\beta-DT_j+1 \tag{5.26}$$

$$\sum_{n=k}^{\beta}\left\{1-v_{j,n}-[v_{j,k-1}-v_{j,k}]\right\}\geq 0,\quad \forall j\in J,\qquad \forall k=\beta-DT_j+2\cdots\beta \tag{5.27}$$

$$D_j = Min\left\{\beta,[DT_j-D_j^0][1-V_j^0]\right\} \tag{5.28}$$

Emission Constraint: This constraint ensures that the total generated contaminants for pollutant *x* is less than a specified emission cap (5.29). A linear emission coefficient $F_{em,x}$ is considered in this work for the sake of simplicity. Some references are available that use quadratic emission factors [59].

$$\sum_{k\in K}\sum_{j\in J} F_{em,x}\times P_{j,k}\leq E_{cap,x} \tag{5.29}$$

Positive Variables: These constraints (5-30)-(5-32) ensure that the following variables are positive.

$$step_{\ell,j,k}\geq 0,\ \forall j\in J,\forall k\in K,\forall \ell=1\cdots M \tag{5.30}$$

$$c_{j,k}^{u}\geq 0,\ \forall j\in J,\ \forall k\in K \tag{5.31}$$

$$c_{j,k}^{d}\geq 0,\forall j\in J,\forall k\in K \tag{5.32}$$

The short-term operation model is a mixed integer linear programming model and is solved using the CPLEX solver in GAMS [64].

5.3 Market Dispatch Model with WF Generation and Environmental Constraints

In this section a market dispatch and clearing model is presented based on uniform price auction and considering the penetration of wind generation sources. The UMP model presented next, is an extension of the short-term operation model discussed in Section 5.2 and also a simplification of the LMP market dispatch model presented in Chapter 4. The UMP market is considered here, in that any

loss of generality, to examine the impact of wind generation on social welfare, UMPs and environmental emissions. The objective function is the maximization of social welfare, given by (5.33):

$$J_{s\in S} = \sum_{k\in K}\sum_{i\in I}\sum_{h=1}^{N_i} \gamma_{h,i,k} \times H_{h,i,k} - \sum_{k\in K}\sum_{j\in J}\left(c^{u}_{j,k} + c^{d}_{j,k} + \sum_{\ell=1}^{M_j} \mu_{\ell,j,k} \times step_{\ell,j,k} \right) \tag{5.33}$$

The UMP market clearing and dispatch model constraints are the same as in Section 5.2, and are briefly listed below:

- Demand Supply Balance
- Spinning Reserve
- Generation Limits
- Ramp-up and Start-up Ramp Rate
- Shut-down Ramp Rate
- Ramp-down and Shut-down Ramp Rate
- Minimum Up-time and Down-time
- Emission Constraint

5.4 System under Study

The overall system under study is the three area IEEE RTS high-voltage transmission system, discussed in Chapter 4. Figure 5-3 shows that the WF is injecting power directly to the transmission system, at a specific bus 101. The WF is considered to comprise 10 WTs, of type VESTAS V82-1.65 MW, with a total capacity of 16.5 MW. The complete data of this system is given in [78].

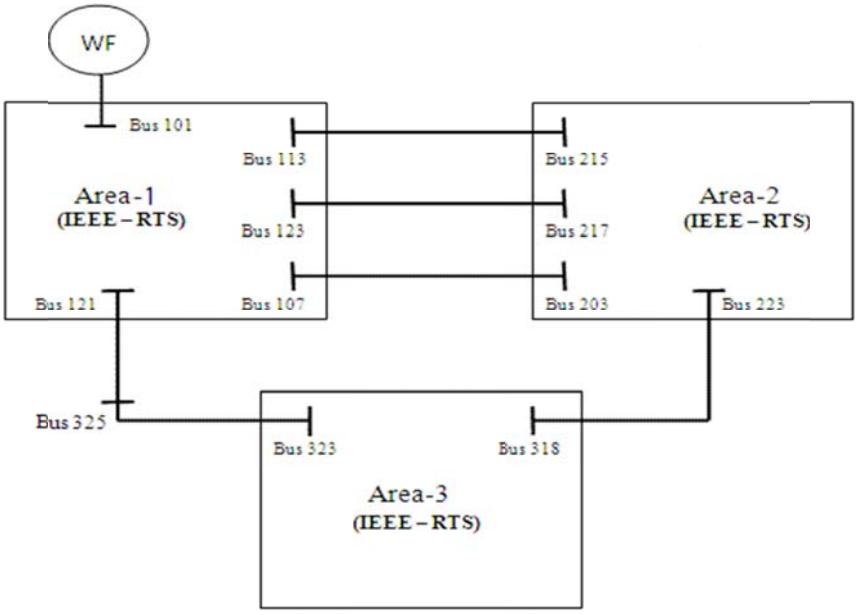

Figure 5-3 Overall transmission system configuration

5.4.1 Wind Data Clustering and Classification

The wind speed data used in this work is extracted from [65]. The hourly wind speed data over three years is clustered into 12 sets, one for each month. The data for July is used to present the results of the research in this chapter. Figure 5-4 shows the hourly mean wind speed profile for July for the WF.

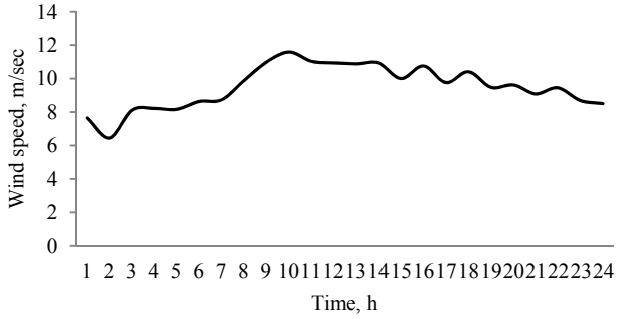

Figure 5-4 Hourly mean wind speed profile for July

Hourly average wind speed values, is used to calculate the hourly PDFs and CDFs using (2.1) and (2.4). Then MCS and Markov-chains are applied to generate N different wind speed

samples for each hour. These wind speed samples are used to form N, 24-hour profiles (*i.e.* scenarios), same as that used in Chapter 4. Subsequently, the forward selection algorithm is used to reduce the number of scenarios to 64 scenarios. Figure 5-5 shows three typical wind speed scenarios after scenario reduction, the shown scenarios (1, 2 and 3) are selected based on the daily average wind power generated; they have the lowest, medium and highest daily average wind generated power respectively.

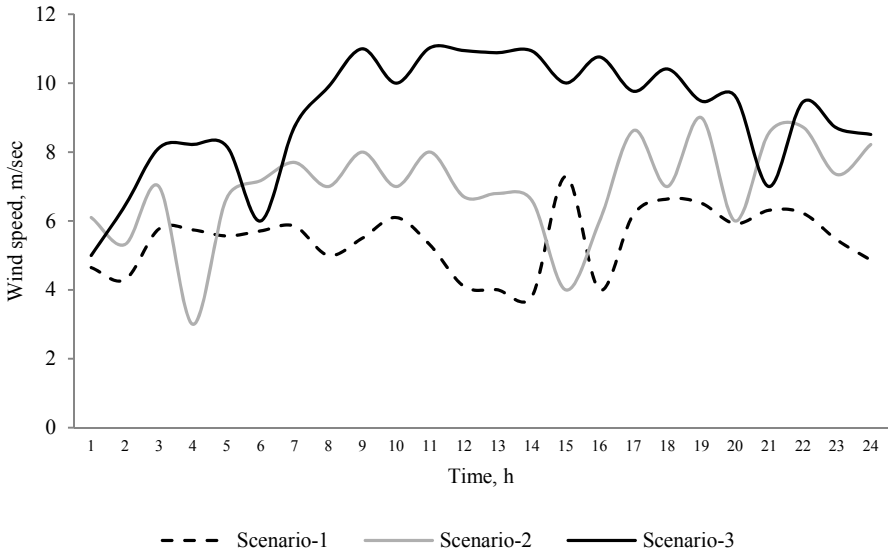

Figure 5-5 Wind speed 24-hour profiles (scenarios)

5.5 Analysis and Results

Using [82] and [83], where all the generator types are defined, different emission contaminant factors ($F_{em,x}$) in (5.29) are calculated. Detailed tables pertaining to these calculations are given in Appendix C.

5.5.1 Short-term Operation with Wind Generation: Environmental Impacts

The short-term operation model, presented in Section 5.2 is solved for the reduced set of 64-*scenarios*. A comparison is carried out between the total operation cost with and without emission cap *i.e.* constraint (5.29). It can be observed from Figure 5-6, that the total system expected operation cost with emission cap is higher than that without emission cap (*i.e.* when

the problem is relaxed) for most of the 64 wind generation scenarios. However, in some wind generation scenarios, the cost is higher without emission cap, specifically at off-peak hours when some of the conventional units are de-committed when emission cap are imposed. Table 5-1 shows the changes in UC decisions with and without the emission constraint for Scenario-2 (medium average wind). The grey cells are the ones that change from ON-state to OFF-state when the emission constraint is applied. It is noted that some of the coal generators have to be de-committed during off-peak hours to reduce the total daily system emissions.

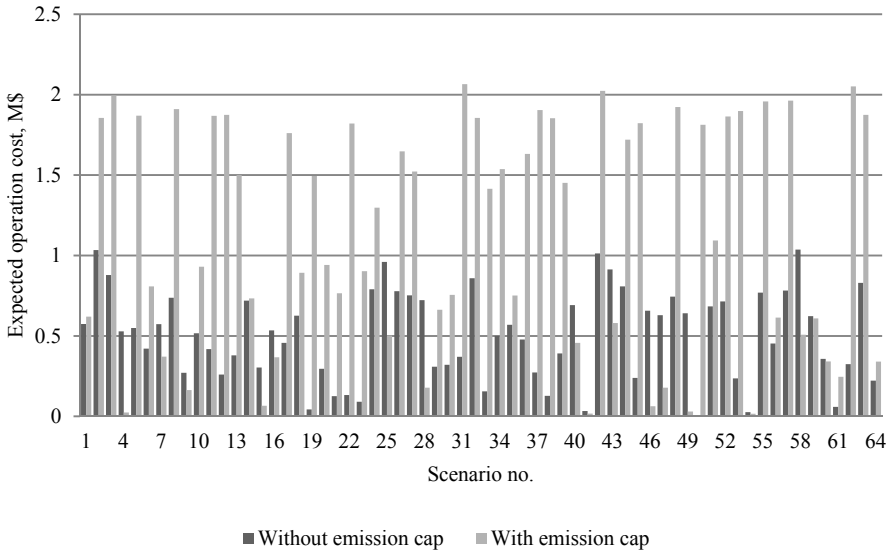

Figure 5-6 Total expected system cost with and without emission cap

Table 5-1 UC decisions with and without emission cap
(Grey cells denote change in UC decisions when emission constraint is applied)

Time / Generator	1	2	3	4	5	6	7	8	9	10	11	12	13	14	15	16	17	18	19	1	21	1	1	24
G24	0	0	0	0	0	0	1	1	1	1	1	0	0	1	0	0	1	1	1	0	0	1	0	1
G25	0	0	0	0	0	0	1	1	1	1	1	0	1	1	0	1	1	0	1	1	0	1	0	1
G26	0	0	0	0	0	0	1	1	0	0	1	0	1	1	0	0	1	1	1	1	0	0	0	1
G27	0	0	0	0	0	0	0	1	1	1	1	1	1	9	0	0	0	1	1	1	0	0	0	1
G28	0	6	0	0	0	0	0	1	1	1	0	0	1	1	0	0	1	1	1	1	0	0	0	1
G29	1	0	0	0	0	0	0	1	1	1	1	1	0	0	0	0	1	0	1	1	0	0	1	0
G32	0	0	0	0	0	0	0	0	0	0	0	1	1	1	1	1	1	1	1	1	1	0	0	0
G56	1	1	0	0	0	0	0	0	0	0	1	1	0	0	0	0	1	1	0	1	0	1	1	1
G57	1	0	0	0	0	0	0	0	0	0	0	1	1	1	0	0	1	0	1	1	1	1	1	1
G58	0	0	0	0	0	0	0	1	1	1	0	1	1	0	0	0	0	0	1	1	0	1	1	1
G59	1	0	0	0	0	0	0	1	1	1	1	0	0	1	0	0	0	0	1	0	1	1	1	0
G60	0	0	0	0	0	0	0	1	0	1	1	1	0	0	0	0	0	0	1	1	1	1	1	1
G61	1	0	0	0	0	0	0	0	0	0	1	1	1	0	0	0	1	1	0	1	1	1	1	0
G64	1	0	0	0	0	0	0	0	0	0	0	1	1	1	1	1	1	1	1	1	1	1	1	0
G88	0	0	0	0	0	0	1	1	0	1	1	0	0	0	0	1	0	1	0	0	1	1	1	1
G89	0	0	0	0	0	0	0	1	1	0	1	0	0	1	0	1	1	1	0	0	1	1	1	0
G90	0	0	0	0	0	0	1	1	1	1	0	0	1	1	1	0	1	0	0	0	1	0	1	0
G91	0	0	0	0	0	0	0	1	1	1	1	0	1	1	0	1	1	0	1	0	0	0	1	0
G92	0	0	0	0	0	0	0	1	0	1	1	0	1	0	0	1	1	0	0	1	1	1	1	0
G93	0	0	0	0	0	0	0	1	1	1	1	1	1	1	0	0	0	0	0	0	1	1	1	0
G96	0	0	0	0	0	0	0	0	0	0	0	1	1	1	1	1	1	1	1	1	1	0	0	0

5.5.1.1 Effect of Changing WF Capacity and Emission Cap

The effect of changing the level of WF penetration capacity and the emission cap values on short-term system operations is discussed in this section. The WF capacity is assumed to be a percentage of the total system generation capacity, changing from 0% to 40%. The emission cap is tightened and assumed to be changing from 50% to 100% of E_{cap}, where E_{cap} is the toal system emissions when no emission constraints are imposed, and there are no WFs. The model is solved for the reduced set of 64-scenarios and Figure 5-7 shows the variations of total expected operation cost with changing the levels of WF capacity as well as changing the percentage of emission cap.

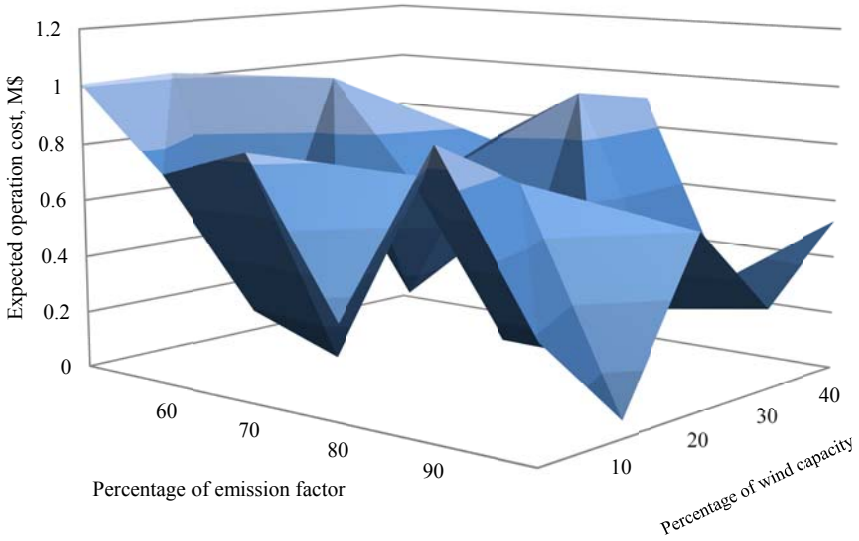

Figure 5-7 Total expected cost variations

Figure 5-8 depicts the relation between the total expected operation cost and percentage of wind capacity at an emission constraint of E_{cap}. It is observed that the expected operation cost decreases with increasing level of WF capacity. However, the expected operation cost slightly increases when the level of WF capacity between 20% - 30% because of the tradeoff between shut-down of coal/oil-fired stations or de-committing a nuclear station. Initially, when wind generation penetration is low, only some of the coal and oil-fired conventional generators with less capacity need to shut-down. However, when WF penetration increases, and because of the minimum generation constraint, one of the bulk power stations needs to be de-committed.

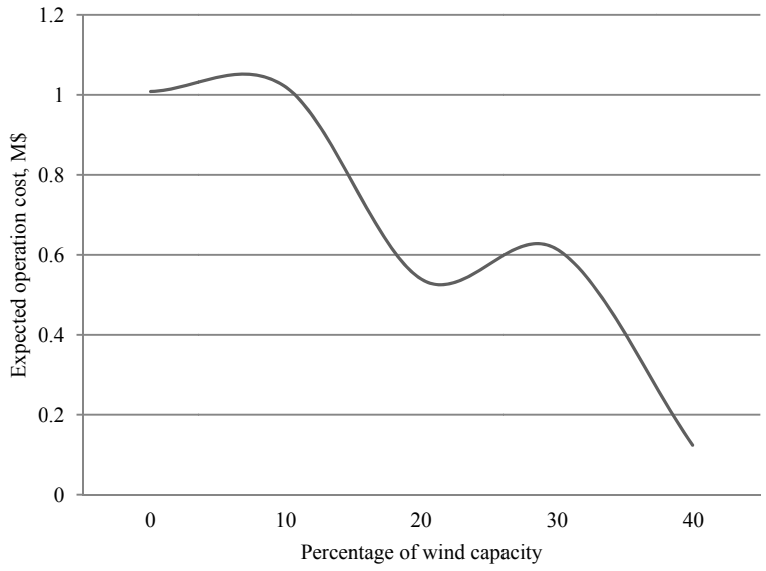

Figure 5-8 Relation between expected cost and percentage level of wind capacity

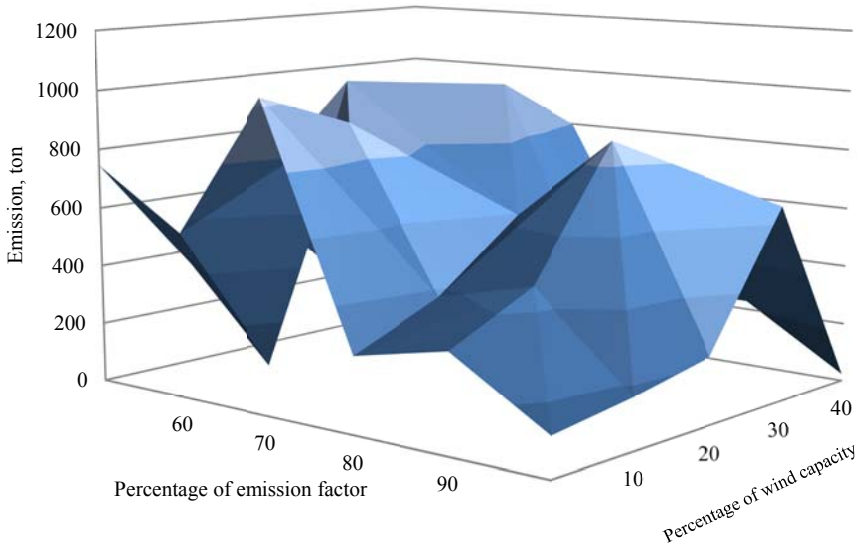

Figure 5-9 Total expected emissions variations

Figure 5-9 shows the variations of total expected system emissions with changing the levels of WF capacity and the percentage of emission cap. Figure 5-10 represents the relation between the expected emissions and wind capacity penetration at an emission cap of E_{cap}. The expected emission decreases with increasing the capacity level of WF, but because of nuclear station de-commitment at 20% capacity level of WF penetration, there is a slight increase in the total expected emissions.

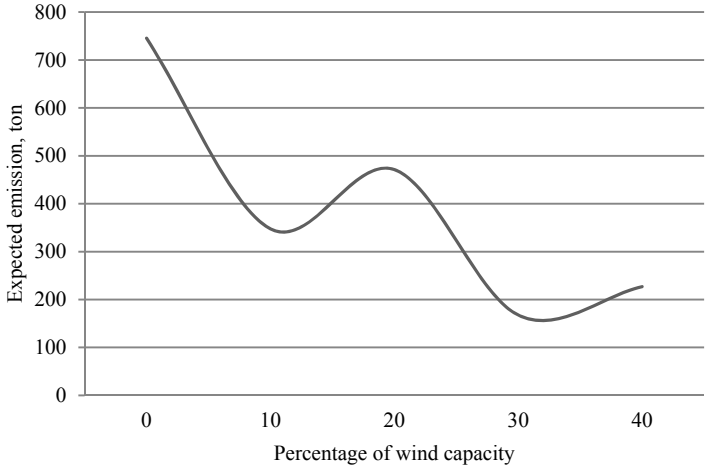

Figure 5-10 Relation between expected emissions and percentage level of wind capacity

5.5.2 Market Dispatch with Wind Generation: Environmental Impacts

The UMP market settlement and dispatch model presented in Section 5.3, is solved for the reduced set of 64 scenarios of wind generation.

Figure 5-11 presents the PDF for UMP at 6 PM, constructed considering all *scenarios* of wind generation. The PDF can be used to calculate the probability of achieving an UMP within a specified range of prices. For example, it can be inferred that the probability that UMP is between 37.5 $/MWh and 38 $/MWh is 0.32.

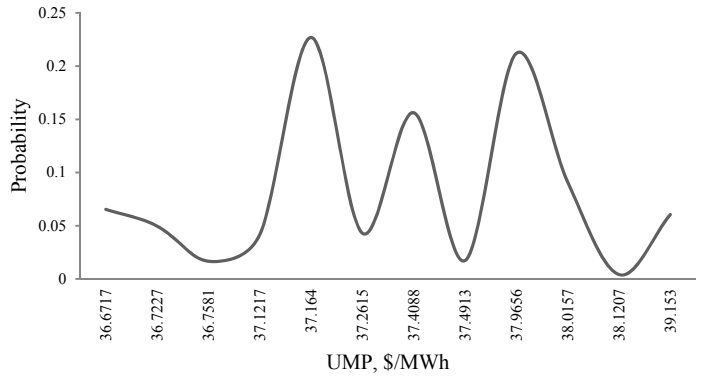

Figure 5-11 PDF for UMP at 6 PM

The expected social welfare of the system considering the 16.5 MW WF at bus-101 is $1,041,358 for the whole day, whereas, it is only $936,146 when the emission constraint is applied. It can be observed that the social welfare decreases when the emission constraint affects the system.

Figure 5-12 shows the change in expected UMP over a period of 24-hours and compared to with no wind generation. It is clear that the spot price is lower when wind generation penetration takes place.

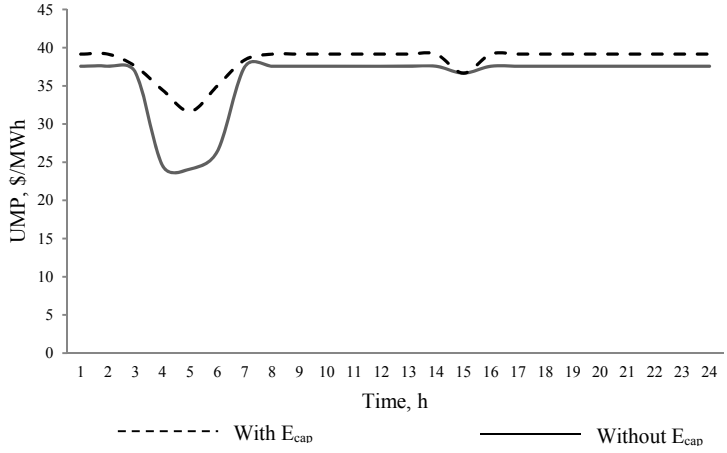

Figure 5-12 Expected UMP with and without WF with the existence of the emission cap

5.5.2.1 Effect of Large Capacity WFs on UMP Market

In this case study, the level of total wind generation capacity is increased to 20% of total generation capacity of the system. Each WF is now considered to comprise 100 WTs, of type VESTAS V82-1.65 MW, with a total capacity of 165 MW. The WTs are assumed to be placed in a rectangular

configuration, arranged in 5 rows with each row having 20 WTs. A comparison of the effect of WF capacity on expected UMPs (Figure 5-13) shows that the UMPs are significantly lower with large capacity WFs especially during peak load hours.

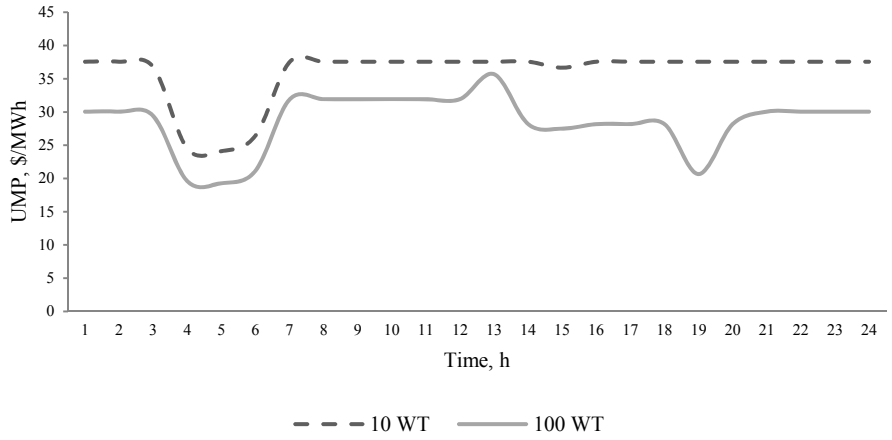

Figure 5-13 Expected UMP for different levels of WF capacity

5.6 Summary

The Government policy in Ontario requires that all connected wind generation capacity must be used. The current perception is that adding more wind energy to the generation system will reduce emissions. A short-term operations model of the power systems is developed; the model includes unit commitment constraints, and wind generation effects to examine the impact of wind generation on UC decisions when emission caps are imposed. The work further examines using a market clearing and dispatch model, how the UMP markets are affected by wind farm capacity when emissions constraint is considered.

The results of the study in this chapter indicate that the relationship between the capacity level of wind generation penetration and the reduction in emissions is not straightforward. By increasing the capacity level of wind penetration, the emissions are reduced up to a certain capacity level. After this level, one of the base-power stations (Nuclear) needs to be de-committed because it reaches a generation level that is less than the minimum operation capacity of the station. This generation has to be substituted by other generation stations and most likely it will be thermal.

Because of the need for reserves in the systems with large wind generation, thermal generators should be useful for backup. The thermal power stations produce large amounts of

emissions and hence, the trade-off between replacing these and increasing the level of penetration of wind generation must be kept with a certain limit. This limit needs to be determined by the system operator based on the generation system and operating conditions.

The analysis also reveals that UMPs are significantly affected by emission constraints. The analysis can be used by market operators and planners to understand the expected range of variation of UMPs when there is significant penetration of wind in the system where emission caps are imposed by the IESO.

Chapter 6
Summary, Contributions and Future Work

6.1 Summary

Wind power generation is characterized by its variability and uncertainty. Therefore, the integration of wind facilities to utility grids has impact on power flow, transmission congestion, load dispatch, economic analysis and electricity market clearing prices. These impacts present major challenges to power system operators; this thesis tackles some of these challenges. Accurate modeling of wind turbines and wind farms play an important role in studying the impact of wind facilities integration to utility grids. The thesis introduces novel analytical frameworks to accurately consider the impacts of high penetration of wind generation sources within the distribution and transmission networks. In particular, two main operational problems are addressed- the Distribution Load Flow (DLF) problem and the Unit Commitment (UC) problem in the presence of wind generation.

In Chapter 1, the motivations of the research work presented in this thesis are discussed, and the research objectives are presented. In Chapter 2, a literature survey of the reported techniques for wind modeling and wind farm output power simulation is presented. The chapter is divided into two main parts; the first dwells upon the power system operational aspects such as, load flow. Different methods used for distribution load flow are presented while the second part deals with the short-term operational problems in power systems with and without wind generation penetration. The short-term operational problems includes inter-hour constraints that require a new wind generation model that can handle the correlation of hourly wind speed transitions. Chapter 2 also discusses the current practices of including emission constraints in short-term system operations problems.

In Chapter 3, a set of new PDLF formulations that include a probabilistic WT model is presented. Three different classes of WT models are considered, a constant power factor WTs, a Induction generator WT, and a constant voltage WT. These WT models are integrated within the PDLF to examine and compare their performance. The different formulations of the PDLF are solved using the forward-backward sweep algorithm and compensation based power flow algorithm, the analysis providing insight into the effects on system losses, voltage regulation and sub-station power import/export in the presence of WT units at different locations. Simultaneous connection of different WT models to the distribution system is considered as well.

In Chapter 4, a mathematical modeling framework to examine the effect of wind generation penetration on power systems is presented. A new clustering and classification technique for

developing 24-hour wind speed clusters for every month is developed. MCS and Markov-Chains are used to generate correlated large amount of 24-hour wind speed scenarios. Thereafter, a novel forward selection, scenario reduction algorithm is proposed to arrive at a reduced set of wind generation scenarios. Subsequently, an LMP energy market model is developed by incorporating the reduced set of scenarios of wind power generation. The model include unit commitment constraints, transmission constraints and wind generation effects to examine the impact of wind generation on price settlement, load dispatch, and reserve requirements. The work further examines how the LMP markets are affected by wind farm capacity and when wake effect is considered. The market model is formulated as an MILP problem and solved using the CPLEX solver in GAMS environment. This model is used to investigate the impact of wind power variability, wind energy penetration level and wind farm location.

In Chapter 5, a short-term operations model is developed to determine the optimum level of wind capacity penetration as well as to set the optimum emissions cap. The effect of wind generation penetration on short-term system operation problems in the presence of an emission cap is also discussed. An UMP-based electricity market dispatch model is presented and the impact of wind generators on market price settlement and emissions reduction is investigated.

6.2 Contributions of this Thesis

The main contributions and conclusions of this research are as follows:

- A new probabilistic model of wind generation profiles, taking into account the wind speed as a random variable with a given PDF, has been proposed in the thesis. Thereafter, the traditional DLF problem has been modified to formulate a PDLF problem that includes these probabilistic models of wind generation, for further analysis. The proposed PDLF formulation yields closer results to the DLF with historical wind data, than that obtained with a deterministic DLF with fixed wind capacity factors.
- The thesis proposes a new clustering and classification technique for developing 24-hour wind speed clusters for every month, using real wind speed data over a period of three years. These wind speed clusters are then used to develop wind speed cluster PDFs. MCS are carried out using the wind speed cluster PDFs to produce hourly wind speed vectors. Markov chain models are applied on the wind speed vectors to improve the correlation between inter-hour changes in wind speed variations. Thereafter, a novel forward selection, scenario reduction algorithm is proposed to arrive at a reduced set of wind generation scenarios.

- The thesis presents an LMP-based electricity market settlement and dispatch model to examine the effects of wind generation on various market variables and on system operation. The effect of wind generation capacity is also examined and results depict that LMPs are expected to reduce with penetration of large capacity WFs into the power systems. Inclusion of wake effect in large WFs shows that the social welfare is reduced because of differential levels of intercepts by different WTs, which highlights the importance of including the dynamic wake model of WTs.
- The thesis proposes a modeling framework for analysis of the environmental impact of wind generation penetration into power systems. Two different models- one pertaining to short-term operations of power systems and the other, a UMP-based market clearing and dispatch model, are presented for the purpose..

6.3 Future Work

Based on the research work reported in this thesis, future research may be pursued in the following directions:

- The developed probabilistic model of WT can be used to examine the effect of wind generation penetration on the reliability of distribution systems as well as to study the impact of WT on protection coordination and system upgrade costs.
- With the availability of sufficient historical data of WF generation, the developed wind power scenario generation and reduction algorithm can be used to validate large scale WF production models.
- In the work presented in this thesis, only the wind output uncertainty is considered. The problem formulations may be extended to include demand uncertainty and generator outages.
- The work can be extended to develop optimal bidding strategies for the WF owners to participate in electricity markets, so as to maximize the revenue of WF owners.
- A multi-stage stochastic programming model that includes all wind power scenarios can be developed, and solved using either the Bender Decomposition or L-Shape decomposition methods.

Publications from this Research

Journal Papers:

1. **M.H. Ahmed**, K. Bhattacharya, M.M.A. Salama, "Stochastic Unit Commitment with Wind Generation Penetration", Electric Power Components and Systems - Manuscript ID UEMP-2012-0112. **Accepted**
2. **M.H. Ahmed**, K. Bhattacharya, M.M.A. Salama, "Probabilistic Distribution Load Flow with Different Wind Turbine Models", IEEE Transaction on Power Systems, TPWRS-00254-2012 – **Minor Reviews**
3. **M.H. Ahmed**, K. Bhattacharya, M.M.A. Salama, "Forward Selection Scenario Reduction for Analysis of Wind Generation Uncertainty Effects", IET proceedings on Renewable Power Generation – **In review**

Conference Papers:

4. **M. H. Ahmed**, K. Bhattacharya, M.M.A. Salama, "Evaluation of the Environmental Impact of Wind Generation Penetration", IEEE PES General Meeting 2012– California, San Diego. July 22 -26, 2012. Accepted.
5. **M. H. Ahmed**, K. Bhattacharya, M.M.A. Salama, "Environmental Modeling of Power System with Wind Power Generation", ICGST- International Conference on Recent Advances in Energy Systems, RAEPS – 12, Alexandria, Egypt, April 3 – 5, 2012.
6. **M. H. Ahmed**, K. Bhattacharya, M.M.A. Salama, "Operations Analysis of Wind Penetration into Distribution Systems Using PDLF", Middle East - Innovative Smart Grid Technologies – ME (ISGT) – Saudi Arabia – Jeddah – December 17 – 20, 2011.
7. **M. H. Ahmed**, K. Bhattacharya, M.M.A. Salama, "Analysis of Uncertainty Model to Incorporate Wind Penetration in LMP-Based Energy Markets", International Conference on Electric Power and Energy Conversion Systems, American University of Sharjah, UAE – November 15 -17, 2011. Digital Object Identifier: 10.1109/EPECS.2011.6126826.
8. **M. H. Ahmed**, K. Bhattacharya, M.M.A. Salama, "Stochastic Analysis of Wind Penetration Impact on Electricity Market Prices", IEEE PES General Meeting 2011 – Michigan, Detroit. July 26 -28, 2011. Digital Object Identifier: 10.1109/PES.2011.6039089.

Appendix A

IEEE 33-Bus Distribution System Network data

Table A.1 IEEE 33-Bus Distribution System Network data

From	To	R (p.u.)	X (p.u.)	B (p.u.)
1	2	0.0922	0.0477	0.0052
2	3	0.493	0.2511	0.0277
3	4	0.366	0.1864	0.0206
4	5	0.3811	0.1941	0.0214
5	6	0.819	0.707	0.046
6	7	0.1872	0.6188	0.0105
7	8	0.7114	0.2351	0.0961
8	9	1.03	0.74	0.0578
9	10	1.044	0.74	0.0586
10	11	0.1966	0.065	0.011
11	12	0.3744	0.1238	0.021
12	13	1.468	1.155	0.0824
13	14	0.5416	0.7129	0.0304
14	15	0.591	0.526	0.0332
15	16	0.7463	0.545	0.0419
16	17	1.289	1.721	0.0724
17	18	0.732	0.574	0.0411
2	19	0.164	0.1565	0.0092
19	20	1.5042	1.3554	0.0845
20	21	0.4095	0.4784	0.023
21	22	0.7089	0.9373	0.0398
3	23	0.4512	0.3083	0.0253
23	24	0.898	0.7091	0.0504
24	25	0.896	0.7011	0.0503
6	26	0.203	0.1034	0.0114
26	27	0.2842	0.1447	0.016
27	28	1.059	0.9337	0.0595
28	29	0.8042	0.7006	0.0452
29	30	0.5075	0.2585	0.0285
30	31	0.9744	0.963	0.0547
31	32	0.3105	0.3619	0.0174
32	33	0.341	0.5302	0.0191

Table A.2 IEEE 33-Bus Distribution Load data

Load at Bus No.	Real Power (kW)	Reactive Power (kVAr)
1	----	----
2	100	60
3	90	40
4	120	80
5	60	30
6	60	20
7	200	100
8	200	100
9	60	20
10	60	20
11	45	30
12	60	35
13	60	35
14	120	80
15	60	10
16	60	20
17	60	20
18	90	40
19	90	40
20	90	40
21	90	40
22	90	40
23	90	50
24	420	200
25	420	200
26	60	25
27	60	25
28	60	20
29	120	70
30	200	600
31	150	70
32	210	100
33	60	40

Appendix B

IEEE RTS Data

Table B.1 RTS Network data

From	To	Length (Miles)	R (p.u.)	X (p.u.)	B (p.u.)	Cont Rating (MW)
101	102	3	0.003	0.014	0.461	175
101	103	55	0.055	0.211	0.057	175
101	105	22	0.022	0.085	0.023	175
102	104	33	0.033	0.127	0.034	175
102	106	50	0.05	0.192	0.052	175
103	109	31	0.031	0.119	0.032	175
103	124	0	0.002	0.084	0	400
104	109	27	0.027	0.104	0.028	175
105	110	23	0.023	0.088	0.024	175
106	110	16	0.014	0.061	2.459	175
107	108	16	0.016	0.061	0.017	175
108	109	43	0.043	0.165	0.045	175
108	110	43	0.043	0.165	0.045	175
109	111	0	0.002	0.084	0	400
109	112	0	0.002	0.084	0	400
110	111	0	0.002	0.084	0	400
110	112	0	0.002	0.084	0	400
111	113	33	0.006	0.048	0.1	500
111	114	29	0.005	0.042	0.088	500
112	113	33	0.006	0.048	0.1	500
112	123	67	0.012	0.097	0.203	500
113	123	60	0.011	0.087	0.182	500
114	116	27	0.005	0.059	0.082	500
115	116	12	0.002	0.017	0.036	500
115	121	34	0.006	0.049	0.103	500
115	121	34	0.006	0.049	0.103	500
115	124	36	0.007	0.052	0.109	500
116	117	18	0.003	0.026	0.055	500
116	119	16	0.003	0.023	0.049	500
117	118	10	0.002	0.014	0.03	500
117	122	73	0.014	0.105	0.221	500
118	121	18	0.003	0.026	0.055	500
118	121	18	0.003	0.026	0.055	500
119	120	27.5	0.005	0.04	0.083	500

119	120	27.5	0.005	0.04	0.083	500
120	123	15	0.003	0.022	0.046	500
120	123	15	0.003	0.022	0.046	500
121	122	47	0.009	0.068	0.142	500
123	217	51	0.01	0.074	0.155	500
107	203	42	0.042	0.161	0.044	175
113	215	52	0.01	0.075	0.158	500
121	325	67	0.012	0.097	0.203	500
325	323	0	0	0.009	0	722
223	318	72	0.013	0.104	0.218	500

Table B.2 Heat Rates of Different Generators

Generator Symbol	Type	Fuel	Output %	MW	Heat Rate Btu/kwh
U12	Fossil Steam	#6 Oil	20	2.4	16017
			50	6	12500
			80	9.6	11900
			100	12	12000
U20	Combustion Turbine	#2 Oil	79	15.8	15063
			80	16	15000
			99	19.8	14500
			100	20	14499
U50	Hydro		N/A		
U76	Fossil Steam	Coal	20	15.2	17107
			50	38	12637
			80	60.8	11900
			100	76	12000
U100	Fossil Steam	#6 Oil	25	25	12999
			50	50	10700
			80	80	10087
			100	100	10000
U155	Fossil Steam	Coal	35	54.25	11244
			60	93	10053
			80	124	9718
			100	155	9600
U197	Fossil Steam	#6 Oil	35	68.95	10750
			60	118.2	9850
			80	157.6	9644
			100	197	9600
U350	Fossil Steam	Coal	40	140	10200
			65	227.5	9600
			80	280	9500
			100	350	9500
U400	Nuclear Steam	LWR	25	100	12751
			50	200	10825
			80	320	10170
			100	400	10000

Table B.3 Generator Data for IEEE RTS system

Type / Gen	Gen Bus	Gen Type	Pmax (MW)	Pmin (MW)	DT (Hour)	UT (Hour)	th (Hour)	tc (Hour)	RU (MW)	RD (MW)	hc (MBTU)	cc (MBTU)	SU (MW)	SD (MW)	C_j ($)
G1	101	U20	20	5	1	1	0	0	180	180	5	5	180	180	100
G2	101	U20	20	5	1	1	0	0	180	180	5	5	180	180	100
G3	101	U76	76	25	4	8	3	12	120	120	596	596	120	120	100
G4	101	U76	76	25	4	8	3	12	120	120	596	596	120	120	100
G5	102	U20	20	5	1	1	0	0	180	180	5	5	180	180	100
G6	102	U20	20	5	1	1	0	0	180	180	5	5	180	180	100
G7	102	U76	76	25	4	8	3	12	120	120	596	596	120	120	100
G8	102	U76	76	25	4	8	3	12	120	120	596	596	120	120	100
G9	107	U100	100	35	8	8	2	7	420	420	250	566	420	420	100
G10	107	U100	100	35	8	8	2	7	420	420	250	566	420	420	100
G11	107	U100	100	35	8	8	2	7	420	420	250	566	420	420	100
G12	113	U197	197	60	10	12	4	7	180	180	443	775	180	180	100
G13	113	U197	197	60	10	12	4	7	180	180	443	775	180	180	100
G14	113	U197	197	60	10	12	4	7	180	180	443	775	180	180	100
G15	115	U12	12	5	2	4	2	4	60	60	38	68	60	60	100
G16	115	U12	12	5	2	4	2	4	60	60	38	68	60	60	100
G17	115	U12	12	5	2	4	2	4	60	60	38	68	60	60	100
G18	115	U12	12	5	2	4	2	4	60	60	38	68	60	60	100
G19	115	U12	12	5	2	4	2	4	60	60	38	68	60	60	100
G20	115	U155	155	50	8	8	3	11	180	180	260	953	180	180	100
G21	116	U155	155	50	8	8	3	11	180	180	260	953	180	180	100
G22	118	U400	400	150	1	1	0	0	1200	1200	0.1	0.1	1200	1200	100
G23	121	U400	400	150	1	1	0	0	1200	1200	0.1	0.1	1200	1200	100
G24	122	U50	50	1	1	1	0	0	50	50	0.1	0.1	50	50	10
G25	122	U50	50	1	1	1	0	0	50	50	0.1	0.1	50	50	10
G26	122	U50	50	1	1	1	0	0	50	50	0.1	0.1	50	50	10
G27	122	U50	50	1	1	1	0	0	50	50	0.1	0.1	50	50	10
G28	122	U50	50	1	1	1	0	0	50	50	0.1	0.1	50	50	10
G29	122	U50	50	1	1	1	0	0	50	50	0.1	0.1	50	50	10
G30	123	U155	155	50	8	8	3	11	180	180	260	953	180	180	100
G31	123	U155	155	50	8	8	3	11	180	180	260	953	180	180	100
G32	123	U350	350	120	10	10	8	12	240	240	1915	4468	240	240	100

Table B.4 Generator Data for IEEE RTS system for Unit Commitment Problem

Type / Gen	a_j ($/Hour)	b_j ($/MWhr)	c_j ($/MWhr^2)	U_j^0 (Hour)	S_j^0 (Hour)	$/MBTU
G1	957.7892	32.0558	2.4353	1	0	4.451
G2	957.7892	32.0558	2.4353	1	0	4.451
G3	171.0059	10.0279	0.0394	8	0	1.275
G4	171.0059	10.0279	0.0394	8	0	1.275
G5	957.7892	32.0558	2.4353	1	0	4.451
G6	957.7892	32.0558	2.4353	1	0	4.451
G7	171.0059	10.0279	0.0394	8	0	1.275
G8	171.0059	10.0279	0.0394	8	0	1.275
G9	577.5272	33.4256	0.0531	8	0	4.451
G10	577.5272	33.4256	0.0531	8	0	4.451
G11	577.5272	33.4256	0.0531	8	0	4.451
G12	843.9887	34.0817	0.0221	12	0	4.451
G13	843.9887	34.0817	0.0221	12	0	4.451
G14	843.9887	34.0817	0.0221	12	0	4.451
G15	74.8676	38.6375	0.7044	4	0	4.451
G16	74.8676	38.6375	0.7044	4	0	4.451
G17	74.8676	38.6375	0.7044	4	0	4.451
G18	74.8676	38.6375	0.7044	4	0	4.451
G19	74.8676	38.6375	0.7044	4	0	4.451
G20	235.085	9.6217	0.0071	8	0	1.275
G21	235.085	9.6217	0.0071	8	0	1.275
G22	264.4836	5.5822	0.0006	1	0	0.65
G23	264.4836	5.5822	0.0006	1	0	0.65
G24	0	0	0	1	0	N/A
G25	0	0	0	1	0	N/A
G26	0	0	0	1	0	N/A
G27	0	0	0	1	0	N/A
G28	0	0	0	1	0	N/A
G29	0	0	0	1	0	N/A
G30	235.085	9.6217	0.0071	8	0	1.275
G31	235.085	9.6217	0.0071	8	0	1.275
G32	412.5176	9.4771	0.0042	10	0	1.275

Table B.5 Load Data Energy Bid for RTS (area 1) system Two Steps

Load Step	Step (1)		Step (2)	
Data ~~Bus No.~~	Pload (MW)	Price ($/MWhr)	Pload (MW)	Price ($/MWhr)
101	70	29.68	108	27.18
102	40	17.74	97	15.24
103	120	23.47	180	20.97
104	40	13.21	74	10.71
105	44	26.72	71	24.22
106	89	17.44	136	14.94
107	80	26.52	125	24.02
108	110	16.92	171	14.42
109	120	26.46	175	23.96
110	130	12.63	195	10.13
111	0	N/A	0	N/A
112	0	N/A	0	N/A
113	190	11.43	265	8.93
114	100	29.87	194	27.37
115	230	20.08	317	17.58
116	60	12.98	100	10.48
117	0	N/A	0	N/A
118	260	12.26	333	9.76
119	160	9.88	181	7.38
120	90	14.48	128	11.98
121	0	N/A	0	N/A
122	0	N/A	0	N/A
123	0	N/A	0	N/A
124	0	N/A	0	N/A

Table B.6 Load Data Energy Bid for RTS (area 2) system Two Steps

Load Step	Step (1)		Step (2)	
Data / Bus No.	Pload (MW)	Price ($/MWhr)	Pload (MW)	Price ($/MWhr)
201	60	19.96	108	17.46
202	60	30.72	97	28.22
203	120	26.67	180	24.17
204	40	18.42	74	15.92
205	44	30.50	71	28.00
206	80	13.72	136	11.22
207	90	21.06	125	18.56
208	120	20.50	171	18.00
209	120	20.04	175	17.54
210	133	17.71	195	15.21
211	0	N/A	0	N/A
212	0	N/A	0	N/A
213	160	13.98	265	11.48
214	130	17.95	194	15.45
215	260	10.39	317	7.89
216	60	16.10	100	13.60
217	0	N/A	0	N/A
218	260	24.43	333	21.93
219	120	28.85	181	26.35
220	60	11.18	128	8.68
221	0	N/A	0	N/A
222	0	N/A	0	N/A
223	0	N/A	0	N/A
224	0	N/A	0	N/A

Table B.7 Load Data Energy Bid for RTS (area 3) system Two Steps

Load Step	Step (1)		Step (2)	
Data / Bus No.	Pload (MW)	Price ($/MWhr)	Pload (MW)	Price ($/MWhr)
301	60	12.91	108	10.41
302	60	17.93	97	15.43
303	100	30.72	180	28.22
304	40	10.84	74	8.34
305	44	16.36	71	13.86
306	90	12.17	136	9.67
307	70	11.93	125	9.43
308	140	13.00	171	10.50
309	160	11.45	175	8.95
310	160	21.12	195	18.62
311	0	N/A	0	N/A
312	0	N/A	0	N/A
313	160	27.81	265	25.31
314	145	27.13	194	24.63
315	233	9.57	317	7.07
316	60	23.60	100	21.10
317	0	N/A	0	N/A
318	300	14.13	333	11.63
319	160	29.44	181	26.94
320	99	12.57	128	10.07
321	0	N/A	0	N/A
322	0	N/A	0	N/A
323	0	N/A	0	N/A
324	0	N/A	0	N/A
325	0	N/A	0	N/A

Table B.8 Variation of Load with Different hours as a percentage of load peaks

Hour	%Loading Of Peak load
1	78
2	72
3	68
4	66
5	64
6	65
7	66
8	70
9	80
10	88
11	90
12	91
13	90
14	88
15	87
16	87
17	91
18	100
19	99
20	97
21	94
22	92
23	87
24	81

Appendix C

Data of Environmental Emission Factors

Table C.1 Average Cost of Fuels for the Electric Power Industry[84].

Fuel Type	Coal	Petroleum	Natural Gas	All Fossil Fuels
Year	Cents/MBTU	Cents/MBTU	Cents/MBTU	Cents/MBTU
1992	141.2	251.4	232.8	158.9
1993	138.5	237.3	256	159.4
1994	135.5	242.3	223	152.5
1995	131.8	256.6	198.4	145.2
1996	128.9	302.6	264.1	151.8
1997	127.3	273	276	152
1998	125.2	202.1	238.1	143.5
1999	121.6	235.9	257.4	143.8
2000	120	417.9	430.2	173.5
2001	123.2	369.3	448.7	173
2002	125.5	334.3	356	151.5
2003	127.5	445.1	536.6	218.7

Anthracite, bituminous coal, subs bituminous coal, lignite, waste coal, and synthetic coal.

Distillate fuel oil (all diesel and No. 1, No. 2, and No. 4 fuel oils), residual fuel oil (No. 5 and No. 6 fuel oils and bunker C fuel oil), jet fuel, kerosene, petroleum coke (converted to liquid petroleum, see Technical Notes for conversion methodology), and waste oil.

Natural gas, including a small amount of supplemental gaseous fuels that cannot be identified separately. Natural gas values for 2001 forward do not include blast furnace gas or other gas.

Average costs of uranium are about $0.65/MBTU

Table C.2 Fuel Energy content and unit conversion to BTU

Energy Source	Unit of Measure	Btu/Unit of Measure
Chilled Water	Ton Hours	11.2
Chilled Water	Daily Tons	267.8
Chilled Water	Gallons	0.0093333
Coal (anthracite)	Lbs. (pounds)	12.5008
Coal (anthracite)	kLbs. (thousand pounds)	11625
Coal (anthracite)	MLbs. (million pounds)	11625000
Coal (anthracite)	Tons	25001.5
Coal (bituminous)	Lbs. (pounds)	12.0007
Coal (bituminous)	kLbs. (thousand pounds)	11160
Coal (bituminous)	MLbs. (million pounds)	11160000
Coal (bituminous)	Tons	24001.44
Coke	Lbs. (pounds)	12.40007
Coke	kLbs. (thousand pounds)	11532
Coke	MLbs. (million pounds)	11532000
Coke	Tons 2	4801.488
Diesel (No. 2)	Gallons	138.1083
Electricity	kWh (thousand Watt-hours)	3.412
Electricity	MWh (million Watt-hours)	3412
Fuel Oil (No. 1)	Gallons	134.9999811
Fuel Oil (No. 2)	Gallons	139.99998
Fuel Oil (No. 5 & No. 6)	Gallons	149.689979
Kerosene	Gallons	134.9838
Liquid Propane	kcf (thousand cubic feet)	1000.06
Liquid Propane	Gallons	90.0054
Liquid Propane	cf (cubic feet)	1.0336235
Natural Gas	ccf (hundred cubic feet)	100
Natural Gas	therms	100
Natural Gas	kcf (thousand cubic feet)	1123.9
Natural Gas	cf (cubic feet)	1.1239
Natural Gas	MCF (million cubic feet)	1123900
Propane	kcf (thousand cubic feet)	1000.06
Propane	Gallons	90.0054
Propane	cf (cubic feet)	1.0336235
Steam	Lbs. (pounds)	1.0789
Steam	kLbs. (thousand pounds)	1003.342
Steam	MLbs. (million pounds)	1003342
Wood	Tons	16783.2

Table C.3 Pollution contaminants of different generators

Pollutant / Gen.	Sox (lb/MWhr)	Nox (lb/MWhr)	PM10 (lb/MWhr)	CO (lb/MWhr)	VOC (lb/MWhr)	Lead (lb/MWhr)	CH4 (lb/MWhr)	N2O (lb/MWhr)	CO2 (lb/MWhr)
G1	0.2	0.5	0.036	0.11	0.04	0.000014	0.002	0.004	160
G2	0.2	0.5	0.036	0.11	0.04	0.000014	0.002	0.004	160
G3	0.019182	0.430435	0.516522	0.02	0.003	0.000507	0.001	0.004	210
G4	0.019182	0.430435	0.516522	0.02	0.003	0.000507	0.001	0.004	210
G5	0.2	0.5	0.036	0.11	0.04	0.000014	0.002	0.004	160
G6	0.2	0.5	0.036	0.11	0.04	0.000014	0.002	0.004	160
G7	0.019182	0.430435	0.516522	0.02	0.003	0.000507	0.001	0.004	210
G8	0.019182	0.430435	0.516522	0.02	0.003	0.000507	0.001	0.004	210
G9	0.016807	0.5	0.1	0.04	0.007	9.86E-06	0.002	0.004	170
G10	0.016807	0.5	0.1	0.04	0.007	9.86E-06	0.002	0.004	170
G11	0.016807	0.5	0.1	0.04	0.007	9.86E-06	0.002	0.004	170
G12	0.016807	0.5	0.1	0.04	0.007	9.86E-06	0.002	0.004	170
G13	0.016807	0.5	0.1	0.04	0.007	9.86E-06	0.002	0.004	170
G14	0.016807	0.5	0.1	0.04	0.007	9.86E-06	0.002	0.004	170
G15	0.016807	0.5	0.1	0.04	0.007	9.86E-06	0.002	0.004	170
G16	0.016807	0.5	0.1	0.04	0.007	9.86E-06	0.002	0.004	170
G17	0.016807	0.5	0.1	0.04	0.007	9.86E-06	0.002	0.004	170
G18	0.016807	0.5	0.1	0.04	0.007	9.86E-06	0.002	0.004	170
G19	0.016807	0.5	0.1	0.04	0.007	9.86E-06	0.002	0.004	170
G20	0.019182	0.430435	0.516522	0.02	0.003	0.000507	0.001	0.004	210
G21	0.019182	0.430435	0.516522	0.02	0.003	0.000507	0.001	0.004	210
G22	1E-08	1E-08	1E-08	1E-08	1E-08	1E-08	1E-08	1E-08	1E-08
G23	1E-08	1E-08	1E-08	1E-08	1E-08	1E-08	1E-08	1E-08	1E-08
G24	1E-08	1E-08	1E-08	1E-08	1E-08	1E-08	1E-08	1E-08	1E-08
G25	1E-08	1E-08	1E-08	1E-08	1E-08	1E-08	1E-08	1E-08	1E-08
G26	1E-08	1E-08	1E-08	1E-08	1E-08	1E-08	1E-08	1E-08	1E-08
G27	1E-08	1E-08	1E-08	1E-08	1E-08	1E-08	1E-08	1E-08	1E-08
G28	1E-08	1E-08	1E-08	1E-08	1E-08	1E-08	1E-08	1E-08	1E-08
G29	1E-08	1E-08	1E-08	1E-08	1E-08	1E-08	1E-08	1E-08	1E-08
G30	0.019182	0.430435	0.516522	0.02	0.003	0.000507	0.001	0.004	210
G31	0.019182	0.430435	0.516522	0.02	0.003	0.000507	0.001	0.004	210
G32	0.019182	0.430435	0.516522	0.02	0.003	0.000507	0.001	0.004	210

This table is deduced from the data given in [82].

Bibliography

[1] *GWEC (Global Wind Energy Council), "Global Wind Statistics 2010,". Available: http://www.gwec.net/fileadmin/documents/Publications/GWEC_PRstats_02-02-2011_final.pdf.*

[2] *Canadian Wind Energy Association www.canwea.ca.*

[3] *"ecoEnergy for Renewable Power Program,". Available: http://www.ecoaction.gc.ca/ecoenergy-ecoenergie/power-electricite/index-eng.cfm*

[4] *Ontario Power Authority (OPA) "Ontario's Integrated Power System Plan,". Available: http://www.powerauthority.on.ca/integrated-power-system-plan.*

[5] *OPA. (2009), "Ontarians get the green light for 700 rooftop solar projects,". Available: http://www.powerauthority.on.ca/news/ontarians-get-green-light-700-rooftop-solar-projects.*

[6] D. Weisser, "A wind energy analysis of Grenada: an estimation using the 'Weibull'density function," *Renewable Energy,* vol. 28, no. 11, pp. 1803-1812, 2003.

[7] K. Divya, and P. Rao, "Models for wind turbine generating systems and their application in load flow studies," *Electric Power Systems Research,* vol. 76, no. 9, pp. 844-856, 2006.

[8] N. Hatziargyriou, T. Karakatsanis, and M. Papadopoulos, "Probabilistic load flow in distribution systems containingdispersed wind power generation," *IEEE Transactions on Power Systems,* vol. 8, no. 1, pp. 159-165, 1993.

[9] C. L. Su, "Probabilistic load-flow computation using point estimate method," *Power Systems, IEEE Transactions on,* vol. 20, no. 4, pp. 1843-1851, 2005.

[10] J. H. Teng, "Modelling distributed generations in three-phase distribution load flow," *Generation, Transmission & Distribution, IET,* vol. 2, no. 3, pp. 330-340, 2008.

[11] H. Sun, D. Nikovski, T. Ohno *et al.*, "A Fast and Robust Load Flow Method for Distribution Systems with Distributed Generations," *Energy Procedia,* vol. 12, pp. 236-244, 2011.

[12] D. Rajicic, and A. Bose, "A modification to the fast decoupled power flow for networks withhigh R/X ratios," *IEEE Transactions on Power Systems,* vol. 3, no. 2, pp. 743-746, 1988.

[13] S. Iwamoto, and Y. Tamura, "A load flow calculation method for ill-conditioned power systems," *IEEE Transactions on Power Apparatus and Systems*, pp. 1736-1743, 1981.

[14] S. Tripathy, G. Prasad, O. Malik *et al.*, "Load-flow solutions for ill-conditioned power systems by a Newton-like method," *IEEE Transactions on Power Apparatus and Systems*, pp. 3648-3657, 1982.

[15] W. Kersting, "A method to teach the design and operation of a distribution system," *IEEE Transactions on Power Apparatus and Systems*, pp. 1945-1952, 1984.

[16] D. Shirmohammadi, H. Hong, A. Semlyen *et al.*, "A compensation-based power flow method for weakly mesheddistribution and transmission networks," *IEEE Transactions on Power Systems,* vol. 3, no. 2, pp. 753-762, 1988.

[17] G. Jasmon, and L. Lee, "Distribution network reduction for voltage stability analysis and loadflow calculations," *ELECTR. POWER ENERGY SYST.,* vol. 13, no. 1, pp. 9-13, 1991.

[18] D. Das, H. Nagi, and D. Kothari, "Novel method for solving radial distribution networks," *IEE Proceedings-Generation, Transmission and Distribution,* vol. 141, pp. 291, 1994.

[19] S. Ghosh, and D. Das, "Method for load-flow solution of radial distribution networks," *IEE Proceedings-Generation, Transmission and Distribution,* vol. 146, pp. 641, 1999.

[20] E. Bompard, E. Carpaneto, G. Chicco *et al.*, "Convergence of the backward/forward sweep method for the load-flow analysis of radial distribution systems," *International journal of electrical power & energy systems,* vol. 22, no. 7, pp. 521-530, 2000.

[21] T. Gözel, and M. H. Hocaoglu, "An analytical method for the sizing and siting of distributed generators in radial systems," *Electric Power Systems Research,* vol. 79, no. 6, pp. 912-918, 2009.

[22] J. H. Teng, "A direct approach for distribution system load flow solutions," *IEEE Transactions on Power Delivery,,* vol. 18, no. 3, pp. 882-887, 2003.

[23] G. A. T. Ackermann, and L. Soder, "Distributed generation: A definition," *Elect. Power Syst. Res.,* vol. 57, pp. 195–204, 2001.

[24] R. Allan, and A. Leite da Silva, "Probabilistic load flow using multilinearisations," *IEE Proceedings Generation, Transmission and Distribution,* vol. 128, no. 5, pp. 280-287, 1981.

[25] G. Verbic, and C. A. Cañizares, "Probabilistic optimal power flow in electricity markets based on a two-point estimate method," *IEEE Transactions on Power Systems,* vol. 21, no. 4, pp. 1883-1893, 2006.
[26] M. Shahidehpour, H. Yamin, and Z. Li, *Market operations in electric power systems: forecasting, scheduling, and risk management*: Wiley-IEEE Press, 2002.
[27] K. Bhattacharya, M. Bollen, and J. Daalder, *Operation of restructured power systems*: Springer Netherlands, 2001.
[28] C. Li, R. Johnson, A. Svoboda *et al.*, "A new unit commitment method," *IEEE Transactions on Power Systems,* vol. 12, no. 1, pp. 113-119, 1997.
[29] T. Senjyu, K. Shimabukuro, K. Uezato *et al.*, "A fast technique for unit commitment problem by extended priority list," *IEEE Transactions on Power Systems,* vol. 18, no. 2, pp. 882-888, 2003.
[30] T. Dillon, K. Edwin, H. Kochs *et al.*, "Integer programming approach to the problem of optimal unit commitment with probabilistic reserve determination," *IEEE Transactions on Power Apparatus and Systems*, pp. 2154-2166, 1978.
[31] F. Zhuang, and F. Galiana, "Towards a more rigorous and practical unit commitment by Lagrangianrelaxation," *IEEE Transactions on Power Systems,* vol. 3, no. 2, pp. 763-773, 1988.
[32] G. Purushothama, and L. Jenkins, "Simulated annealing with local search-a hybrid algorithm for unit commitment," *IEEE Transactions on Power Systems,* vol. 18, no. 1, pp. 273-278, 2003.
[33] I. Damousis, A. Bakirtzis, and P. Dokopoulos, "A solution to the unit-commitment problem using integer-coded genetic algorithm," *IEEE Transactions on Power Systems,* vol. 19, no. 2, pp. 1165-1172, 2004.
[34] N. Padhy, "Unit commitment-a bibliographical survey," *IEEE Transactions on Power Systems,* vol. 19, no. 2, pp. 1196-1205, 2004.
[35] G. Nemhauser, and L. Wolsey, *Integer and combinatorial optimization*: Wiley New York, 1999.
[36] J. Arroyo, and A. Conejo, "Optimal response of a thermal unit to an electricity spot market," *IEEE Transactions on Power Systems,* vol. 15, no. 3, pp. 1098-1104, 2000.
[37] M. Carrion, and J. Arroyo, "A computationally efficient mixed-integer linear formulation for the thermal unit commitment problem," *IEEE Transactions on Power Systems,* vol. 21, no. 3, pp. 1371–1378, 2006.
[38] V. Pappala, I. Erlich, K. Rohrig *et al.*, "A stochastic model for the optimal operation of a wind-thermal power system," *IEEE Transactions on Power Systems,* vol. 24, no. 2, pp. 940-950, 2009.
[39] K. Høyland, and S. Wallace, "Generating scenario trees for multistage decision problems," *Management Science,* vol. 47, no. 2, pp. 295-307, 2001.
[40] F. Bouffard, and F. Galiana, "Stochastic security for operations planning with significant wind power generation," *IEEE Transactions on Power Systems,* vol. 23, no. 2, pp. 306-316, 2008.
[41] M. Pereira, and L. Pinto, "Multi-stage stochastic optimization applied to energy planning," *Mathematical Programming,* vol. 52, no. 1, pp. 359-375, 1991.
[42] J. Wang, M. Shahidehpour, and Z. Li, "Security-constrained unit commitment with volatile wind power generation," *IEEE Transactions on Power Systems,* vol. 23, no. 3, pp. 1319-1327, 2008.
[43] G. Sideratos, and N. Hatziargyriou, "An advanced statistical method for wind power forecasting," *IEEE Transactions on Power Systems,* vol. 22, no. 1, pp. 258-265, 2007.
[44] B. Ummels, M. Gibescu, E. Pelgrum *et al.*, "Impacts of wind power on thermal generation unit commitment and dispatch," *IEEE Transactions on energy conversion,* vol. 22, no. 1, pp. 44-51, 2007.
[45] A. Tuohy, P. Meibom, E. Denny *et al.*, "Unit commitment for systems with significant wind penetration," *IEEE Transactions on Power Systems,* vol. 24, no. 2, pp. 592–601, 2009.
[46] L. Soder, "Reserve margin planning in a wind-hydro-thermal power system," *IEEE Transactions on Power Systems,* vol. 8, no. 2, pp. 564-571, 1993.
[47] H. Yan, P. Luh, X. Guan *et al.*, "Scheduling of hydrothermal power systems," *IEEE Transactions on Power Systems,* vol. 8, no. 3, pp. 1358-1365, 1993.
[48] S. Dekrajangpetch, G. Sheble, and A. Conejo, "Auction implementation problems using Lagrangian relaxation," *IEEE Transactions on Power Systems,* vol. 14, no. 1, pp. 82-88, 1999.
[49] S. Takriti, B. Krasenbrink, and S. Lilian, "Incorporating fuel constraints and electricity spot prices into the stochastic unit commitment problem," *Operations Research,* vol. 48, no. 2, pp. 268-280, 2000.

[50] M. H. Ahmed, K. Bhattacharya, and M. Salama, "Analysis of uncertainty model to incorporate wind penetration in LMP-based energy markets." pp. 1-8.
[51] "GAMS Release 2.50," A User's Guide, GAMS Development Corporation, 1999.
[52] T. L. Baldwin, and S. A. Lewis, "Distribution load flow methods for shipboard power systems," *IEEE Transaction on Industry Applications,* vol. 40, no. 5, pp. 1183-1190, 2004.
[53] G. Bathurst, and G. Strbac, "Value of combining energy storage and wind in short-term energy and balancing markets," *Electric Power Systems Research,* vol. 67, no. 1, pp. 1-8, 2003.
[54] J. Morales, A. Conejo, and J. Pérez-Ruiz, "Economic valuation of reserves in power systems with high penetration of wind power," *IEEE Transactions on Power Systems,* vol. 24, no. 2, 2009.
[55] C. Chompoo-inwai, W. Lee, P. Fuangfoo *et al.*, "System impact study for the interconnection of wind generation and utility system," *IEEE transactions on Industry Applications,* vol. 41, no. 1, pp. 163-168, 2005.
[56] M. Ortega-Vazquez, and D. Kirschen, "Estimating the Spinning Reserve Requirements in Systems With Significant Wind Power Generation Penetration," *IEEE Transactions on Power Systems,* vol. 24, no. 1, pp. 114-124, 2009.
[57] P. Schweizer, "Determining optimal fuel mix for environmental dispatch," *IEEE Transactions on Automatic Control,* vol. 19, no. 5, pp. 534-537, 1974.
[58] A. Tsuji, "Optimal Fuel Mix and Load Dispatching Under Environemental Constraints," *IEEE Transactions on Power Apparatus and Systems*, pp. 2357-2364, 1981.
[59] M. Tsay, W. Lin, and J. Lee, "Application of evolutionary programming for economic dispatch of cogeneration systems under emission constraints," *International Journal of Electrical Power and Energy Systems,* vol. 23, no. 8, pp. 805-812, 2001.
[60] M. Tsay, "Applying the multi-objective approach for operation strategy of cogeneration systems under environmental constraints," *International Journal of Electrical Power and Energy Systems,* vol. 25, no. 3, pp. 219-226, 2003.
[61] C. Cormio, M. Dicorato, A. Minoia *et al.*, "A regional energy planning methodology including renewable energy sources and environmental constraints," *Renewable and Sustainable Energy Reviews,* vol. 7, no. 2, pp. 99-130, 2003.
[62] A. Augugliaro, L. Dusonchet, S. Favuzza *et al.*, "A backward sweep method for power flow solution in distribution networks," *International journal of electrical power & energy systems,* vol. 32, no. 4, pp. 271-280, 2010.
[63] E. F. Schuster, "Estimation of a probability density function and its derivatives," *The Annals of Mathematical Statistics*, pp. 1187-1195, 1969.
[64] A. E. Feijoo, and J. Cidras, "Modeling of wind farms in the load flow analysis," *IEEE Transactions on Power Systems,,* vol. 15, no. 1, pp. 110-115, 2000.
[65] http://www.knmi.nl/klimatologie/onderzoeksgegevens/potentiele_wind/.
[66] B. Venkatesh, R. Ranjan, and H. Gooi, "Optimal reconfiguration of radial distribution systems to maximize loadability," *Power Systems, IEEE Transactions on,* vol. 19, no. 1, pp. 260-266, 2004.
[67] Y. Atwa, and E. El-Saadany, "Reliability Evaluation for Distribution System With Renewable Distributed Generation During Islanded Mode of Operation," *IEEE Transactions on Power Systems,* vol. 24, no. 2, 2009.
[68] H. Holttinen, P. Meibom, A. Orths *et al.*, "Impacts of large amounts of wind power on design and operation of power systems, results of IEA collaboration," *Wind Energy,* vol. 14, no. 2, pp. 179-192, 2011.
[69] M. Nowak, and W. Römisch, "Stochastic Lagrangian relaxation applied to power scheduling in a hydro-thermal system under uncertainty," *Ann. Oper. Res.,* vol. 100, no. 1, pp. 251-272, 2000.
[70] R. Srikanthan, and T. McMahon, *Stochastic generation of rainfall and evaporation data*: Australian Government Pub. Service, 1985.
[71] A. J. Frost, M. A. Thyer, R. Srikanthan *et al.*, "A general Bayesian framework for calibrating and evaluating stochastic models of annual multi-site hydrological data," *Journal of Hydrology,* vol. 340, no. 3, pp. 129-148, 2007.
[72] S. Ahmad, I. H. Khan, and B. Parida, "Performance of stochastic approaches for forecasting river water quality," *Water research,* vol. 35, no. 18, pp. 4261-4266, 2001.

[73] A. D. Sahin, and Z. Sen, "First-order Markov chain approach to wind speed modelling," *Journal of Wind Engineering and Industrial Aerodynamics,* vol. 89, no. 3, pp. 263-269, 2001.
[74] F. Kaminsky, R. Kirchhoff, C. Syu *et al.*, "A comparison of alternative approaches for the synthetic generation of a wind speed time series," *Journal of solar energy engineering,* vol. 113, pp. 280, 1991.
[75] M. Torre, P. Poggi, and A. Louche, "Markovian model for studying wind speed time series in Corsica," *International Journal of Renewable Energy Engineering,* vol. 3, no. 2, pp. 311-319, 2001.
[76] D. O. Logofet, and E. V. Lesnaya, "The mathematics of Markov models: what Markov chains can really predict in forest successions," *Ecological Modelling,* vol. 126, no. 2, pp. 285-298, 2000.
[77] P. Poggi, G. Notton, M. Muselli *et al.*, "Stochastic study of hourly total solar radiation in Corsica using a Markov model," *International journal of climatology,* vol. 20, no. 14, pp. 1843-1860, 2000.
[78] C. Grigg, P. Wong, P. Albrecht *et al.*, "The IEEE Reliability Test System-1996. A report prepared by theReliability Test System Task Force of the Application of ProbabilityMethods Subcommittee," *IEEE Transactions on Power Systems,* vol. 14, no. 3, pp. 1010-1020, 1999.
[79] R. Barth, L. Soeder, C. Weber *et al.*, "Methodology of the Scenario Tree Tool-Deliverable 6.2 (d)," *Report of the EU Project: Wind Power Generation in Liberalised Electricity Markets (Wilmar).¡ http://www.wilmar.com, Stuttgart, Tech. Rep*, 2006.
[80] S. Grady, M. Hussaini, and M. Abdullah, "Placement of wind turbines using genetic algorithms," *Renewable Energy,* vol. 30, no. 2, pp. 259-270, 2005.
[81] I. Katic, J. Højstrup, and N. Jensen, "A simple model for cluster efficiency." pp. 407-10.
[82] C. Volume II, "Uncontrolled Emission Factor Listing For Criteria Air Pollutants", July 2001. Prepared by: Eastern Research Group, Point Sources Committee and Emission Inventory Improvement Program, located at <http://www.epa.gov/ttnchie1/eiip/techreport/volume02/index.html>
[83] B.-H. Lee, Y.-H. Baek, H.-S. Choi *et al.*, "Impulse breakdown characteristics of the plane-to-plane electrode system with a needle-shaped protrusion in SF₆," *Current Applied Physics,* vol. 7, no. 3, pp. 289-295, 2007.
[84] E. I. A. w. U.S. Department of Energy, located at < http://www.eia.doe.gov/epa/epat4p5.html >.